Government of Western Australia

Department of
Mines and Petroleum

REPORT
164

GEOLOGY OF THE EASTERN ZONE OF THE LAMBOO PROVINCE, HALLS CREEK OROGEN, WESTERN AUSTRALIA

by C Phillips, K Orth, JA Hollis, CL Kirkland, S Bodorkos, AIS Kemp, MTD Wingate, Y Lu, L Iaccheri, and RW Page

John de Laeter Centre

GEMOC

CCFS

EXPLORATION INCENTIVE SCHEME

Geological Survey of Western Australia

Government of Western Australia
Department of Mines and Petroleum

REPORT 164

GEOLOGY OF THE EASTERN ZONE OF THE LAMBOO PROVINCE, HALLS CREEK OROGEN, WESTERN AUSTRALIA

by
C Phillips, K Orth[1], JA Hollis[2], CL Kirkland[3], S Bodorkos[4], AIS Kemp[5], MTD Wingate, Y Lu, L Iaccheri[5], and RW Page[4]

1 Department of Geology, University of Tasmania, Sandy Bay Campus, Private Bag 79, Hobart TAS 7001, Australia

2 Ministry of Mineral Resources, PO Box 930, 3900 Nuuk, Greenland

3 Department of Applied Geology, Curtin University, GPO Box U1987, Perth WA 6845, Australia

4 Geoscience Australia, GPO Box 378, Canberra ACT 2601, Australia

5 School of Earth and Environment, The University of Western Australia, 35 Stirling Highway, Crawley WA 6009, Australia

Perth 2016

Geological Survey of Western Australia

MINISTER FOR MINES AND PETROLEUM
Hon. Sean K L'Estrange MLA

ACTING DIRECTOR GENERAL, DEPARTMENT OF MINES AND PETROLEUM
Tim Griffin

EXECUTIVE DIRECTOR, GEOLOGICAL SURVEY OF WESTERN AUSTRALIA
Rick Rogerson

REFERENCE
The recommended reference for this publication is:
Phillips, C, Orth, K, Hollis, JA, Kirkland, CL, Bodorkos, S, Kemp, AIS, Wingate, MTD, Lu, Y, Iaccheri, L and Page, RW 2016, Geology of the Eastern Zone of the Lamboo Province, Halls Creek Orogen, Western Australia: Geological Survey of Western Australia, Report 164, 57p.

National Library of Australia Cataloguing-in-Publication entry

Creator:	Phillips, Christopher, author.
Title:	Geology of the eastern zone of the Lamboo Province, Halls Creek Orogen, Western Australia / Christopher Phillips, Karen Orth, Julie Hollis, Chris Kirkland, Simon Bodorkos, Tony Kemp, Michael Wingate, Yongjun Lu, Linda Iaccheri and RW Page.
ISBN:	9781741687132
Subjects:	Geology--Western Australia--Halls Creek region. Geology, Structural--Western Australia--Halls Creek Region. Halls Creek Region (W.A.)
Other Authors/Contributors:	Orth, K. author. Hollis, Julie, author. Kirkland, Chris, author. Bodorkos, Simon, author. Kemp, Tony, author. Wingate, Michael, author. Lu, Yongjun, author. Laccheri, Linda, author. Page, R. W., author. Geological Survey of Western Australia
Dewey Decimal Classification:	

ISSN 0508–4741

U–Pb measurements of GSWA samples were conducted using the SHRIMP II ion microprobes at the John de Laeter Centre of Isotope Research at Curtin University in Perth, Western Australia. Isotope analyses were funded in part by the Western Australian Government Exploration Incentive Scheme (EIS). Lu–Hf measurements were conducted using LA–ICPMS at the ARC National Key Centre for Geochemical Evolution and Metallogeny of Continents (GEMOC), via the ARC Centre of Excellence in Core to Crust Fluid Systems (CCFS), based in the Department of Earth and Planetary Sciences at Macquarie University, Australia.

Grid references in this publication refer to the Geocentric Datum of Australia 1994 (GDA94). Locations mentioned in the text are referenced using Map Grid Australia (MGA) coordinates, Zone 52. All locations are quoted to at least the nearest 100 m.

Copy editor: RS Bower
Cartography: AK Symonds
Desktop publishing: RL Hitchings

Published 2016 by Geological Survey of Western Australia
This Report is published in digital format as part of a digital dataset on USB, and is available online at <www.dmp.wa.gov.au/GSWApublications>.

Further details of geological publications and maps produced by the Geological Survey of Western Australia are available from:
Information Centre
Department of Mines and Petroleum
100 Plain Street | EAST PERTH WESTERN AUSTRALIA 6004
Telephone: +61 8 9222 3459 Facsimile: +61 8 9222 3444
www.dmp.wa.gov.au/GSWApublications

Cover photograph: Tightly folded marble and calcareous metasiltstone in the c. 1881 Ma Brim Rockhole Formation, 15 km north-northeast of Sophie Downs Homestead

Contents

Abstract 1
Introduction 2
Geology of the Lamboo Province 2
Western Zone (1879–1810 Ma) 2
Central Zone (1865–1810 Ma) 5
Halls Creek Orogeny (1832–1808 Ma) 6
Yampi Orogeny (1000–800 Ma) 6
King Leopold Orogeny (c. 560 Ma) 6
Geology of the Eastern Zone 6
Sophie Downs Suite 8
Halls Creek Group 10
Woodward Dolerite 18
Geochemistry 19
Major and trace element geochemistry 19
Sm–Nd whole-rock isotope data 27
Zircon U–Pb geochronology and Lu–Hf isotopes 30
Sophie Downs Suite 30
Halls Creek Group 33
Discussion 42
Evolution of the Eastern Zone 42
Correlations with the Granites–Tanami Orogen 46
Conclusions 48
References 48

Appendices

1 Analytical data and methodology for geochemistry 53
2 Zircon U–Pb geochronology and Lu–Hf isotopes 55
3 Definition of the Brim Rockhole Formation (new formation) 57

Note: Appendix 1 and 2 are available as a downloadable zip file on eBookshop

Figures

1. Location map and simplified geology of the Halls Creek Orogen 3
2. Location and geology of the study area 4
3. Time–space plot of the Lamboo Province and west Tanami region 5
4. Generalized stratigraphic column through the Eastern Zone 7
5. Field photographs of the Ding Dong Downs Volcanics 9
6. Field photographs of the Saunders Creek Formation 11
7. Field photographs of the Brim Rockhole Formation 13
8. The unconformable surface between the Brim Rockhole and Biscay Formations 14
9. Field photographs of the Biscay Formation 15
10. Field photographs of the Olympio Formation 17
11. Classification diagrams for volcanic rocks in the Ding Dong Downs Volcanics 19
12. Major elements against MgO for samples from the Ding Dong Downs Volcanics 20
13. Geochemical diagrams of Ding Dong Downs Volcanics samples 21
14. REE trends of Halls Creek Group and Tanami Group metasandstone samples 22
15. Geochemical classification diagrams of Brim Rockhole Formation and Biscay Formation metavolcanic rocks 23
16. Major element plots of Brim Rockhole Formation and Biscay Formation mafic metavolcanic rocks 24, 25
17. Trace and REE trends in Brim Rockhole Formation and Biscay Formation mafic metavolcanic rocks 26
18. Volcanic rock classification plots of Woodward Dolerite samples 27
19. Major and trace element plots against MgO of Woodward Dolerite samples 28, 29
20. Trace and REE spider diagrams of Woodward Dolerite samples 29
21. εNd values vs time of samples from the Eastern Zone 30
22. U–Pb and Lu–Hf analytical data from Sophie Downs Suite samples 31
23. U–Pb and Lu–Hf analytical data from Saunders Creek Formation and Brim Rockhole Formation samples 34, 35

24. U–Pb and Lu–Hf analytical data from Biscay Formation samples 37
25. U–Pb and Lu–Hf analytical data from lower Olympio Formation metasedimentary rocks and the Maude Headley Member, Olympio Formation 39
26. U–Pb and Lu–Hf analytical data of the Butchers Gully Member, Olympio Formation 40
27. U–Pb and Lu–Hf analytical data of metasedimentary rocks from the upper Olympio Formation 41
28. Depositional models of the Halls Creek Group 45

Table

1. Summary of age data of samples analysed from the Eastern Zone 32

The geology of the Eastern Zone of the Lamboo Province, Halls Creek Orogen, Western Australia

by

C Phillips, K Orth[1], JA Hollis[2], CL Kirkland[3], S Bodorkos[4], AIS Kemp[5], MTD Wingate, Y Lu, L Iaccheri[5], and RW Page[4]

Abstract

The Eastern Zone of the Lamboo Province records magmatism, volcanism and sedimentation on the western margin of the North Australian Craton from c. 1912 to 1788 Ma. The oldest exposed rocks in the Eastern Zone comprise the Sophie Downs Suite (including the Ding Dong Downs Volcanics) which record passive margin magmatism and sedimentation between c. 1912 and 1904 Ma. The unconformably overlying Halls Creek Group consists of four formations that (in ascending order) are the fluvial Saunders Creek Formation, lacustrine or shallow-marine Brim Rockhole Formation (new formation proposed here), shallow-marine Biscay Formation and deep-marine Olympio Formation. The Brim Rockhole Formation, formerly part of the lower Biscay Formation, is raised to formation status based on sedimentology and SHRIMP U–Pb zircon age data. Saunders Creek Formation and Brim Rockhole Formation metasandstone units contain detrital zircons dominated by Archean age components, whereas Biscay Formation metasandstone units contain detrital zircons with dominant Paleoproterozoic age components. Furthermore, calcareous and dolomitic metasedimentary rocks in the Brim Rockhole Formation are intercalated with felsic metavolcanic rocks dated at c. 1881 Ma, interpreted as the age of volcanism. The Biscay Formation is younger with constituent psammitic and pelitic metasedimentary rocks yielding a maximum depositional age of c. 1861 Ma. Both the Brim Rockhole Formation and Biscay Formation include intercalated basaltic metavolcanic rocks. Overall, metabasalt rocks have similar whole-rock geochemistry and fall on a trend consistent with progressive fractionation, increasing crustal contamination from c. 1881 to 1861 Ma. The Olympio Formation is disconformable or unconformable on the Biscay Formation and represents marine transgression accompanying subsidence. Turbidite metasandstones in the lower Olympio Formation contain 1875–1860 Ma detrital zircon grains with unradiogenic Hf values. These data are similar to turbidite metasandstones from the 1864–1840 Ma Killi Killi Formation in the Granites–Tanami Orogen to the southeast that also contain detrital zircons with dominant age components at 1870–1860 Ma. This Report suggests a large turbidite system was active along the western margin of the North Australian Craton feeding sedimentary detritus to deep-marine basins in the Halls Creek and Granites–Tanami Orogens. Based on similar age components and Hf isotope data, possible detrital sources for the turbidite system could be the 1864–1852 Ma Paperbark Supersuite in the Western Zone of the Lamboo Province or the 1867–1862 Ma Nimbuwah Complex in the Pine Creek Orogen. The entire Halls Creek Group and Sophie Downs Suite are intruded by the c. 1835 Ma Woodward Dolerite with the onset of the Halls Creek Orogeny at c. 1832–1808 Ma.

KEYWORDS: geochronology, lutetium hafnium dating, Proterozoic, regional geology, sedimentary geology, uranium lead dating, zircon

1 Department of Geology, University of Tasmania, Sandy Bay Campus, Private Bag 79, Hobart TAS 7001, Australia

2 Ministry of Mineral Resources, PO Box 930, 3900 Nuuk, Greenland

3 Department of Applied Geology, Curtin University, GPO Box U1987, Perth WA 6845, Australia

4 Geoscience Australia, GPO Box 378, Canberra ACT 2601, Australia

5 School of Earth and Environment, The University of Western Australia, 35 Stirling Highway, Crawley WA 6009, Australia

Introduction

The Paleoproterozoic Kimberley and Speewah Basins dominate the geology of the Kimberley region of northern Western Australia. The southern and eastern margins of these basins unconformably overlie older Paleoproterozoic meta-igneous and metasedimentary rocks of the Lamboo Province (Thom, 1975; Griffin and Grey, 1990; Tyler et al., 1995, 2012; Sheppard et al., 2012). The Lamboo Province, the deformed margins of the Kimberley and Speewah Basins and small localized sedimentary basins constitute the northeast-trending Halls Creek Orogen and northwest-trending King Leopold Orogen (Griffin and Grey, 1990; Grey and Griffin, 1990). Current tectonic models suggest that the Halls Creek Orogen records the collision between the Kimberley Craton and the North Australian Craton during the Halls Creek Orogeny at 1832–1808 Ma (Tyler et al., 1998; Griffin et al., 2000a; Page et al., 2001; Sheppard et al., 2012). The Halls Creek Orogen and Lamboo Province are divided by major north-northeast-trending strike-slip faults which define the boundaries of three tectonostratigraphic terranes defined by Griffin and Tyler (1993) and Tyler et al. (1995) as the Western, Central and Eastern Zones (Fig. 1). The Western Zone records sedimentation, plutonism and volcanism on the eastern margin of the Kimberley Craton. Rocks of the Central Zone are considered to have been deposited in either an oceanic arc or back-arc setting outboard of the Kimberley Craton (Sheppard et al., 1999b; Blake et al., 2000). This Report focuses on the Eastern Zone, which consists of a volcanic and plutonic basement (the Sophie Downs Suite, including the Ding Dong Downs Volcanics) overlain by a volcano-sedimentary succession (the Halls Creek Group) deposited on the western margin of the North Australian Craton.

There are relatively few published data on the Halls Creek Group or the Sophie Downs Suite despite significant mapping of the Lamboo Province and Halls Creek Orogen in the 1980s and 1990s (Tyler et al., 1995, 1998; Warren, 1997; Blake et al., 1997, 1999b, 2000; Griffin et al., 1998, 2000a; Tyler, 2004). Field mapping and sampling by the Geological Survey of Western Australia (GSWA) in 2012 investigated the tectonostratigraphy of the Eastern Zone. Accessible outcrops on the Halls Creek, Mcintosh, Dixon and Ruby Plains 1:100 000 map sheets defined the study area of this Report (Fig. 2). Outcrops were accessible on Sophie Downs and Ruby Plains Stations using station tracks as well as accessible areas along the Duncan Road and Tanami Road (Fig. 2). This study presents the results of new mapping and sampling as well as new and previously unpublished analytical data describing and reinterpreting the tectonostratigraphy of the Eastern Zone and addressing its relevance to understanding the evolution of the North Australian Craton. Regional correlations with the Granites–Tanami Orogen to the southeast are explored incorporating these new data.

Geology of the Lamboo Province

Western Zone (1879–1810 Ma)

The Western Zone includes all deformed Paleoproterozoic crystalline rocks west of the Ramsay Range and Springvale Faults (Fig. 1). The basement does not crop out, but is assumed to be the eastern extent of the inferred Archean to Paleoproterozoic Kimberley Craton (Gunn and Meixner, 1998; Tyler et al., 1999; Griffin et al., 2000a; Collins et al., 2003; Downes et al., 2007; Saygin and Kennett, 2010; Sheppard et al., 2012). The oldest exposed rocks in the Western Zone are greenschist to granulite facies turbiditic metasedimentary rocks of the Marboo Formation and Mount Joseph Migmatite. Detrital zircons from a metasandstone in the Marboo Formation provide a maximum depositional age of 1872 ± 9 Ma (Figs 1 and 3; Tyler et al., 1999). The Marboo Formation was divided into an upper and lower unit by Hancock and Rutland (1984) and Hancock (1991). The lower unit consists of metamorphosed quartzofeldspathic greywacke with lesser metasiltstone and metamudstone deposited in a middle fan setting sourced from a continental province (Griffin et al., 1993; Tyler et al., 1999). The majority of the upper unit contains <1 m thick beds of metamudstone and metasiltstone with lesser metamorphosed quartzofeldspathic greywacke deposited in a lower fan setting (Griffin et al., 1993). Constituent felsic volcanic fragments in the upper unit indicate a magmatic arc or orogenic source (Griffin et al., 1998; Tyler et al., 1999). Current structures from both units indicate a paleocurrent from the north and northwest (Hancock, 1991; Tyler et al., 1999). Metadolerite and metagabbro sills of the 1872–1861 Ma Ruins Dolerite intrude the Marboo Formation (Griffin et al., 1993; Tyler et al., 1999). These sills are commonly at amphibolite facies and the Marboo Formation is hornfelsed along the contacts. Griffin et al. (1993) identified seven steeply dipping sills with individual units up to 270 m thick.

The 1864–1852 Ma Paperbark Supersuite intrudes the Marboo Formation and Ruins Dolerite. The supersuite comprises the Whitewater Volcanics, high-level porphyry intrusions and voluminous plutonic rocks (Griffin et al., 1993, 2000a). The Whitewater Volcanics are composed of volcaniclastic rocks interlayered with felsic to intermediate volcanic rocks considered volcanic and subvolcanic equivalents of plutonic rocks in the Paperbark Supersuite (Dow and Gemuts, 1967; Roberts et al., 1968; Gellatly and Halligan, 1971; Griffin et al., 1994; Thorne et al., 1999). Three samples from the Whitewater Volcanics yielded dates of 1854 ± 5, 1854 ± 6 and 1857 ± 4 Ma interpreted as the age of igneous crystallization and suggest contemporaneous felsic volcanism over a strike length >600 km (Griffin et al., 2000a). Plutonic rocks

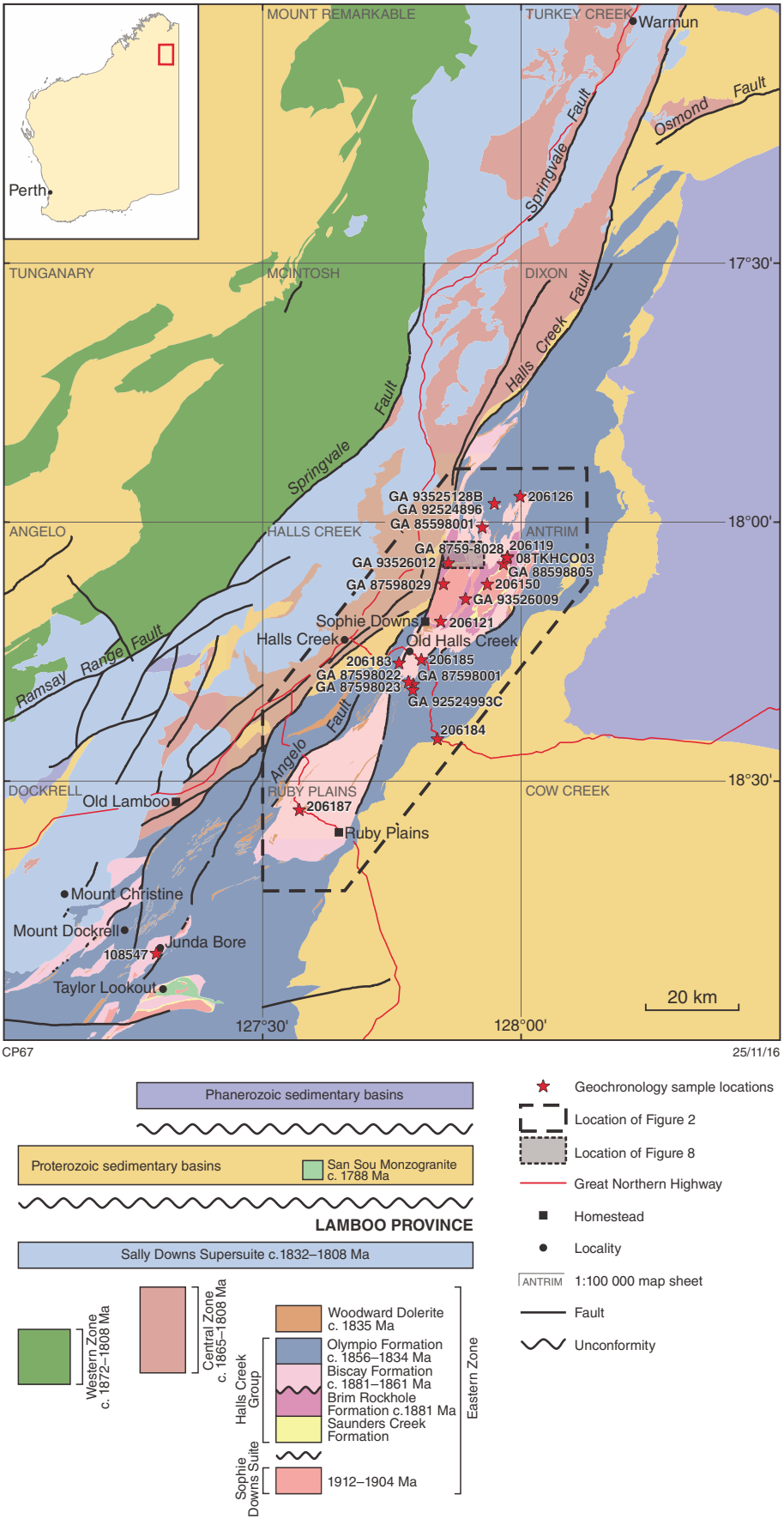

Figure 1. Location and regional geology of the Halls Creek Orogen. The inset box shows the location of the study area and location of Figure 2.

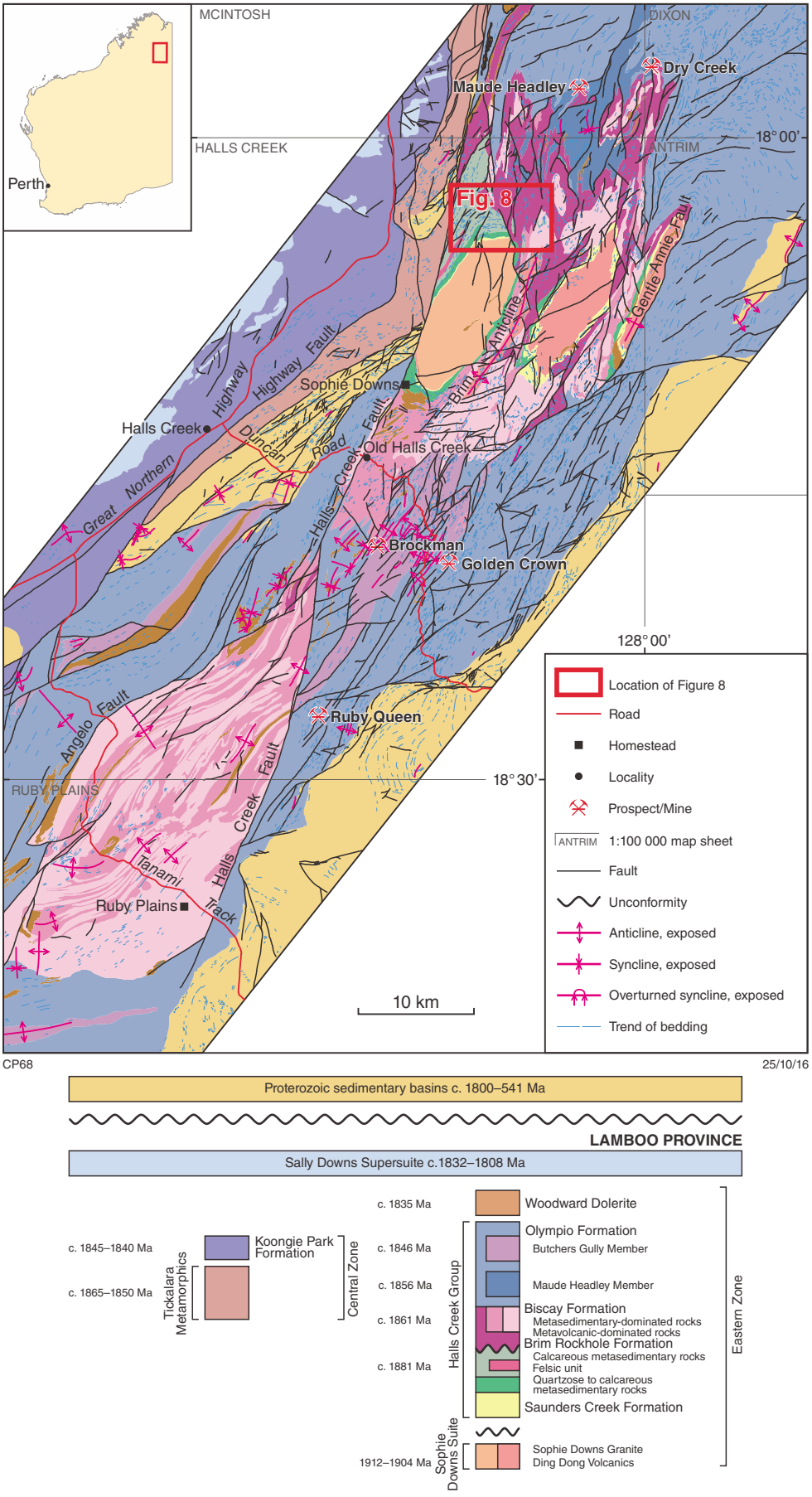

Figure 2. Location and geology of the study area. The inset box shows the location of Figure 8.

include medium- to coarse-grained high-K, I-type granites dominated by monzogranite with granodiorite, syenogranite and lesser tonalite (Griffin et al., 2000a). Mafic plutonic rocks include biotite-bearing norite, gabbronorite, gabbro and diorite (Sheppard, 1997a,b; Griffin et al., 2000a).

The Western Zone and Central Zone experienced two phases of deformation and metamorphism associated with the 1870–1850 Ma Hooper Orogeny (Fig. 3; Bodorkos et al., 1999; Tyler et al., 1999). The Hooper Orogeny marks the collision of an oceanic- or back-arc, represented by rocks of the Central Zone, with rocks of the Western Zone deposited on the inferred passive margin of the Kimberley Craton. In the Western Zone, the Marboo Formation and Ruins Dolerite were overprinted by a layer-parallel foliation and metamorphosed to greenschist facies during D_1/M_1 at 1870–1864 Ma (Tyler et al., 1999; Griffin et al., 2000a). Subsequent deformation of the Marboo Formation resulted in upright to isoclinal folds at all scales (D_2/M_2), accompanied by greenschist to granulite facies metamorphism before and during intrusion of the Paperbark Supersuite. Younger magmatism associated with the Sally Downs Supersuite intruded the entire Lamboo Province at c. 1832–1808 Ma (see Halls Creek Orogeny; Page et al., 2001).

Central Zone (1865–1810 Ma)

The Central Zone crops out between the Ramsay Range and Springvale Faults to the west and the Angelo, Halls Creek and Osmond Faults to the east (Fig. 1). Basement rocks are not exposed. The Tickalara Metamorphics dominate the Central Zone and consist of middle to upper amphibolite to granulite facies mafic volcanic and intrusive rocks with interlayered metasedimentary and volcaniclastic rocks. Turbiditic metasedimentary sequences and the presence of pillow lavas indicate a marine depositional setting (Plumb et al., 1985; Sheppard et al., 1999a; Tyler, 2004). Detrital zircons from metasedimentary samples in the Tickalara Metamorphics provide a maximum depositional age of c. 1865 Ma (Bodorkos et al., 1999). Mafic rocks in the lower parts of the

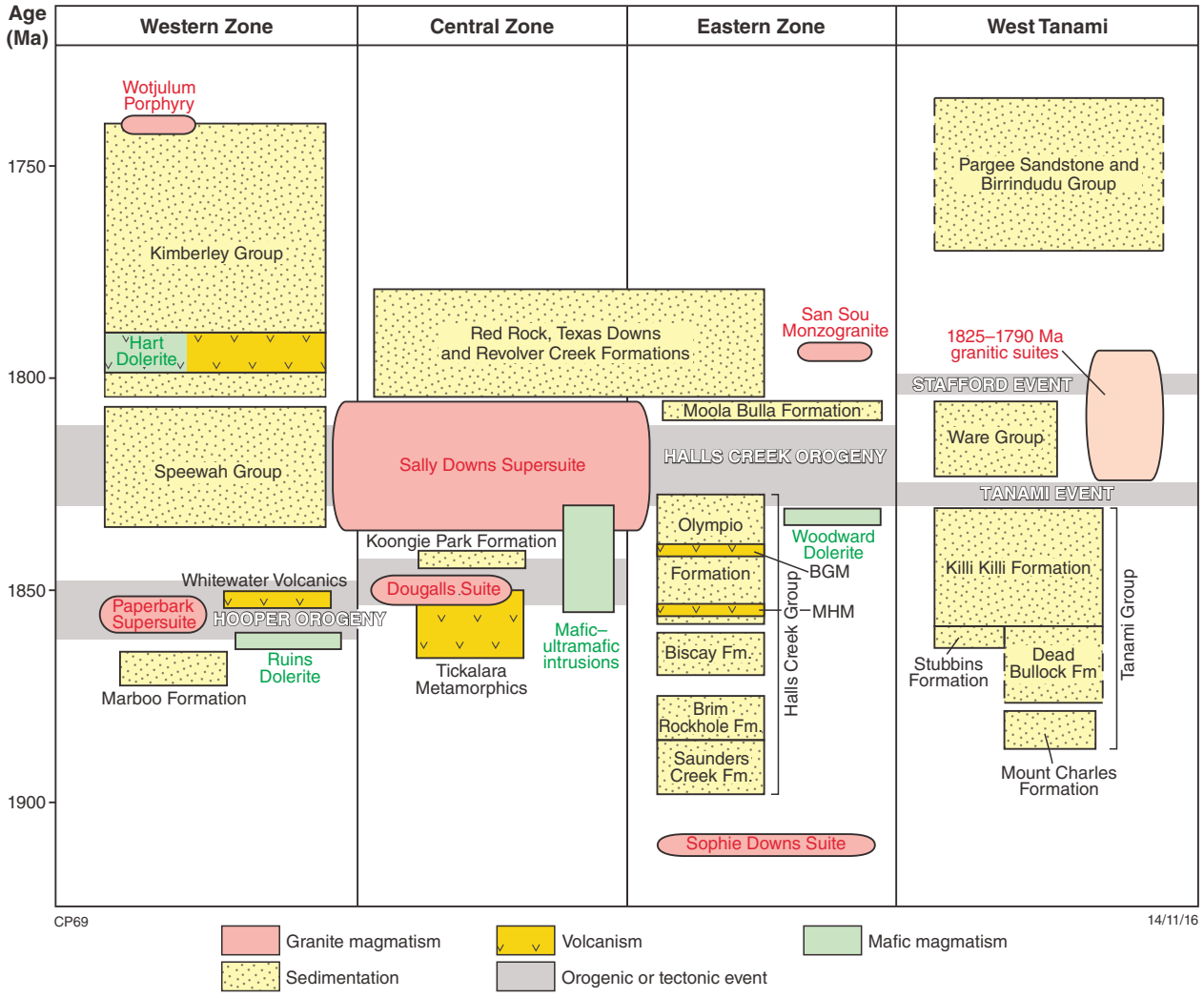

Figure 3. A time–space plot showing the regional stratigraphy and timing of deformation events across the Lamboo Province and Tanami region of Western Australia. MHM = Maude Headley Member, BGM = Butchers Gully Member. Modified from Hollis et al. (2014).

Tickalara Metamorphics are MORB-like in composition (Page et al., 1994; Griffin et al., 1998). The Tickalara Metamorphics were deposited in either an oceanic island-arc/back-arc setting or an ensialic basin margin outboard of the Kimberley Craton during east-directed subduction (Sheppard et al., 1999b; Griffin et al., 2000a).

Deformation events in the Central Zone are similar in style to those described in the Western Zone; however, Central Zone events are younger. D_1/M_1 in the Central Zone occurred at c. 1863–1850 Ma evidenced by layer-parallel foliation and isoclinal folding in the Tickalara Metamorphics (Tyler et al., 1995; Sheppard et al., 1997c). Tight to isoclinal folding and medium to high-temperature, low-pressure metamorphism associated with D_2/M_2 affected the Tickalara Metamorphics at c. 1845 Ma, which suggests that the Western and Central Zones were amalgamated by this time (Page and Hancock, 1988; Tyler et al., 1995; Myers et al., 1996; Sheppard et al., 1997b; Bodorkos et al., 1999; Page et al., 2001).

Back-arc or arc extension at 1845–1840 Ma in the southern extent of the Central Zone led to deposition of marine sedimentary rocks and bimodal volcanic and volcaniclastic rocks of the Koongie Park Formation (Page et al., 1994; Page and Sun, 1994; Orth, 1997). Clasts of metamorphic and granitic rocks within the Koongie Park Formation sedimentary units indicate a continental source. The Koongie Park Formation was metamorphosed to greenschist facies accompanied by tight to isoclinal folding followed by intrusion of the 1827–1808 Ma Kevins Dam Suite of the Sally Downs Supersuite during the 1832–1808 Ma Halls Creek Orogeny.

The Tickalara Metamorphics and the Koongie Park Formation host mafic–ultramafic layered intrusions (Figs 1 and 3). Page and Hoatson (2000) identified three main episodes of mafic–ultramafic intrusion at c. 1855, 1845 and 1830 Ma. Some of these intrusions contain significant Ni, Cu, Cr and PGE mineralization (Hoatson and Blake, 2000).

Halls Creek Orogeny (1832–1808 Ma)

Current models suggest northwest-directed subduction led to collision between the Kimberley Craton (including the Western and Central Zones) and the North Australian Craton and Eastern Zone during the Halls Creek Orogeny (Tyler et al., 1998; Page et al., 2001). The orogeny was accompanied by emplacement of the 1832–1808 Ma Sally Downs Supersuite (Figs 1 and 3; Page et al., 2001). The Sally Downs Supersuite is composed of granitic rocks and gabbros that intrude all zones of the Lamboo Province, but dominantly the Central Zone (Griffin et al., 1998; Tyler et al., 1998). Final accretion of the Kimberley Craton to the North Australian Craton was completed by the end of the Halls Creek Orogeny at c. 1808 Ma evidenced by undeformed Sally Downs Supersuite granites (Myers et al., 1996; Bodorkos et al., 1999).

Yampi Orogeny (1000–800 Ma)

The timing of the Yampi Orogeny is poorly constrained. The event must have taken place after deposition of the c. 1740 Ma Wotjulum Porphyry that intrudes the upper Kimberley Group (Wingate et al., 2011) but before deposition of Neoproterozoic cover sequences. The Yampi Orogeny was probably an intracratonic event, which in the Western Zone produced major northwest-trending ductile faults that dip to the southwest (Tyler and Griffin, 1990). Metamorphism associated with the orogeny is generally low, reaching greenschist facies in the Eastern Zone and amphibolite facies in some Western Zone rocks (Griffin et al., 1993; Blake et al., 1999b). In the Eastern Zone major north–northeast-trending sinistral strike-slip structures such as the Springvale, Halls Creek and Gentle Annie Faults may have been initiated, or reactivated, during the Yampi Orogeny (Blake et al., 1999b). Mylonites in the Halls Creek Group and on the margins of the c. 1800 Ma Speewah and Kimberley Groups are probably associated with the Yampi Orogeny (Tyler and Griffin, 1990; Tyler et al., 1995).

King Leopold Orogeny (c. 560 Ma)

The King Leopold Orogeny of Griffin et al. (1993) is an intracratonic event with deformation dated at c. 560 Ma (Shaw et al., 1992). This deformation is coeval with the Paterson Orogeny east of the Pilbara Craton and the Petermann Orogeny in central Australia (Myers et al., 1996). Large-scale folding and southwest-directed thrusting associated with the King Leopold Orogeny are present on the margins of the Kimberley and Speewah Basins, unconformable or in thrust-contact with the Western Zone (Tyler and Griffin, 1990; Griffin et al., 1993). In the Eastern Zone, the King Leopold Orogeny produced west–northwest-plunging open refolded folds (Tyler and Griffin, 1990; Tyler et al., 1998; Blake et al., 2000).

Geology of the Eastern Zone

This section describes the results of new mapping in the Eastern Zone conducted by GSWA in 2012. Lithofacies are described in ascending order from the basement to basin rocks (Figs 3 and 4). Magnetic susceptibility measurements used in this Report were taken using a hand-held KT–10 magnetic susceptibility meter with values presented in SI units.

The Eastern Zone of the Lamboo Province records sedimentation and magmatism on the western margin of the North Australian Craton from c. 1912 to 1788 Ma. Rocks of the Eastern Zone crop out east of the Angelo, Halls Creek and Osmond Faults and are unconformably overlain by Proterozoic and Phanerozoic rocks (Figs 1 and 2). The oldest exposed rocks of the Eastern Zone comprise greenschist to lower amphibolite facies granitic rocks, bimodal metavolcanic rocks and interbedded metasedimentary rocks of the 1912–1904 Ma Sophie

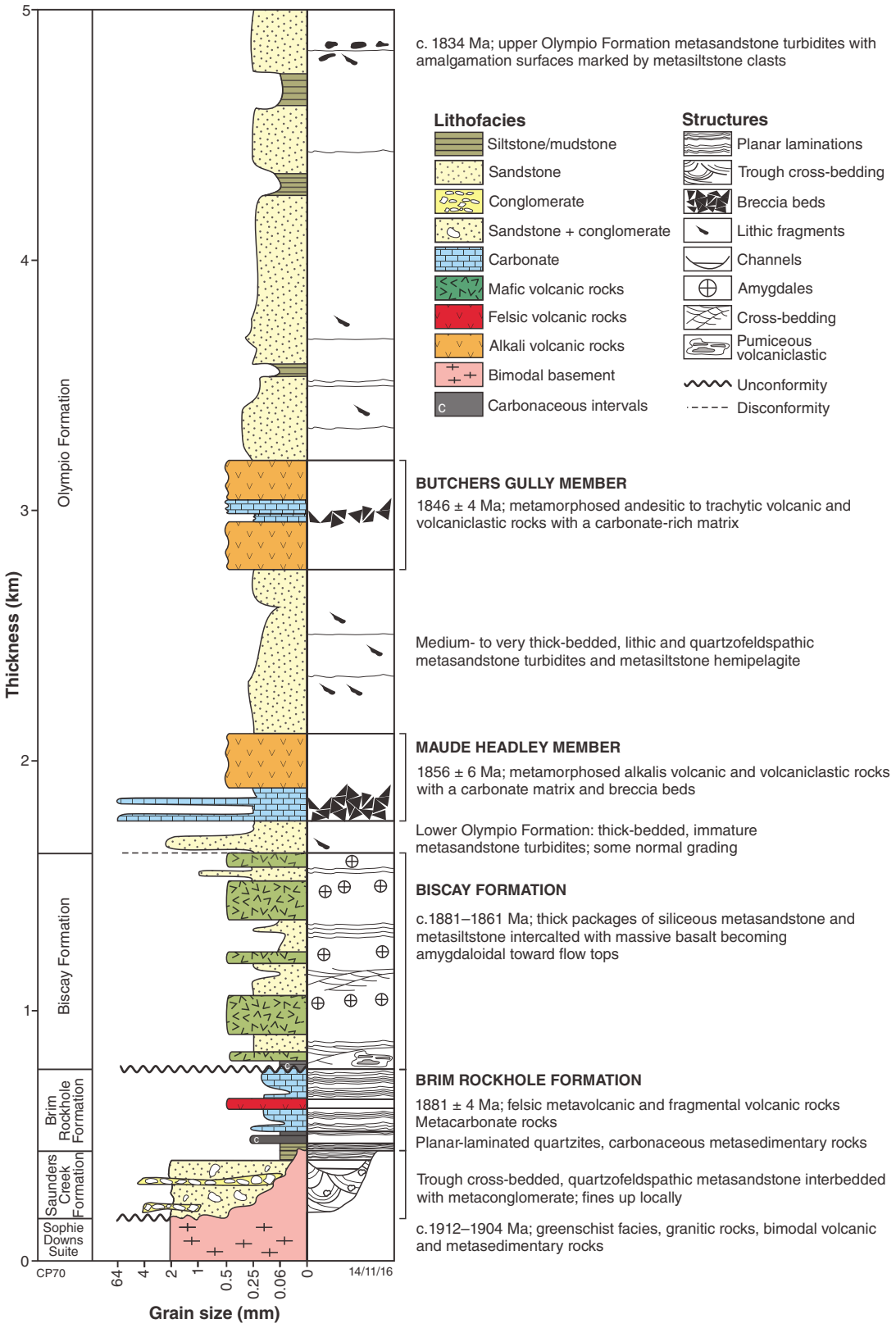

Figure 4. A generalized stratigraphic column through the Eastern Zone

Downs Suite. The Sophie Downs Suite forms restricted inliers in the widespread volcano-sedimentary sequences of the Halls Creek Group. The Halls Creek Group is unconformable on the Sophie Downs Suite and is exposed in a >275 km long, north–northeast-trending belt of greenschist facies metasedimentary and metavolcanic rocks. The group contains four formations that (in ascending order) are the Saunders Creek Formation, Brim Rockhole Formation (new formation), Biscay Formation and Olympio Formation (Figs 2 and 4). A felsic metavolcanic rock in the Brim Rockhole Formation is dated at 1881 ± 4 Ma, interpreted as the age of volcanism (Blake et al., 1999b; this study). Detrital zircons from the top of the exposed Olympio Formation provide a maximum depositional age of 1834 ± 8 Ma (GSWA 206184; this study) but which must have been deposited before intrusion of the Mount Christine Granite at 1808 ± 3 Ma (Page et al., 2001).

D_1/M_1 and D_2/M_2 events in the Eastern Zone, which are associated with the Halls Creek Orogeny, are younger than D_1/M_1 and D_2/M_2 events in the Western and Central Zones, and are equivalent to D_3/M_3 and D_4/M_4 respectively, in the Central Zone (Griffin and Tyler, 1993; Tyler, 2004). The Halls Creek Orogeny affected the entire Lamboo Province, and it must have been ongoing since c. 1834 Ma, which is the maximum depositional age of the upper Olympio Formation in the Eastern Zone (this study). The timing of the Halls Creek Orogeny is also constrained by deformed granites of the Sally Downs Supersuite dated at c. 1832 Ma (Page et al., 2001). The Eastern Zone D_1 deformation produced a strong shear zone contact between the Saunders Creek Formation and basement rocks including high-strain zones on the edge of the Saunders Creek Dome. Well-developed south-striking axial planar foliations are associated with small-scale tight to isoclinal folds, bedding-parallel shear zones and mylonitic rocks (Warren, 1997; Blake et al., 1999b). Biscay Formation metasedimentary rocks show south-trending fold axial traces and foliation traces (Hancock, 1991; Tyler et al., 1998). D_1 structures affect the Halls Creek Group, and are equivalent to D_3 in the Tickalara Metamorphics and Mabel Downs Tonalite in the Central Zone. The Mabel Downs Tonalite is dated at 1832 ± 3 Ma and 1829 ± 4 Ma (Page et al., 2001). D_3 structures do not affect the 1821 ± 3 Ma Sally Downs Tonalite (Page et al., 2001) so this event can be constrained between these two ages. D_2 deformation in the Eastern Zone (1821–1808 Ma) produced northeast- to east-northeasterly trending, open to isoclinal, upright to moderately inclined folds with accompanying axial planar cleavage, crenulation cleavage and bedding-cleavage, or crenulation-hinge lineation (Griffin and Tyler, 1993; Tyler et al., 1995; Blake et al., 1999b). Eastern Zone rocks experienced upper greenschist to lower amphibolite facies metamorphism during their M_1 and M_2 events (Tyler et al., 1995).

The Eastern Zone is significantly disrupted by strike-slip faulting. Placing basement blocks of similar age adjacent to each other (i.e. the Junda Microgranite, Esaw Monzogranite and Ding Dong Downs Volcanics on Dockrell alongside the Ding Dong Downs Volcanics and Sophie Downs Granite on Halls Creek) indicates a displacement up to 100 km along the sinistral Halls Creek Fault system (Fig. 1). This reconstruction also places similar Saunders Creek Formation and Brim Rockhole Formation lithofacies, described below, adjacent to each other. This offset corroborates the findings of Tyler et al. (1995) who estimated a sinistral offset of 90 km by stitching together the Angelo and Osmond Faults.

Sophie Downs Suite

The Sophie Downs Suite consists of four coeval formations: the volcano-sedimentary Ding Dong Downs Volcanics and three intrusive granitic formations — the Sophie Downs Granite, Junda Microgranite and Esaw Monzogranite. The Sophie Downs Granite (Gemuts and Smith, 1968; Dow and Gemuts, 1969) was renamed the Sophie Downs Granophyre Member by Blake et al. (2000) and included with the Ding Dong Downs Volcanics. Blake et al. (2000) justified this change to highlight the shallow intrusive nature of the felsic igneous rocks within the Sophie Downs Dome. However, in the absence of contact relationships, this Report uses the original nomenclature.

The 1912–1904 Ma Ding Dong Downs Volcanics crops out in the Brim Anticline, Saunders Creek Dome and Castle Creek Anticline, 20–30 km northeast of Halls Creek on Halls Creek (Fig. 2), with small areas preserved around Taylor Lookout, shown as undivided Sophie Downs Suite on Dockrell (Fig. 1; Tyler et al., 1998). This study describes accessible outcrops north of the Saunders Creek Dome and the Brim Anticline on Halls Creek (Fig. 2). The Ding Dong Downs Volcanics experienced lower amphibolite facies metamorphism and are locally retrogressed to chlorite–epidote–albite-bearing assemblages. Metabasaltic rocks dominate the Ding Dong Downs Volcanics in the Saunders Creek Dome, with felsic units forming thin dykes through the metabasalt (Fig. 5a). The Saunders Creek Dome also preserves felsic-derived volcaniclastic rocks (Fig. 5b). Metabasalt units can be up to 3 m thick with amygdaloidal tops (Fig. 5c) and contain phenocrysts of amphibole and/or plagioclase up to 1 mm across. The groundmass is altered to epidote–quartz–feldspar–chlorite with scattered opaque minerals. In some samples, the opaque minerals are altered to elongate domains of titanite and hematite. Opaque minerals appear to be ilmenite or hematite but crystal shapes are similar to pyrite and magnetite and may be pseudomorphs. Many of the metabasaltic rocks contain amygdales of epidote–quartz with epidote forming outer rims as well as quartz and quartz–epidote in cores. The cores of some amygdales contain chlorite.

Intercalated metasedimentary rocks consist of green thin-bedded, laminated, fine-grained metasandstone, metasiltstone and metamudstone (Fig. 5d). Quartz and carbonate grains with opaque minerals are present along cleavage traces with abundant euhedral minerals altered to hematite–ilmenite. Carbonate veins, along with sheared carbonate–opaque oxides, cut metasedimentary rocks of the Ding Dong Downs Volcanics. No original minerals are preserved. A metabasaltic-clast breccia with a metasandstone and metasiltstone/metamudstone

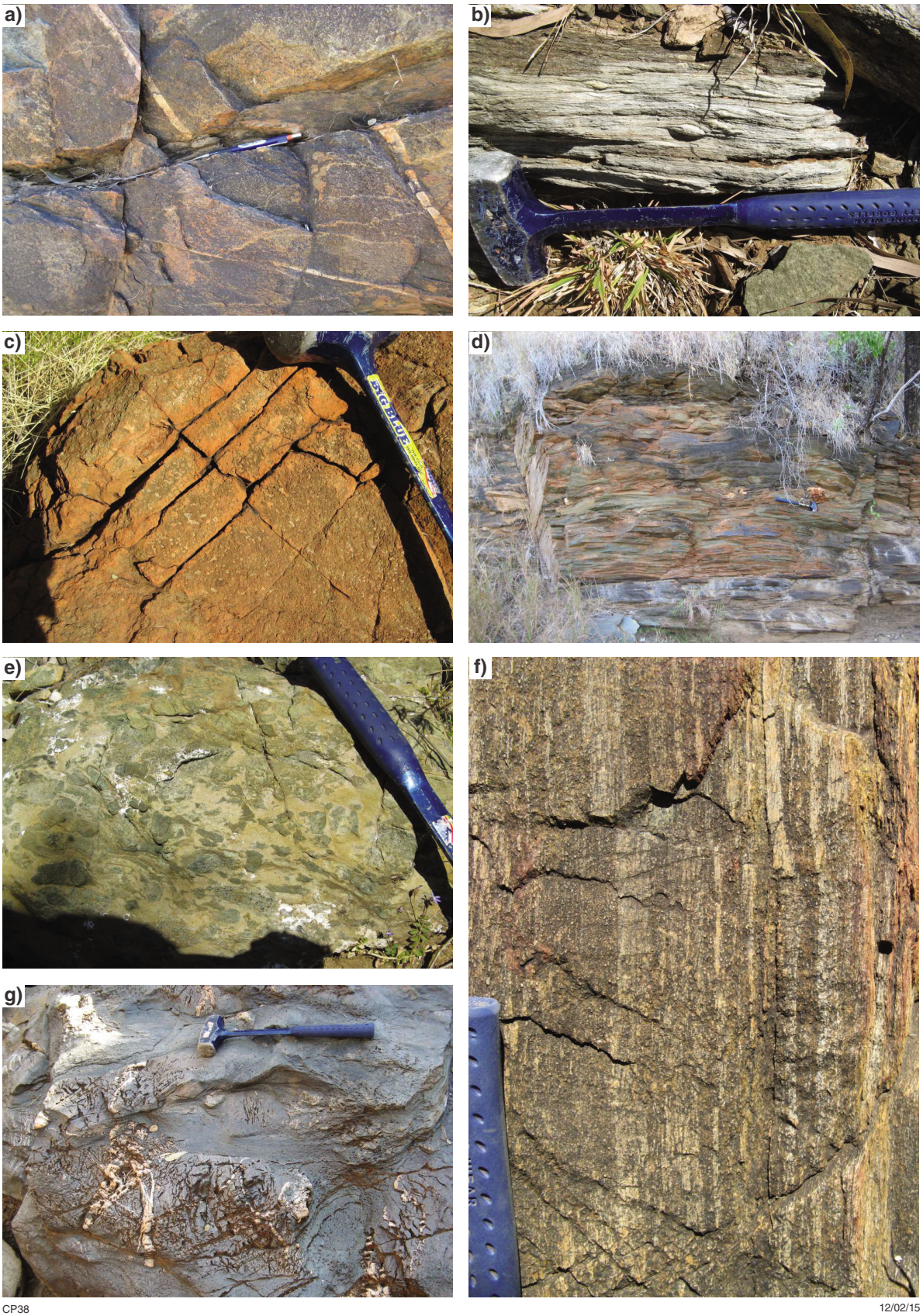

Figure 5. **Field photographs of the Ding Dong Downs Volcanics in the study area: a) light-coloured felsic dyke intruding massive metabasalt; b) mylonitic felsic unit on the western edge of the Saunders Creek Dome; c) irregular quartz amygdales in metabasalt; d) a mafic-derived metasedimentary unit; e) possible peperite formed by the interaction of basalt (now dark-green metabasalt) with wet sediment (now light-green pelitic metasedimentary rock); f) flow-banded metarhyolite; g) veined and boudinaged metabasalt at the western edge of the Saunders Creek Dome**

matrix is present at the margin of one of the metabasalt units (Fig. 5e). Metabasalt and breccia grade into metasedimentary rock. Volcanic clasts disrupt bedding suggesting that this is a peperite. The occurrence of peperite indicates interaction between basalt and wet sediment as a high-level basin intrusion, burrowing of basalt into unconsolidated substrate or loading onto unconsolidated substrate (Schminke, 1967; McPhie et al., 1993; Doyle, 2000).

Intercalated felsic metavolcanic rocks and metasedimentary rocks crop out in the Brim Anticline. Metarhyolite units preserve layering which may represent flow banding (Fig. 5f). The metasedimentary rocks comprise subvertical beds of psammite and phyllite and ridge-forming quartz metasandstone. Felsic metavolcanic rocks include interbedded feldspar-phyric, quartz-phyric and aphyric units. Aphyric felsic metavolcanic rocks comprise lensoidal domains of quartz and white mica with minor biotite. Quartz-phyric felsic metavolcanic rocks contain euhedral quartz phenocrysts up to 0.7 mm across, in a groundmass entirely altered to fine-grained quartz and white mica, locally with epidote, chlorite and opaque minerals. Feldspar-phyric rocks are coarser and contain glomerocrysts of quartz–feldspar where feldspar has been carbonate altered. Granophyric quartz and feldspar occur in coarser grained crystal aggregates and in the groundmass. Veins of epidote and opaques are scattered along mica-rich domains. Foliation, veining and shear zones are well developed. Along the western edge of the Saunders Creek Dome is a north-northeasterly trending 300–400 m wide, high-strain zone with intervals of metabasalt boundins cut by quartz veins and mylonite (Fig. 5g). Epidote is ubiquitous.

The Sophie Downs Granite in the Sophie Downs Dome (Fig. 2) is a leucocratic monzogranite dated at 1912 ± 3 Ma (GA 87598029; Blake et al., 1999b; this study). The granite contains screens and rafts of country rock. The undated Esaw Monzogranite in the core of the Taylor Lookout Anticline on Dockrell (labelled as Sophie Downs Suite on Figure 1) comprises leucocratic biotite–muscovite monzogranite and garnet–muscovite monzogranite (Tyler et al., 1998). The Junda Microgranite crops out in numerous structural domes on Dockrell, and is composed of foliated, leucocratic microgranite dated at 1911 ± 5 Ma (GSWA 108547; this study).

Halls Creek Group

Saunders Creek Formation

Deposition of the Saunders Creek Formation took place in a c. 23 Ma window between c. 1904 Ma, the age of the youngest rocks in the basement, and c. 1881 Ma, the eruption age of a felsic volcanic in the overlying Brim Rockhole Formation. The Saunders Creek Formation crops out as thin veneers, up to 200 m thick, unconformable on basement structural domes (Figs 1 and 2). The formation is entirely siliciclastic and consists dominantly of coarse-grained metasandstone and conglomeratic lithofacies associations.

Poorly sorted quartzofeldspathic metasandstone and quartzite

This lithofacies volumetrically dominates the Saunders Creek Formation. It consists of medium- to very thick-bedded, poorly sorted, fine- to very coarse-grained quartzofeldspathic metasandstone varying from subarkose to arkose and quartz arenite compositions. Trough cross-bedding is abundant (Fig. 6a) with lesser tabular cross-bedding, overturned cross-bedding and planar parallel laminations. Laminations comprise very dark or black, aluminous metasiltstone or metamudstone with abundant heavy minerals like magnetite and rutile, and have high magnetic susceptibilities (50–308 $x10^{-3}$ SI). Floating quartz pebbles are common. Stacked channel bodies 3–9 m wide and up to 3 m deep are locally present. These channel structures generally have a massive fill or are locally normally graded. Intense silicification has subdued or removed many sedimentary structures resulting in massive beds of quartz-dominated metasandstone and quartzite with pseudomorphs of hematite and quartz after feldspar.

Matrix-supported quartz-pebble metaconglomerate

Interbedded with cross-bedded quartzofeldspathic metasandstone, this lithofacies forms thin- to medium-bedded, poorly sorted, matrix-supported, monomictic quartz-granule and quartz-pebble metaconglomerate (Fig. 6b). Metaconglomerates scour into underlying metasandstone beds forming discontinuous beds, lenses and lags. Quartz granules and pebbles are subrounded to well rounded. One pebble clast is a red, massive metasiltstone and is the only example of this clast type. The matrix is composed of fine- or medium-grained subarkose to quartz arenite with cross-laminations of dark grey, aluminous metasiltstone and metamudstone. Laminations within the matrix have moderate magnetic susceptibility values (42–90 $x10^{-3}$ SI) due to magnetite.

Thin-bedded heterolithic lithofacies

This lithofacies consists of a heterolithic package of flaggy, thin-bedded metasandstone beds 1–2 cm thick and interbedded flaggy metasiltstone beds 1–3 cm thick. Metasandstone beds are massive, very fine-grained, quartz-rich subarkose with subordinate muscovite that is probably metamorphic in origin. Interbedded metasiltstone beds are massive. The lithofacies has a planar geometry.

Metasiltstone-dominated lithofacies

Metasiltstone-dominated lithofacies are restricted to the top of the Saunders Creek Formation suggesting that the formation, at least locally, fines upward. This lithofacies is present on the western flank of the Saunders Creek Dome where it consists of thick packages of thin- to medium-bedded, planar parallel-laminated or cross-laminated, siliceous metasiltstone and sandy metasiltstone. Metasiltstone beds are commonly strongly cleaved and have moderate magnetic susceptibilities (23–30 $x10^{-3}$ SI) due to heavy minerals such as magnetite.

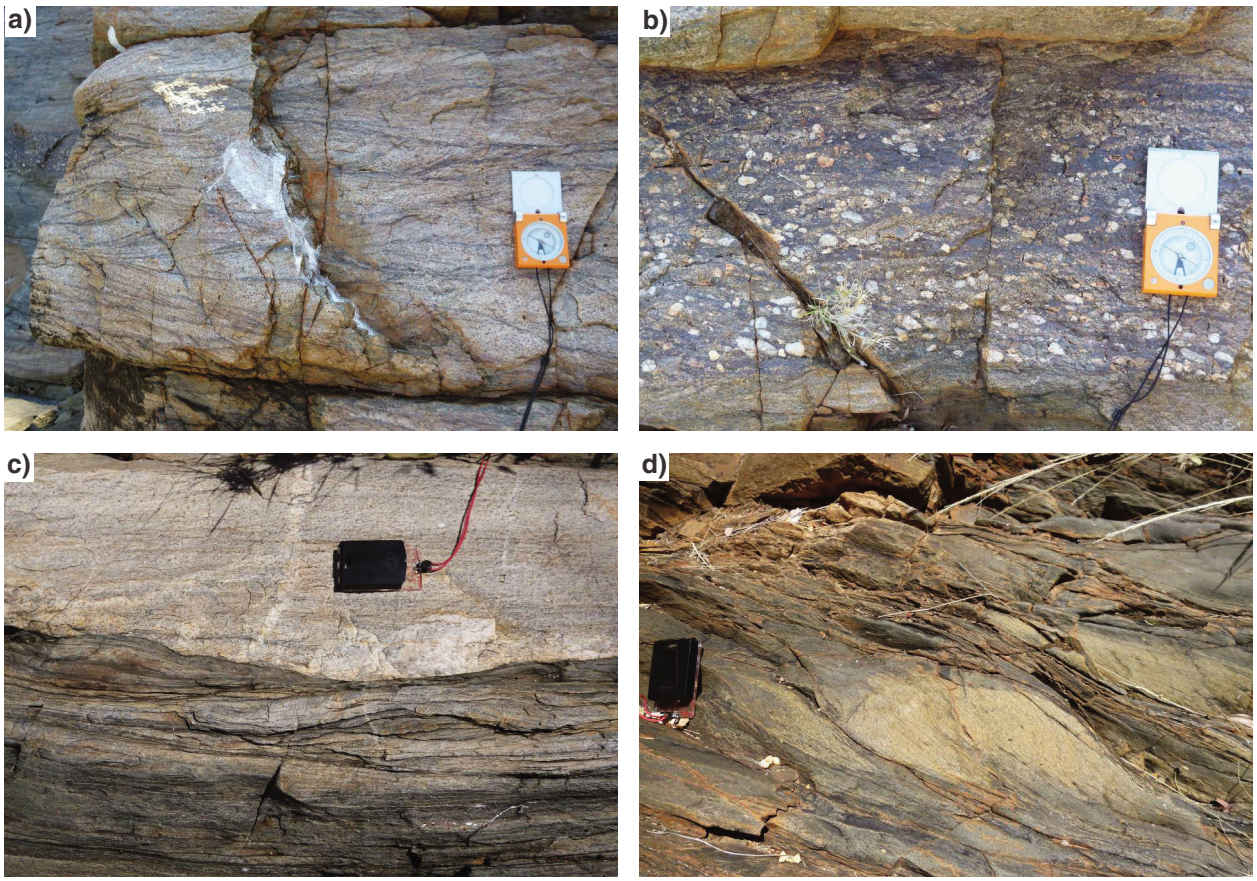

Figure 6. Field photographs of the Saunders Creek Formation in the study area: a) trough cross-bedded feldspathic metasandstone with heavy mineral-rich cross-laminations; b) matrix-supported, quartz-pebble conglomeratic with a heavy mineral-rich metasandstone matrix; c) medium- to coarse-grained metasandstone eroded into laminated metasiltstone; d) deformed metasandstone drawn into cleavage within the metasiltstone-dominated lithofacies. Images a) and b) are interbedded north of the Saunders Creek Dome; c) and d) are observed on the western flank of Saunders Creek Dome. All photographs are taken from above.

Interbedded metasandstone lenses are up to 30 cm thick, massive or planar parallel-laminated, medium- to coarse-grained subarkose to quartz arenite. Contacts between metasandstone and metasiltstone beds are erosive (Fig. 6c). Overturned cross-bedding is observed in some metasandstone interbeds. Metasandstone beds are commonly boudinaged (Fig. 6d). The top of this lithofacies in the Saunders Creek Dome area is gradational into the overlying lower Brim Rockhole Formation.

Brim Rockhole Formation (new formation)

Based on significant differences in sedimentology and SHRIMP U–Pb zircon geochronology, this Report divides the Biscay Formation into two formations. The former lower Biscay Formation that is characterized by carbonaceous and calcareous lithofacies with an intercalated felsic metavolcanic rock dated at 1881 ± 4 Ma, interpreted as the age of volcanism (GA 93526012; Blake et al., 1999b), is here redefined as the Brim Rockhole Formation. The former upper Biscay Formation is redefined as the Biscay Formation. Mafic volcanism was continuous through deposition of the Brim Rockhole Formation and Biscay Formation. In this Report, we describe the metavolcanic units in these formations separately, but discuss these units as part of the same long-lived magmatic event from c. 1881 to 1861 Ma (see Discussion).

The Brim Rockhole Formation crops out on the flanks of the Sophie Downs and Saunders Creek Domes, on the western limb of the north-northeasterly trending Castle Creek Anticline and flanks basement exposures in the Taylor Lookout area (Figs 1 and 2). The formation consists of upper greenschist to lower amphibolite facies thin- to medium-bedded, fine-grained quartzite, grading into locally carbonaceous (graphitic) metasandstone and schist and overlain by metasedimentary carbonate rocks interbedded with subordinate felsic and mafic, metavolcanic rocks. The Brim Rockhole Formation is commonly conformable and locally gradational on the Saunders Creek Formation, but is unconformable on the Sophie Downs Granite on the eastern side of the Sophie Downs Dome (Fig. 2). The formation is up to 200 m thick.

In ascending stratigraphic order, the lithofacies of the Brim Rockhole Formation are described below, based on traverses from the Sophie Downs Dome.

Laminated quartzites and quartz-rich metasandstone

The Brim Rockhole Formation is locally unconformable on the Sophie Downs Granite around the Sophie Downs Dome. On the flanks of the Sophie Downs Dome, the base of the Brim Rockhole Formation consists of white or light grey, thin-bedded, moderately well-sorted, very fine-grained or fine-grained quartz arenite and quartzite. Planar-parallel and wavy laminations ≤1 mm thick are common (Fig. 7a). Planar laminations are 2–10 mm apart or form packages 1 cm thick metasiltstone and metamudstone laminations comprise muscovite and iron oxides including magnetite with low to moderate magnetic susceptibilities (11–12 $x10^{-4}$ SI). On the southeast flank of the Saunders Creek Dome, the Brim Rockhole Formation is gradational on the Saunders Creek Formation where a thick package of very fine-grained, quartz-rich and locally garnetiferous, friable, and foliated metasandstone grades from the metasiltstone-dominated lithofacies at the top of the Saunders Creek Formation.

Carbonaceous metasedimentary rocks

Conformable on laminated quartzites are dark-grey, thin- or medium-bedded, planar-parallel and wavy laminated, very fine-grained or fine-grained sublitharkose (Fig. 7b). This lithofacies is iron rich, carbonaceous and micaceous. Grains of K-feldspar and black lithic clasts of metasiltstone are 1–2 mm across. Lenses up to 15 cm across are common and composed of angular quartz clasts <1 mm wide. The magnetic susceptibility of the lithofacies increases up section from 30 $x10^{-3}$ to 69 $x10^{-3}$ SI over a distance of 10 m due to an increase in fine-grained magnetite with a concomitant increase in graphite and rutile. The increase in carbon up section culminates in a 1 m thick package of very thin-bedded and thin-bedded mica–graphite–quartz schist (Fig. 7c). The schist contains <1 mm wide grains of quartz and minor lithic fragments that define laminations or lenses 2 cm wide and 7 mm thick. On the western limb of the Castle Creek Anticline, the Brim Rockhole Formation similarly consists of carbonaceous metasiltstone and metasandstone (Blake et al., 2000).

Calcareous and dolomitic metasedimentary rocks

Calcareous and dolomitic metasedimentary rocks crop out north and northeast of the Sophie Downs Dome, with minor occurrences west of the Brim Anticline (Fig. 2). The rocks include greenschist facies, variably calcareous and dolomitic metasandstone and metasiltstone, calc-silicate schists, carbonate schists, limestone and marble. The package can be up to 150 m thick, although the exact thickness is difficult to ascertain due to complex folding. Regolith cover commonly obscures the contact between carbonaceous units and calcareous metasedimentary rocks, but both units crop out adjacent to each other indicating an abrupt lithological change. It is possible that the two are separated by a low-angle unconformity or disconformity. Metasedimentary carbonate rocks north of the Sophie Downs Dome comprise thick packages of very thin- to medium-bedded, planar and wavy laminated carbonate schist deformed into tight folds (Fig. 7d). Locally, grey marble is present (Fig. 7e). Carbonate schist and marble are deformed into isoclinal northeast-plunging F_2 (D_2) folds.

Outcrops 2.5 km northeast of the Sophie Downs Dome consist of a heterolithic package of medium-grained calcareous metasandstone, metalimestone and carbonate schist interbedded with quartz arenite (Fig. 7f). These lithofacies are preserved in a north-plunging antiform–synform pair with centimetre-scale folding. Calcareous metasandstone beds are thin bedded to thick bedded, moderately sorted and very fine grained or fine grained. Metasandstone beds have a microcrystalline, calcareous matrix and weakly calcareous metasiltstone laminations. Carbonate schists are very fine grained. In some outcrops, schists contain intraclasts of massive or planar-parallel laminated calcareous metasiltstone, which are probably boudinaged thin-bedded calcareous metasandstone layers. These schistose rocks preserve remnants of an interbedded succession of metalimestone, calcareous metasandstone and metasiltstone/metamudstone. Lesser quartz-dominated metasandstone beds result from increased clastic input into the carbonate depocentre. Siliciclastic beds are discontinuous and form lenses 10–100 cm thick of well-sorted, fine-grained quartz arenite. Some of these quartz-dominated metasandstone beds are boudinaged. Lenses of calcareous metasedimentary rocks are recorded from numerous locations in the overlying Biscay Formation (Warren, 1997) but do not reach the outcrop extent of those described above and are probably carbonate-altered siliciclastic rocks.

Metamafic and metafelsic volcanic and volcaniclastic rocks

Brim Rockhole Formation metasedimentary rocks are intercalated with bimodal metavolcanic rocks. Metamafic volcanic rocks are massive to amygdaloidal metabasalt and are well exposed on the eastern limb of the Brim Anticline. A 150–260 m thick unit of metamorphosed fragmental felsic volcanic and volcaniclastic rock is interbedded with calcareous metasedimentary rocks on the western side of the Sophie Downs Dome (Fig. 2). Lithologies in this unit include metarhyolite, felsic volcaniclastic schist, tuff and cherty tuff, interbedded quartz–mica schist as well as minor metabasalt and mafic metasedimentary rocks. Felsic volcanic and volcaniclastic units contain lesser beds of the calcareous metasedimentary rocks described above. A felsic metavolcanic rock is dated at 1881 ± 4 Ma, interpreted as the age of volcanism (GA 93526012; Blake et al., 1999b; this study). This date also places an age on the concomitant sedimentation in the Brim Rockhole Formation.

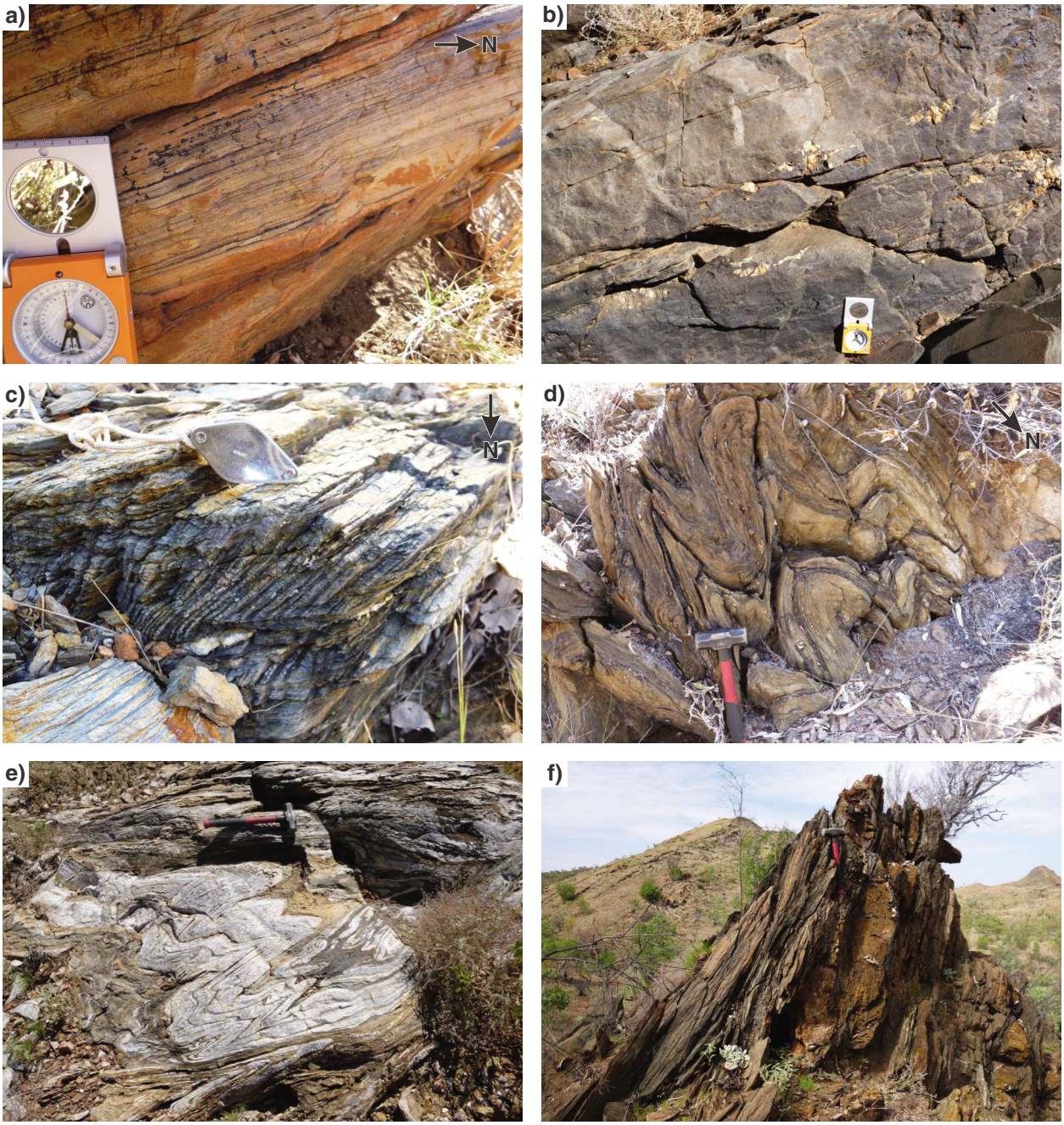

Figure 7. **Field photographs from the Brim Rockhole Formation in the study area: a) laminated quartzite lithofacies at the base of the Formation on the eastern flank of Sophie Downs Dome; b) carbonaceous and micaceous metasedimentary unit on the eastern flank of Sophie Downs Dome, photographed from above; c) graphite–mica–quartz schist east of the Sophie Downs Dome; d) tightly folded calcareous schist north of Sophie Downs Dome; e) tightly folded marble (white to light grey) and very fine-grained calcareous metasedimentary rock (dark grey), north of Sophie Downs Dome, photographed from above; f) schistose heterolithic calcareous metasedimentary lithofacies consisting of calcareous metasandstone (dark brown/grey) and calcareous metaclaystone (light brown), approximately 2.5 km northeast of Sophie Downs Dome. Note calcite veins in the metaclaystone beds.**

Biscay Formation (redefined)

The Biscay Formation, as redefined in this Report, consists of upper greenschist to lower amphibolite facies mafic metavolcanic rocks and fine-grained, volcanic-derived siliciclastic metasedimentary units that lie stratigraphically above the Brim Rockhole Formation. The Biscay Formation is either unconformable or in fault contact with the Brim Rockhole Formation. About 2 km north of the Sophie Downs Dome, the contact between the Brim Rockhole Formation and the Biscay Formation is marked by a low-angle unconformity (Fig. 8). Carbonate schist and metamorphosed limestone (locally boudinaged) are interbedded and in unconformable contact with an overlying package of pelitic schist in the Biscay Formation (Fig. 8). This surface probably represents a depositional hiatus associated with basin subsidence. About 3 km northeast of the Sophie Downs Dome the contact is similarly abrupt with schistose carbonate and quartz-rich metasandstone of the Brim Rockhole Formation underlying laminated metasiltstone and garnetiferous and micaceous metasandstone of the Biscay Formation. The contact is not exposed but the lithological change occurs in <2 m stratigraphic thickness; it may be disconformable here and elsewhere. The formation is deformed into northeast-trending folds, many of which are doubly plunging. Due to extensive deformation and fault repetition, the true thickness of the Biscay Formation is difficult to quantify but may be >700 m thick. This deformation introduces difficulty in establishing a stratigraphy due to the lack of a complete section.

Metasedimentary lithofacies consist of fine-grained mafic schist, lithic to quartz-rich metasandstone, and less common psammitic schist that probably originates from sublitharenite or litharenite protoliths. Thin- and medium-bedded metasiltstone and metamudstone, pelitic schist, phyllite and rare slate result from greenschist facies metamorphism of quartz-rich and micaceous siltstone and mudstone protoliths. Subordinate lithologies include felsic schist, carbonaceous rocks and metachert. Figures 2, 8 and 15 divide the Biscay Formation into metabasalt-dominated and metasedimentary-dominated lithofacies following Blake et al. (1999a,b). Lithological descriptions of metabasalt and metasedimentary rocks are separate in this Report. In reality, however, they are interlayered in varying proportions.

Metasedimentary and metamorphosed volcaniclastic rocks

Metasedimentary rocks comprise thin- to thick-bedded, very fine- and fine-grained, quartz-rich and mafic-derived, biotite-bearing metasandstone and metasiltstone (Fig. 9a). They are commonly well sorted, massive and siliceous with faint planar-parallel laminations and cross-bedding composed of fine-grained aluminous and iron-rich material. Metasiltstone clasts <1 mm wide are common lithic fragments. Ferromagnesian minerals such as pyroxene, biotite and magnetite are also present variably altered to actinolite and chlorite.

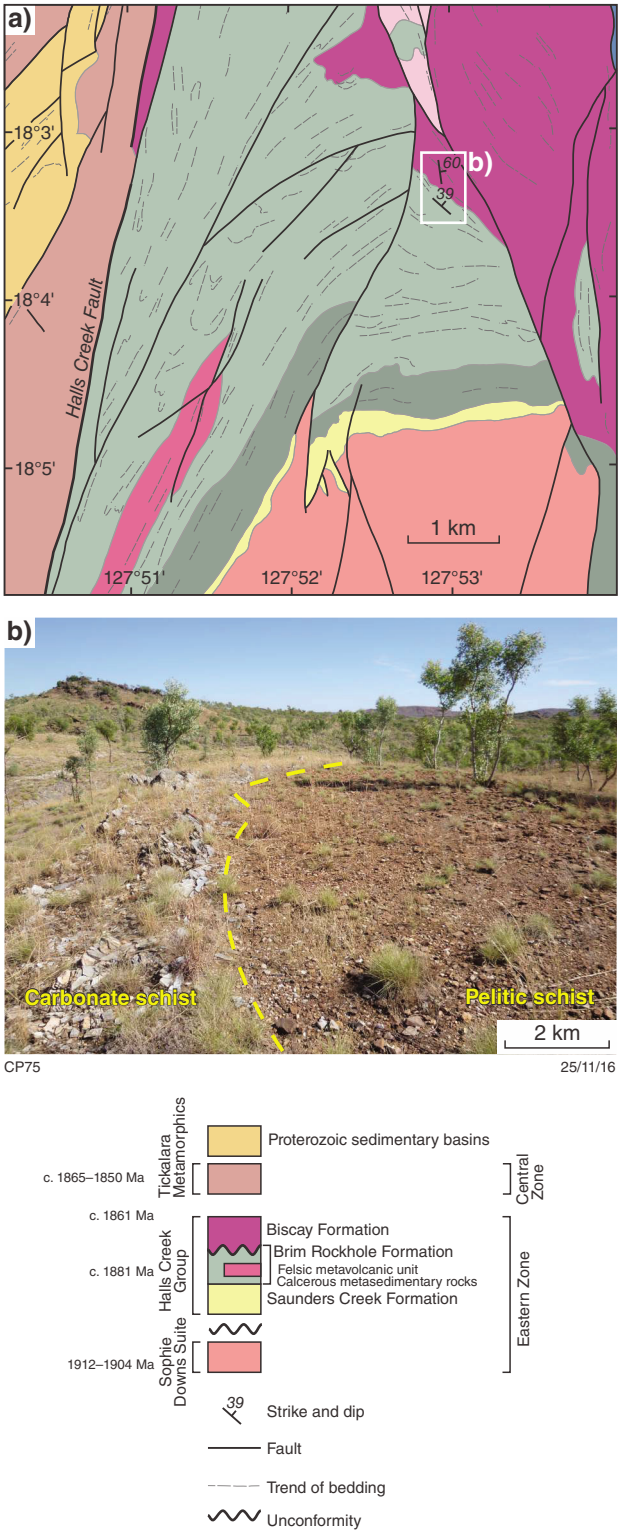

Figure 8. Location and field photograph of the low-angle unconformable surface between Brim Rockhole Formation calcareous metasedimentary units and overlying Biscay Formation pelitic schists. See Figure 2 for location within the study area. The photograph location is outlined in white.

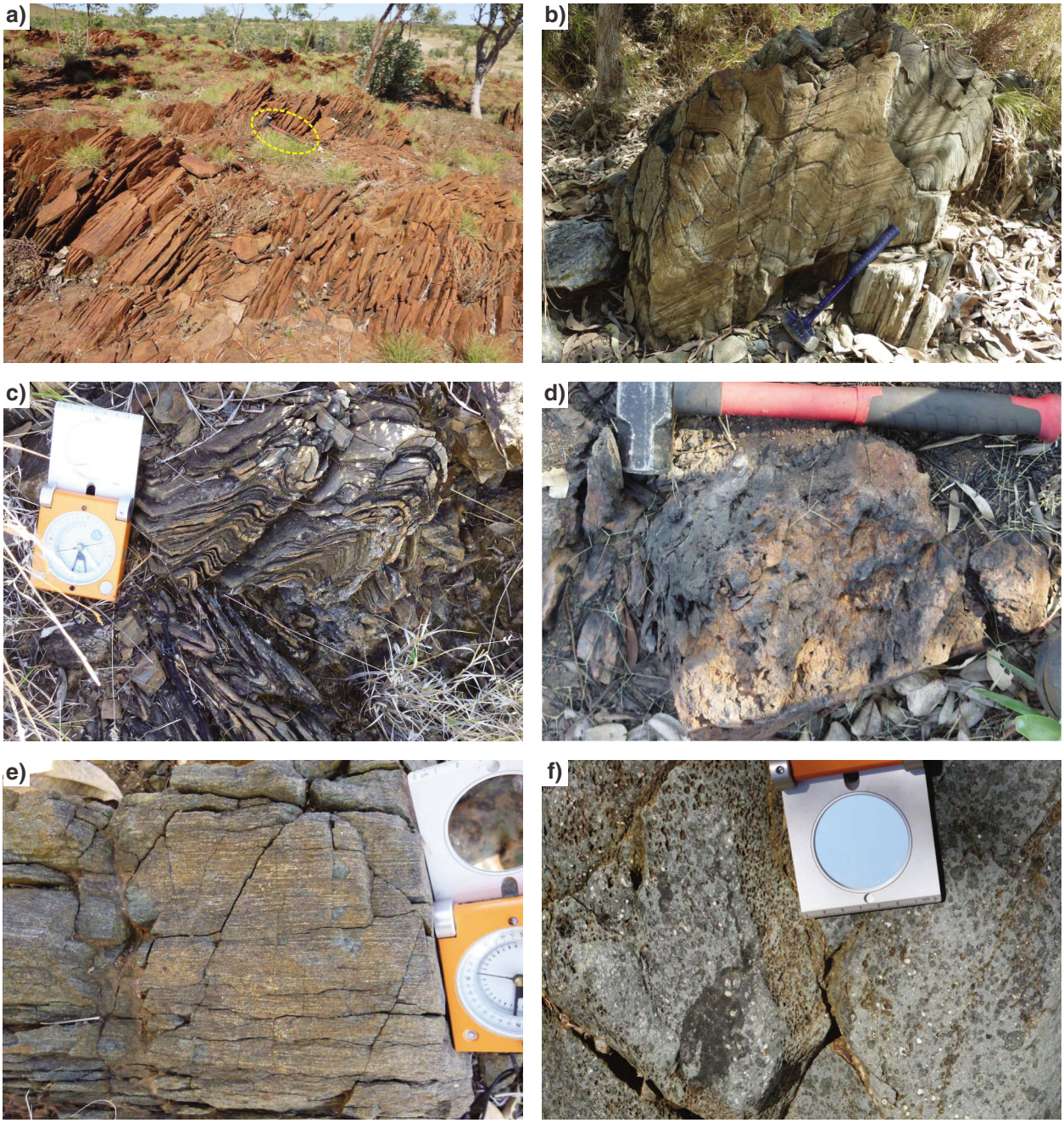

Figure 9. **Field photographs from the Biscay Formation in the study area: a) fissile, quartz-rich metasiltstone along the Tanami Road, hammer highlighted for scale; b) west-verging, south-plunging D_2 folds in metasiltstone; c) F_2 folds in interbedded, very thin-bedded metasandstone and metasiltstone; d) scoriaceous carbon-rich volcaniclastic rock, photographed from above; e) possible flow alignment in metabasalt picked out by feldspar, photographed from above; f) amygdaloidal metabasalt on flow tops, some quartz-filled amygdales, photographed from above**

Rare uppermost Biscay Formation metasandstone beds comprise medium-bedded, normally graded, fine- to medium-grained, quartz metasandstone with fine-grained planar laminations and very coarse-grained lenses of quartz arenite. Interbedded metasiltstone-dominated lithofacies in the upper Biscay Formation are thin or medium bedded, planar-parallel laminated and strongly cleaved. Many Biscay Formation rocks were deformed during D_2, resulting in tight to isoclinal folding (Fig. 9b,c).

Metavolcaniclastic rocks are interbedded with both metavolcanic rocks and metasedimentary units. Warren (1997) noted that the metasedimentary units toward the top of the Biscay Formation include mafic tuff and metasandstone units deposited on top of metabasalt. These metasedimentary units are commonly <1 m thick. Volcaniclastic units near the base of the Biscay Formation are black, very well sorted, friable and carbonaceous with areas that appear scoriaceous (Fig. 9d). Less than 200 m along strike from these carbonaceous volcaniclastic rocks is an interbedded package of phyllitic and pelitic schist. The phyllitic material is very pale, leached and friable. The whole package is muscovite rich with <1 mm quartz grains, which form eyes within the mica foliation. Pseudomorphs of feldspar and possible pyrite are associated with black, graphitic laminations.

Metamafic volcanic rocks

Volcanic units consist of greenschist to lower amphibolite facies metabasalt of variable thickness. The abundance of metabasalt increases toward the top of the Biscay Formation. Thin (<0.5 m thick) units are intercalated with mafic-derived metasandstone and metasiltstone north of Saunders Creek Dome, whereas 250–500 m thick ridges of metabasalt are present near Ruby Plains Homestead. In the old Halls Creek area, metadolerite with interlayered sheared carbonate-altered metadolerite is about 300 m thick. Relationships with the surrounding rocks suggest the metadolerites may represent a series of intrusive units, each 5–10 m thick. Most mafic volcanic samples of the Biscay Formation have been metamorphosed to lower amphibolite facies. Randomly oriented feldspar laths are pseudomorphed by nontwinned feldspar (albite)–carbonate–quartz and locally minor epidote. All ferromagnesian minerals are replaced by amphibole, including green actinolite and yellow to colourless tremolite. Chlorite and chlorite–carbonate with minor epidote also replace ferromagnesian minerals. In most samples, no original igneous textures are preserved. Amphibole defines the foliation with intervening feldspar–quartz–carbonate and opaque oxide minerals. Titanite forms small, poorly defined granular crystals associated with opaque minerals. Opaque minerals are mainly hematite with rare pyrite. Many of these grains are partially altered to hydrated iron oxides. In some outcrops, the orientation of feldspar crystals suggests flow alignment (Fig. 9e). Quartz-filled amygdales are present in the upper portions of metabasalt flows north of the Saunders Creek Dome (Fig. 9f) but are not apparent in units to the south of the study area near Ruby Plains Homestead.

Olympio Formation

The Olympio Formation is a >4000 m thick package of greenschist facies turbiditic metasedimentary rocks interlayered with subaqueous to emergent volcanic and volcaniclastic rocks. In the Dry Creek area on Dixon and the Maude Headley area on McIntosh (Fig. 2), very thick-bedded, immature turbidite metasandstone occurs on top of shallow-marine metabasalt and mafic-derived metasedimentary rocks. These contact relationships indicate that the Olympio Formation is disconformable or locally unconformable on the Biscay Formation. The top of the Biscay Formation is identified either by the uppermost mafic metavolcanic unit (Fig. 10a) or by a chert or siliceous tuff bed overlying the uppermost mafic metavolcanic unit (Warren, 1997). In the Maude Headley area, pebbles of metasedimentary rocks are found above the contact with the Biscay Formation (Warren, 1997), which probably indicates a transgressive surface of erosion. In many other areas, the Biscay Formation – Olympio Formation contact is commonly schistose to mylonitic (Warren, 1997; Blake et al., 2000). The c. 1856 Ma Maude Headley Member, in the lower part of the Olympio Formation, is a sequence of metamorphosed alkali volcanic, volcaniclastic, carbonate and chert rocks conformably overlying turbidite metasandstone. The c. 1846 Ma Butchers Gully Member is a similar sequence of metamorphosed alkali volcanic and volcaniclastic rocks. The c. 10 Ma between the deposition of the Butchers Gully and Maude Headley Members records turbidity current sedimentation in a deep-marine basin (Fig. 4). Another package of turbidite metasandstone and metasiltstone overlies the Butcher Gully Member. All turbidite packages have a planar geometry. There are few reliable paleocurrent data from the Olympio Formation; however, Hancock (1991) describes climbing ripples from which he recorded a paleoflow from the northwest.

Figure 10. (right) Field photographs from the Olympio Formation in the study area: a) contact between the uppermost metabasalt in the Biscay Formation disconformably overlain by thick-bedded quartzofeldspathic turbidite units of the lower Olympio Formation; b) planar turbidite package made of interbedded thick-bedded metasandstone and thin-bedded metasiltstone, Mount Bradley abandoned mine site; c) metasandstone turbidite with an amalgamation surface marked by metasiltstone clasts, Elvire crossing on the Duncan Road; d) very coarse-grained meta-arkose turbidite, southwest of Ruby Plains Homestead, photographed from above; e) strongly cleaved metasiltstone hemipelagite; f) matrix-supported metacarbonate breccia at the base of the Maude Headley Member in the Maude Headley area, photographed from above; g) deformed fine- to medium-grained calcareous metasedimentary rock, Maude Headley Member in the Maude Headley area, photographed from above.

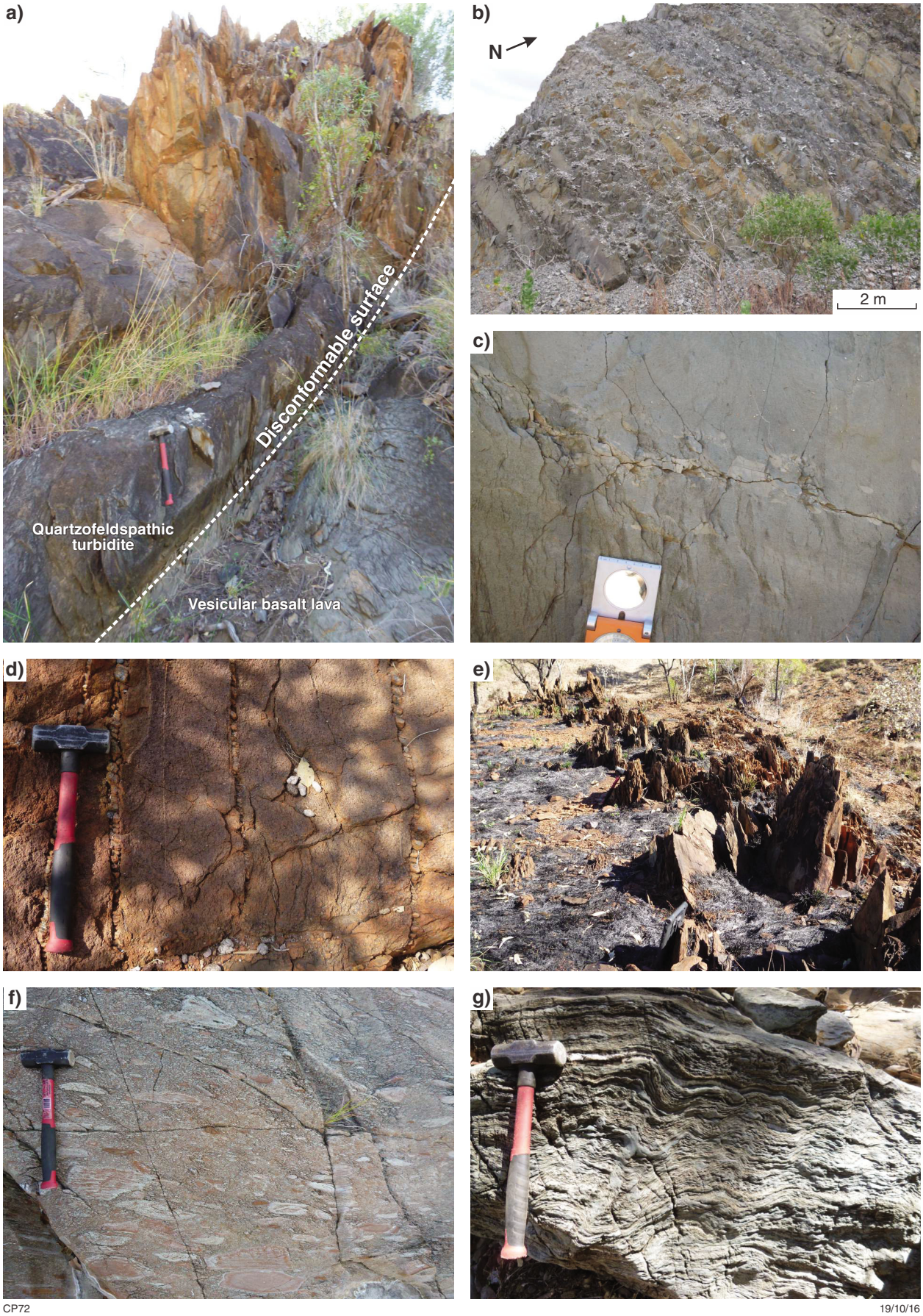
a)
Disconformable surface
Quartzofeldspathic turbidite
Vesicular basalt lava
b)
N
2 m
c)
d)
e)
f)
g)

CP72 19/10/16

Quartzofeldspathic metasandstone

This lithofacies is ubiquitous in the study area. It is composed of thick packages of medium-bedded to very thick-bedded, moderately sorted, very fine-grained to medium-grained arkose, subarkose and feldspathic sublitharenite (Fig. 10b). Feldspar is commonly weathered and altered to limonite and kaolinite. Lithic components include metasiltstone clasts and uncommon quartz sandstone clasts 3–10 mm long. Beds are commonly massive but normal grading from massive, medium-grained beds to planar-laminated, very fine-grained beds occurs at the top of thick metasandstone packages. This lithofacies corresponds to Bouma divisions T_{ABD} (Bouma, 1962). Clasts of planar parallel-laminated or massive siliceous metasiltstone up to 10 cm across mark amalgamation surfaces and erosive contacts between metasandstone beds (Fig. 10c).

Coarse-grained and conglomeratic metasandstone

Conglomeratic and coarse-grained lithofacies are rare and described from a small number of outcrops 12 km southwest of Ruby Plains Homestead on Ruby Plains. Coarser grained turbidite metasandstone units consist of medium- to very thick-bedded, coarse- and very coarse-grained subarkose (Fig. 10d). Normal grading is common. Quartz grains are subangular to subrounded and feldspar grains are angular to subangular. Lags consist of matrix-supported, monomictic, quartz-granule conglomerate. Quartz clasts are subangular to subrounded. The matrix is composed of massive, fine-grained subarkose. These coarse-grained lithofacies correspond to Bouma division T_A (Bouma, 1962).

Metasiltstone and silty metasandstone

Silty metasandstone lithofacies consist of medium- to thick-bedded, fine- to medium-grained, massive or normally graded, silty, quartzofeldspathic metasandstone with 15–30% metasiltstone matrix. Massive beds are common and moderately sorted. Fine- to medium-grained normally graded beds are less common, and medium-grained, quartz-dominated lenses are rare. Silty metasandstones are commonly interbedded with thin- to thick-bedded, massive or cleaved metasiltstone. Contacts are sharp but nonerosional. This lithofacies corresponds to Bouma divisions T_{DEF} (Bouma, 1962). Lithofacies are commonly siliceous, although some outcrops are less siliceous, friable and less competent, having taken up the regional strain. Thick packages of strongly cleaved metasiltstone are common (Fig. 10e).

Maude Headley Member

The Maude Headley Member crops out in a series of north-northeasterly trending outcrops 5 km northeast of the Sophie Downs Dome and the Saunders Creek Dome (Fig. 2). It consists of metamorphosed alkali volcanic and volcaniclastic rocks as well as calcareous metasedimentary rocks. The member occurs 50–100 m stratigraphically above the base of the Olympio Formation. Breccia beds 0.5 – 1.5 m thick identify the base of the Maude Headley Member. Breccia beds are matrix supported, poorly sorted and polymictic (Fig. 10f). Beds are commonly massive but some are normally graded. Breccia clasts are angular, up to 30 cm long, and composed of metacarbonate, metachert, quartz, recrystallized clastic material (some phyllitic), banded and massive aphyric volcanic rock, feldspar-phyric and aphyric volcanic fragments with quartz amygdales as well as vesicular basalt and rhyolite. Breccia matrices are composed of fine-grained, crystalline or schistose metacarbonate or less commonly a metasandstone matrix. Possible volcanic bombs and scoria also occur in breccia beds. Beds of granule-breccia, metasandstone and metasiltstone are intercalated with possible beds of pumice breccia. Breccia beds are overlain by thick-bedded, very fine-grained metacarbonate or calcareous metasandstone with <1 cm thick, highly siliceous discontinuous beds and lenses in a calcareous matrix (Fig. 10g). Thick-bedded and fine-grained, equigranular felsic metavolcanic or fragmentary felsic metavolcanic rocks overlie metasedimentary and volcaniclastic units. Breccia or conglomerate beds are locally interbedded with coherent vesicular felsic and fragmentary metavolcanic rocks.

Butchers Gully Member

The Butchers Gully Member of Griffin and Tyler (1993) consists of metamorphosed andesitic to trachytic volcanic and volcaniclastic rocks with a carbonate-rich matrix. Metachert and ferruginous metachert dominate some beds while metatrachytic lava flows, domes and sills are common in others. The member occurs between packages of thick-bedded turbidite metasandstone and metasiltstone (Fig. 4). The most extensive research on the Butchers Gully Member was carried out on the Brockman prospect, 7 km south of Old Halls Creek (Fig. 2; Buckovic, 1984; Esslemont, 1990; Taylor et al., 1995a,c). At the Brockman Prospect, the Butchers Gully Member is composed of a series of metamorphosed volcanic and volcaniclastic rocks. Taylor et al. (1995a,b) divided the lavas into two compositional and textural types: 1) leucocratic, trachytic and amygdaloidal (amygdales filled with secondary limonite, calcite, biotite, quartz and/or fluorite); and 2) mesocratic, trachytic, pillowed or massive with some scoriaceous tops and interflow breccia beds. Mesocratic and equigranular subvolcanic sills and dykes 1–150 m thick intrude the lavas. Intercalated with the metavolcanic rocks are poorly sorted, matrix-supported volcanic-bomb-breccia beds, some reworked into clast-supported variants. Volcaniclastic rocks show a facies trend from a crystal-bearing zone to a pumiceous zone in more proximal-to-vent facies to volcanic metasandstone beds (Esslemont, 1990; Taylor et al., 1995a,b).

Woodward Dolerite

The Woodward Dolerite forms sill-like intrusive bodies up to 200 m thick. The formation intrudes the Halls Creek Group and its basement but pre-dates deformation and metamorphism associated with the Halls Creek Orogeny (Blake et al., 1999b, 2000). The Woodward Dolerite has been metamorphosed in the upper greenschist to epidote–amphibolite facies (Blake et al., 1999b).

Lithofacies include fine- to coarse-grained metadolerite and metagabbro. Most of the samples collected during this study are of amphibolite grade. Ferromagnesian minerals are pseudomorphed by amphibole(–zoisite) and less commonly by epidote. Carbonate or combinations of albite–quartz–carbonate(–white mica) commonly replace feldspar. Skeletal minerals and granophyric quartz indicate shallow levels of intrusion. Some dolerite sills have chilled margins as well as locally developed ophitic textures (Tyler et al., 1998; Blake et al., 1999b). Opaque minerals are altered to combinations of titanite, hematite, iron oxides/hydroxides and siderite. Minor biotite is present in some samples. Accessory minerals include pyrite and a radioactive brown mineral, possibly baddeleyite.

Geochemistry

The geochemistry section describes the results of new and published whole-rock chemistry from meta-igneous and metasedimentary samples as well as whole-rock Sm–Nd isotope data from mafic rocks in the Eastern Zone. Geochemical analyses are presented in Appendix 1. In the following descriptions of metavolcanic samples, major elements have been recalculated to 100% on a volatile-free basis. All data in Appendix 1 are reported in their original form. Metasedimentary samples were not recalculated and are described and plotted in their original form.

Major and trace-element geochemistry

Sophie Downs Suite

Sixteen samples from the Sophie Downs Suite include nine metamafic samples and seven metafelsic samples from a combination of new data and samples re-analysed by GSWA in 2010 (see Appendix 1 – Tables 1 and 2). On an immobile element plot, most metamafic rocks plot as basaltic andesite (Fig. 11; Winchester and Floyd, 1977). One sample plots as alkaline basalt (GSWA 108573) but is from a metamafic body, which crosscuts the Sophie Downs Granite in the Sophie Downs Dome. Major element plots for Sophie Downs Suite samples show the bimodal geochemistry of rocks in this unit (Fig. 12). Metamafic samples have anomalously high Pb and many show depletions in Sr and Nb and are 4–30 times more enriched in large ion lithophile elements (LILE) compared to Primitive Mantle (PM; Fig. 13a). Metamafic samples are also 20–100 times more enriched in light rare earth elements (LREE) and 10–50 times more enriched in medium to heavy rare earth elements (M–HREE) compared to C1 chondrites (Fig. 13b).

Metafelsic rocks of the Ding Dong Downs Volcanics plot as rhyolite or rhyodacite and one that just plots into the commendite/pantellerite field (GSWA 209744; Fig. 11). On a PM-normalized spider diagram, samples are enriched in most LILE and LREE (50–120 × PM), with a negative

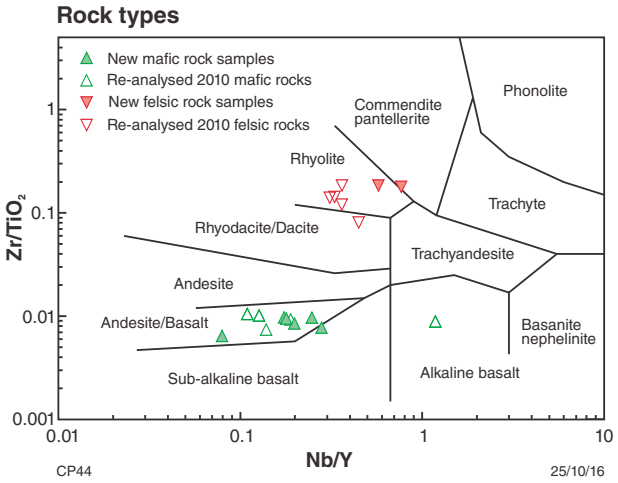

Figure. 11 An immobile element classification diagram after Winchester and Floyd (1977) for samples from the Ding Dong Downs Volcanics. Red symbols represent felsic rocks and green symbols are mafic rocks. New samples (solid fill) were collected during this study. Re-analysed samples (open symbols) are from Sheppard et al. (1997a,b).

anomaly at Nb and Ta and marked depletions of Sr, P and Ti (Fig. 13c). Compared to chondrite, metafelsic samples are 90–110 times more enriched in LREE and 40–70 times more enriched in HREE (Fig. 13b). Metarhyolites display a prominent negative Eu anomaly, Eu/Eu* = 0.3 – 0.6 (Fig. 13b). Metafelsic rocks are metaluminous to peraluminous (Fig. 13d) with geochemistry similar to A-type granites (Fig. 13e).

Saunders Creek Formation

Two metasandstone samples were taken from the Saunders Creek Formation (Appendix 1 – Tables 3 and 4), both from the quartzofeldspathic metasandstone and quartzite lithofacies. Samples are quartz rich (73.31 and 91.24 wt% SiO_2) with low Al_2O_3, CaO, MgO, K_2O and Na_2O due to the lack of clay minerals. Rare earth element (REE) trends normalized to post-Archean Australian shales (PAAS) indicate LREE enrichment with Eu/Eu* values comparable to PAAS (Fig. 14a; Taylor and McLennan, 1995).

Brim Rockhole Formation

Both the Brim Rockhole Formation and Biscay Formation contain intercalated metavolcanic rocks — dominantly basaltic metavolcanic rocks. Basaltic metavolcanic rocks from both formations are petrographically and geochemically similar and may be part of the same magmatic event (see Discussion). In this geochemistry section, metavolcanic rocks from the Brim Rockhole Formation and Biscay Formation are described separately, but are plotted together on Figures 15–17.

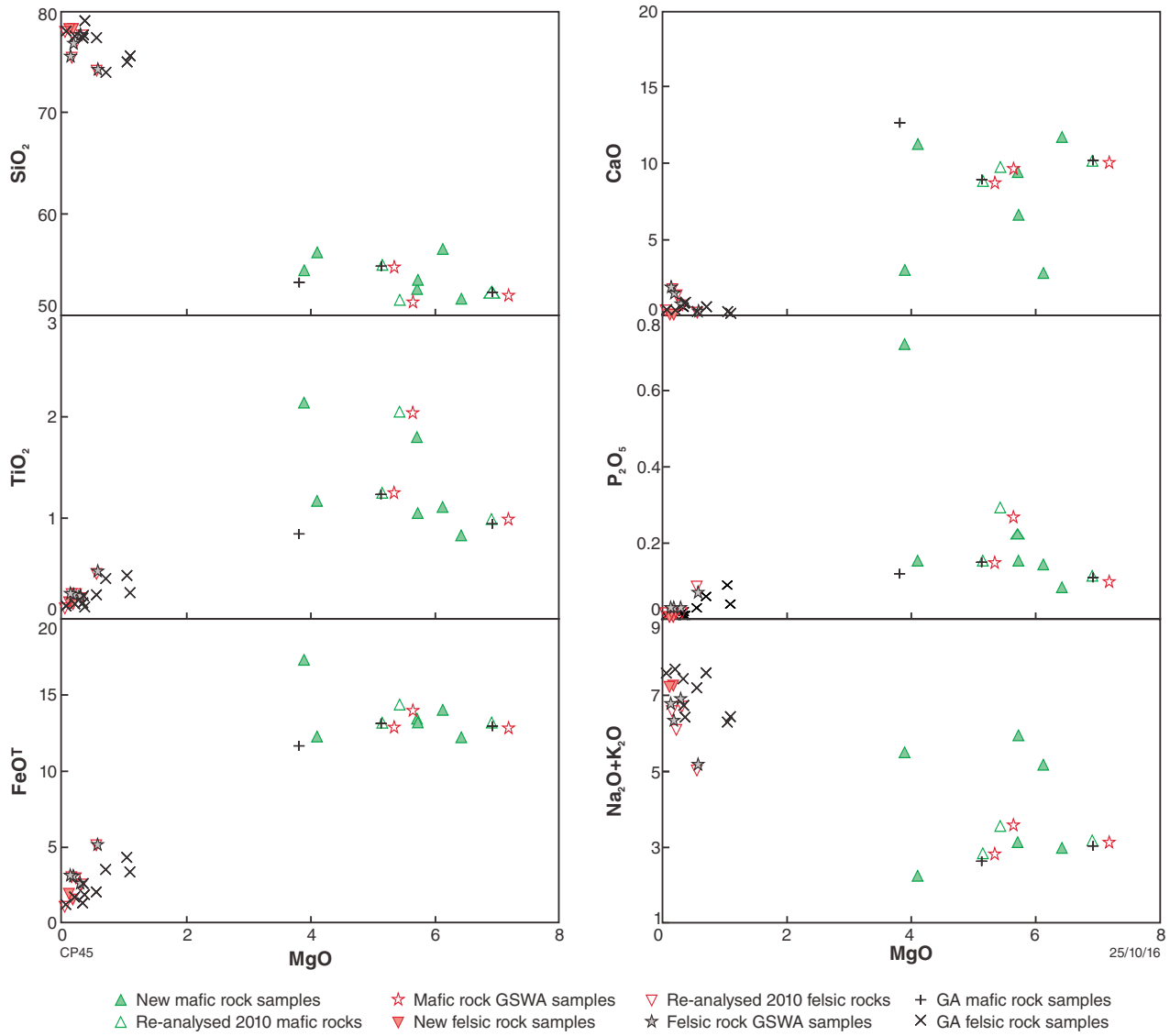

Figure 12. Major elements against MgO for samples from the Ding Dong Downs Volcanics. Mafic rocks are represented by green symbols and felsic rocks by red symbols. Old GSWA analyses are plotted for comparison (Sheppard et al., 1997) along with some felsic rocks from OZCHEM, maintained by Geoscience Australia.

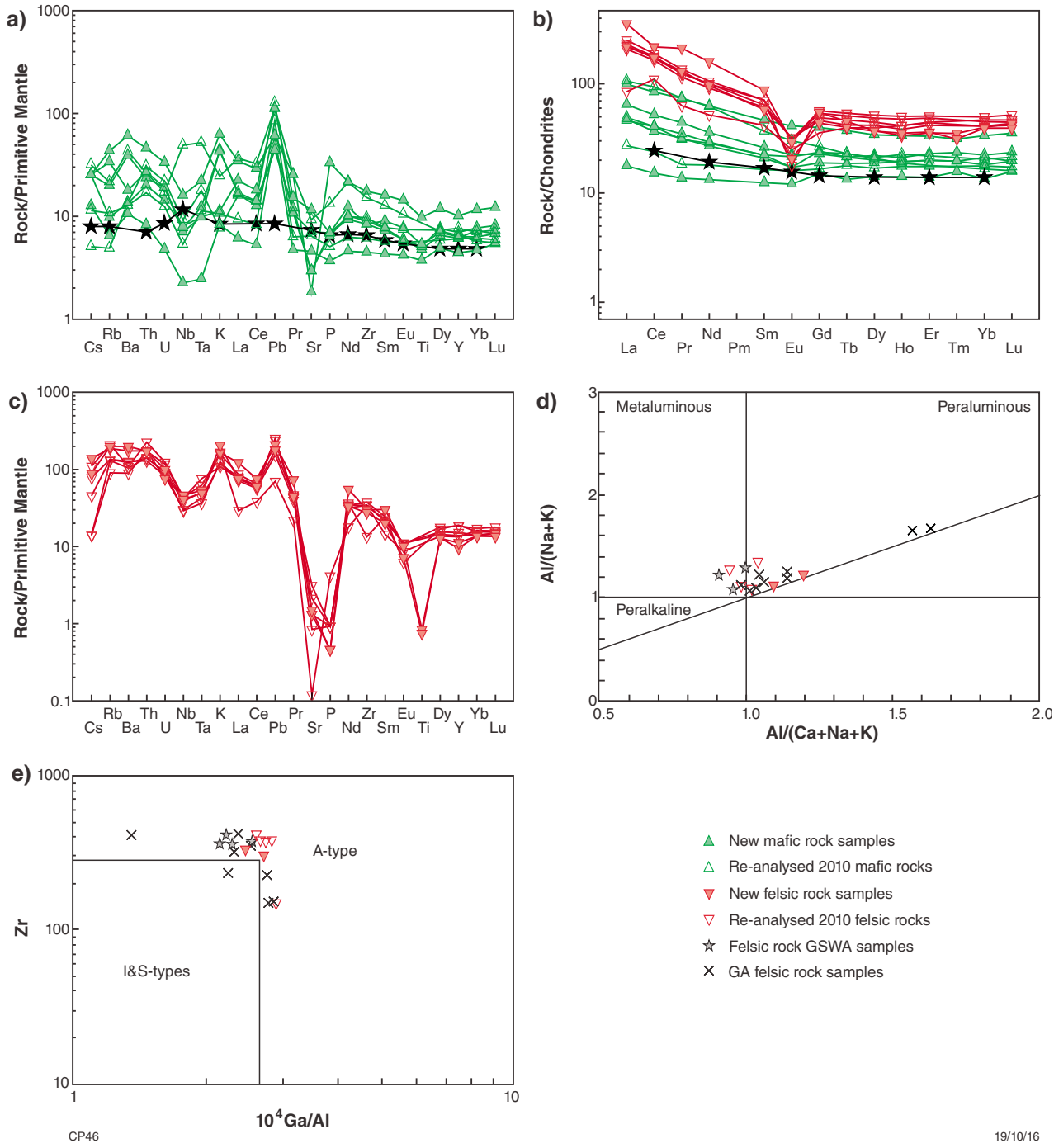

Figure 13. Geochemical diagrams for samples from the Ding Dong Downs Volcanics: a) primitive mantle-normalized trace element plots of mafic metavolcanic samples, after Sun and McDonough (1989); b) chrondrite-normalized trace element plots of mafic and felsic metavolcanic rocks, after Sun and McDonough (1989); c) primitive mantle-normalized trace element plots of felsic metavolcanic samples, after Sun and McDonough (1989); d) geochemistry of felsic metavolcanic rocks, after Maniar and Piccoli (1989); e) geochemical classification of felsic metavolcanic rocks, after Whalen et al. (1987). Black stars in a) and b) are MORB.

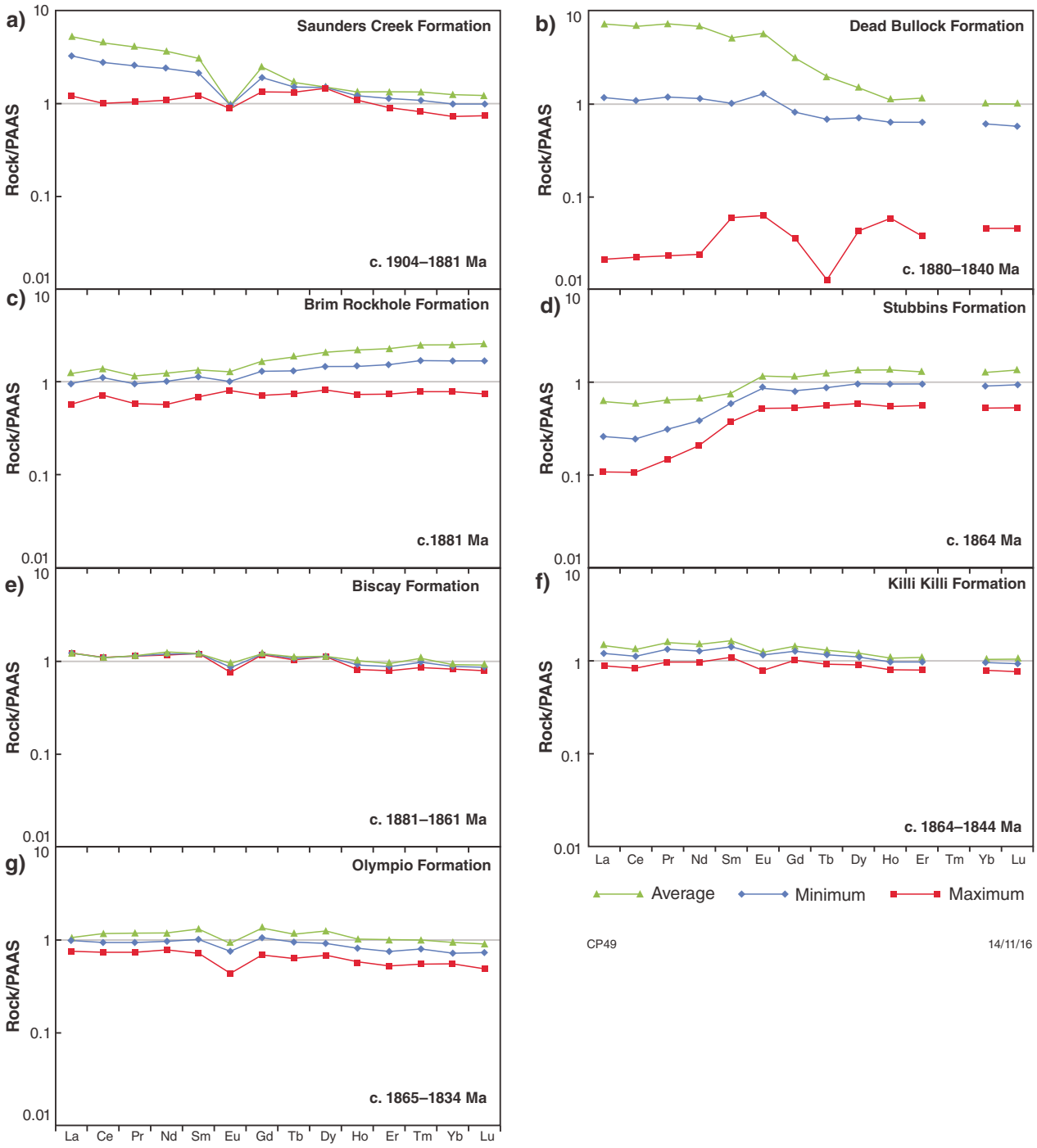

Figure 14. REE trends relative to post-Archean Australian Shale (PAAS) from Halls Creek Group metasandstone samples and metasandstone samples from the Tanami Group of the Granites–Tanami Orogen. Tanami data are from Bagas et al. (2008) and Lambeck et al. (2008).

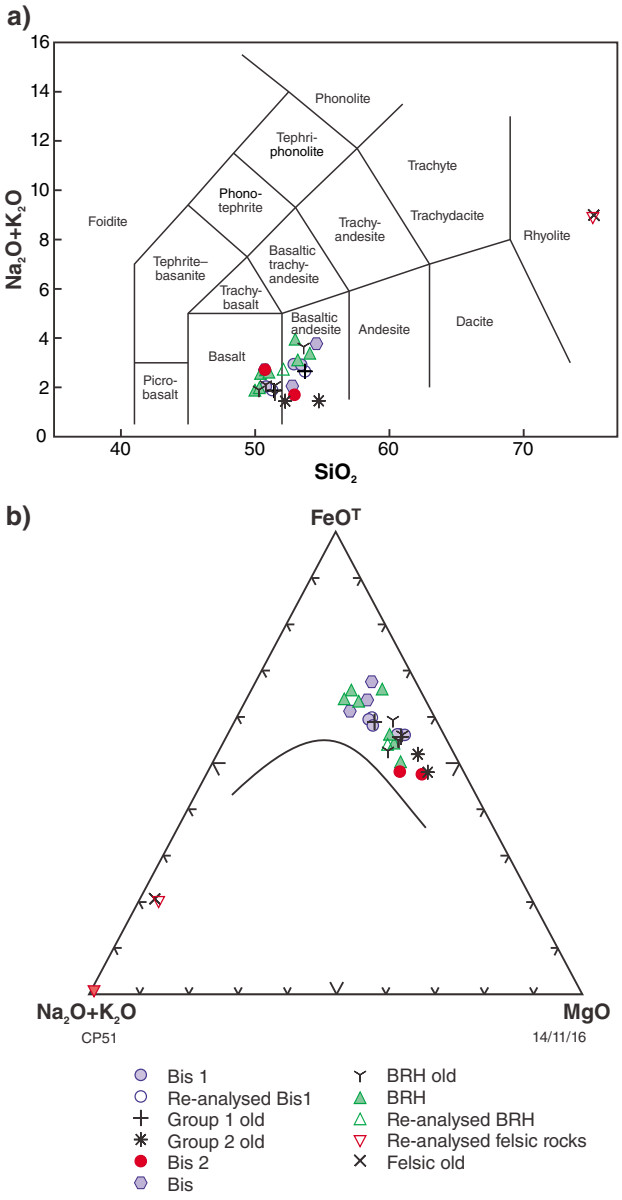

Figure 15. a) A volcanic rock identification diagram of Brim Rockhole Formation and Biscay Formation samples, after Le Bas et al. (1986); b) AFM plot of the Brim Rockhole and Biscay Formation mafic metavolcanic rocks. All samples plot above the curve defining the tholeiitic series (Irvine and Baragar, 1971). Felsic samples are shown as inverted red triangles. Mafic samples are from Brim Rockhole (BRH) and Biscay Formations (Bis). Groups 1 and 2 refer to the groups of Sheppard et al. (1999b). Four samples are re-analysed from the GSWA collection (Sheppard et al., 1997a,b) (re-an). Values are in wt%.

Ten metavolcanic samples from the Brim Rockhole Formation were analysed for whole-rock geochemistry (Appendix 1 — Tables 5 and 6). Metamafic samples are basalt or basaltic andesite and the one metafelsic sample plots as a rhyolite (Fig. 15a; Le Bas et al., 1986). On an AFM ternary diagram, all the metamafic samples fall into the tholeiitic field (Fig. 15b) with Mg# from 40 to 62. MgO displays a positive correlation with Al_2O_3 and CaO and a negative correlation with most other major elements, including SiO_2, TiO_2, FeO^T, K_2O and P_2O_5 (Fig. 16a–f) where FeO^T represents total iron. Nickel and Cr decrease with decreasing MgO (Fig 16g,h), whereas immobile elements such as Zr, Y and Nb and REE increase with decreasing MgO (Fig. 16i,j). Figure 17 shows trace element patterns relative to Primitive Mantle (PM) and chondrite. All Brim Rockhole Formation metamafic samples show positive Pb anomalies on a PM-normalized trace element diagram (Fig. 17a). Many samples have negative anomalies between U and Nb to Ta in the PM-normalized spider diagrams but five samples show no anomaly. Overall, Nb and Ta are less abundant than in island-arc tholeiites (Pearce, 1983; Wilson, 1989). Strontium, P and Ti show negative anomalies in most samples (Fig. 17a).

Nine metasedimentary samples from the Brim Rockhole Formation were analysed, four siliciclastic samples and five carbonate samples (Appendix 1 — Tables 3 and 4). Carbonaceous lithofacies (GSWA 210794 and 206012) contain 7.04 – 19.54 wt% Fe_2O_3 and up to 4.24 wt% C. Compared to average continental crust values, carbonaceous samples show enrichment in Mo, U and V (Taylor and McLennan, 1985). Overall, REE trends normalized to PAAS show enrichment in LREE and increasing enrichment in HREE with no significant Eu anomaly (Fig. 14b). Carbonate metasedimentary samples contain 8.98 – 43.64 wt% CaO and 7.86 – 42.15 wt% SiO_2. High CaO samples have the lowest SiO_2. GSWA 206048 has a 2:1 Mg:Ca ratio and is dolomitized.

Biscay Formation

Fifteen metavolcanic samples from the Biscay Formation were analysed (Appendix 1 — Tables 5 and 6). Four samples are not plotted due to high loss on ignition (LOI) (>3 wt%). All metamafic samples are basalt or basaltic andesite and the metafelsic sample plots as a rhyolite (Fig. 15a; Le Bas et al., 1986). On an AFM ternary diagram all the metamafic samples fall into the tholeiitic field (Fig. 15b). Sheppard et al. (1999b) recognized two geochemical groups within the Biscay Formation, some of which are now part of the Brim Rockhole Formation.

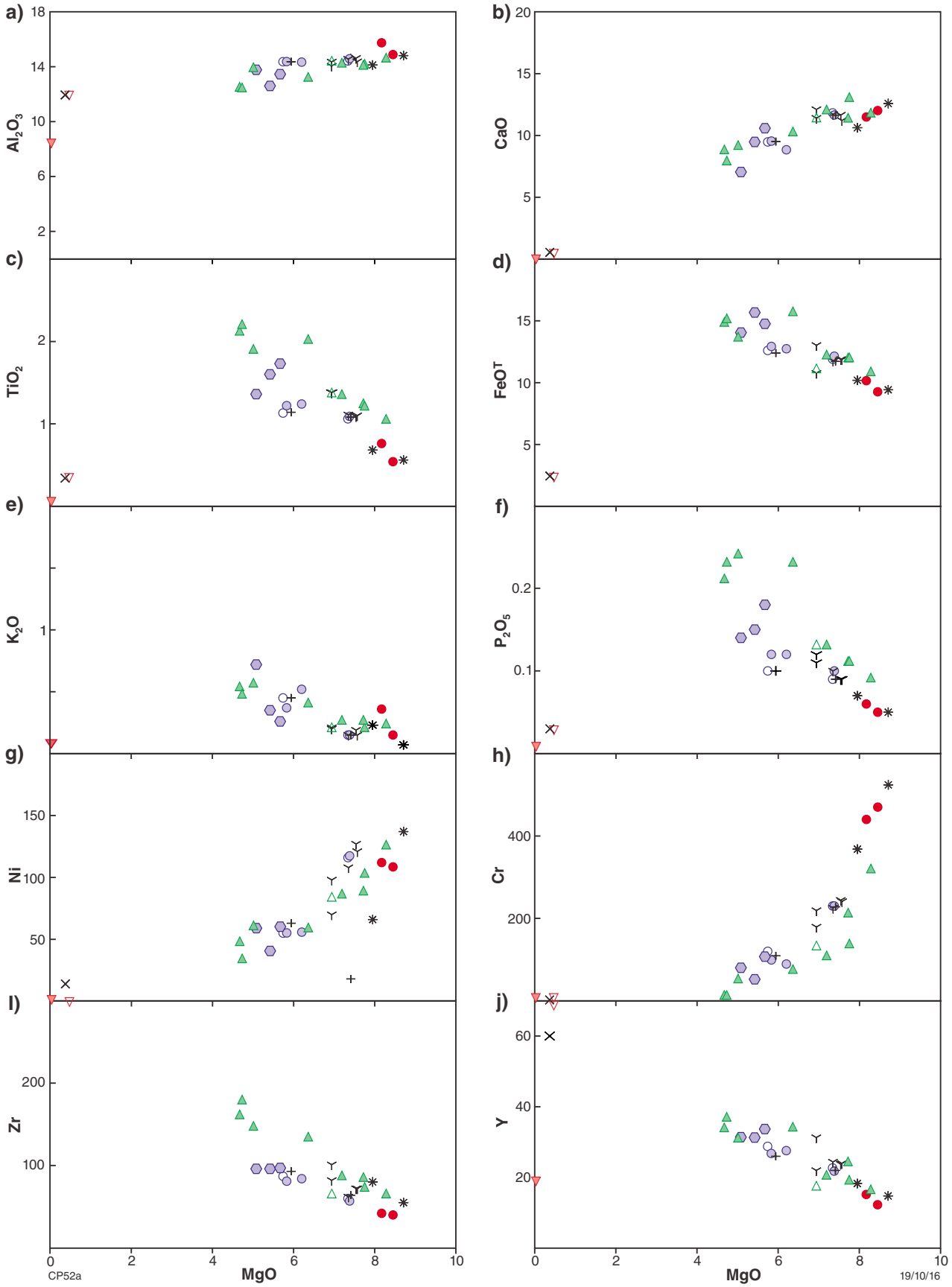

Figure 16. **Bivariate plots of selected major (wt%) and trace elements (ppm) against MgO (wt%) from Brim Rockhole Formation (BRF) and Biscay Formation metavolcanic samples. Bis 1 and Bis 2 refer to the geochemical groups identified by Sheppard et al. (1999b). Other data are taken from Sheppard et al. (1999a).**

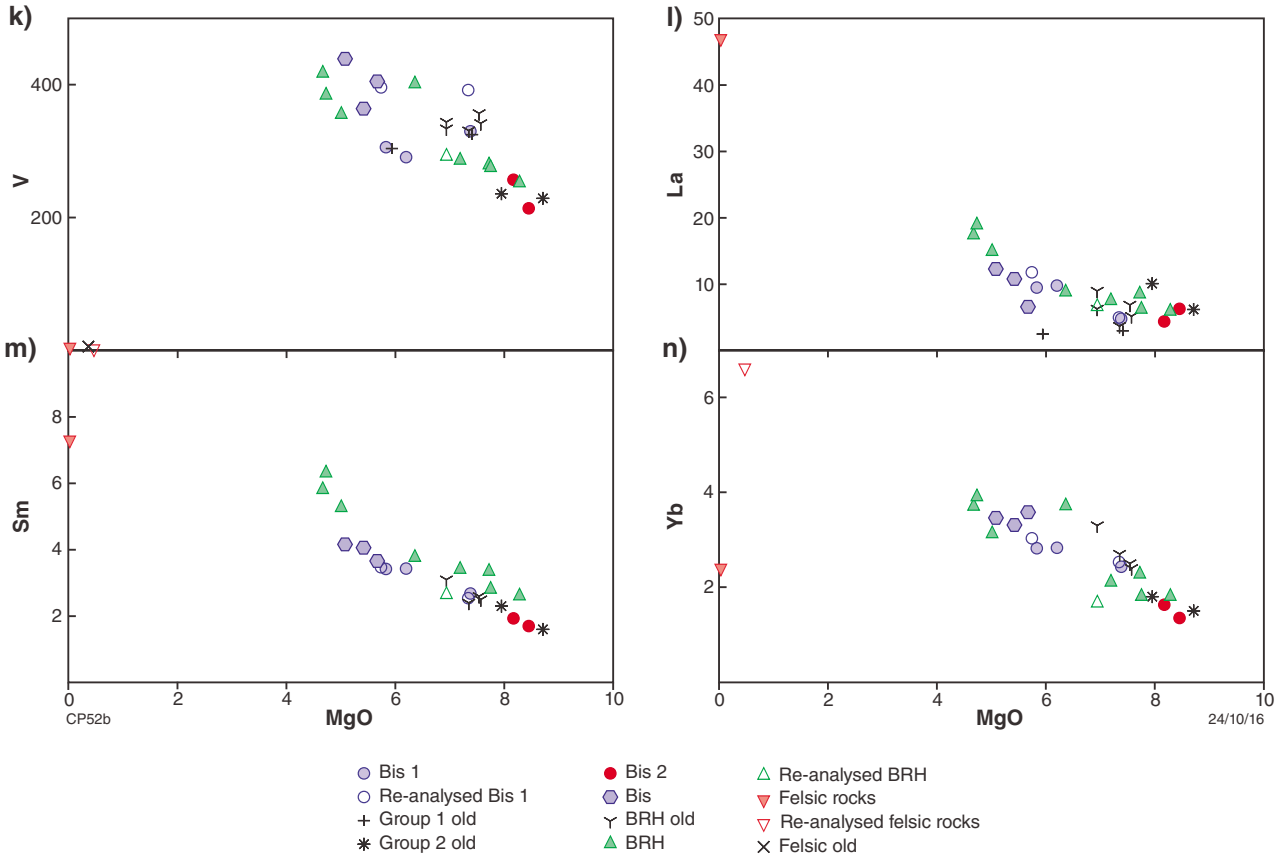

Figure 16. continued

These groups were defined by moderate MgO values with higher TiO_2 concentrations (Group 1) compared to samples with high MgO contents and low TiO_2 (Group 2). New analyses, presented here, overlap these groups and MgO bivariant plots display a greater spread of data (Fig. 16a–n). These new data do not support the separation of Biscay Formation (or Brim Rockhole Formation) metamafic volcanic rocks into geochemical groups. All Biscay Formation metamafic samples contain Pb, enrichment in LREE is evident in most samples and negative anomalies between U and Nb to Ta in the PM-normalized spider diagrams (Fig. 17b). Overall, Nb and Ta are less abundant than in island-arc tholeiites (Pearce, 1983; Wilson, 1989). Strontium, P and Ti show negative anomalies in most samples (Fig. 17b).

Chondrite-normalized REE patterns for Biscay Formation (and Brim Rockhole Formation) metamafic rocks are slightly LREE enriched (20–90 x C1) while M–HREE are less enriched (9–25 x C1) and have flatter HREE patterns (Fig. 17d,e). Samples with the greatest LREE enrichment ($[La/Yb]_N$ = 1.3 – 3.4) also have the most pronounced negative Eu anomalies (Eu/Eu* = 0.8 – 0.9). Biscay Formation metafelsic rocks show negative anomalies in Sr, Nb, Ta and Eu on a chondrite-normalized trace element diagram (Fig 17e).

Normalized to PAAS, the two metasedimentary samples from the Biscay Formation have REE trends, which show a slight enrichment in LREE, a minor Eu anomaly and an overall minor depletion in HREE (Fig. 14c).

Olympio Formation

Thirteen metasedimentary samples from the Olympio Formation were analysed (Appendix 1 — Tables 3 and 4). Metasandstone turbidite samples have a relatively flat LREE profile with depletion in HREE relative to PAAS (Fig. 14d).

Woodward Dolerite

The geochemical characteristics of the Woodward Dolerite are defined by three new samples and re-analysis of 10 existing pulps (Appendix 1 — Tables 7 and 8). The samples plot as subalkaline basalt or basaltic andesite (Fig. 18), with one sample characterized as an alkaline basalt (GSWA 108718). The majority of samples have 50–53 wt% SiO_2 and 3.8 – 8.7 wt% MgO. Bivariant plots of major element oxides against MgO (Fig. 19) show a negative correlation with TiO_2 (0.5 – 1.8 wt%), total iron (FeO^T; 8.5 – 15.7 wt%) and P_2O_5 (0.05 – 0.15 wt%) and a positive correlation with Al_2O_3 (12–16 wt%) and CaO (7.5 – 12 wt%). K_2O content is generally less than 1 wt%. A high CaO content in GSWA 209777 combined with 3 wt% LOI suggests that this sample has undergone some carbonate addition. The patterns in the MgO major oxide plots follow an iron-enrichment trend that defines tholeiitic mafic rocks. Nickel and Cr have a positive correlation with MgO consistent with olivine and pyroxene fractionation.

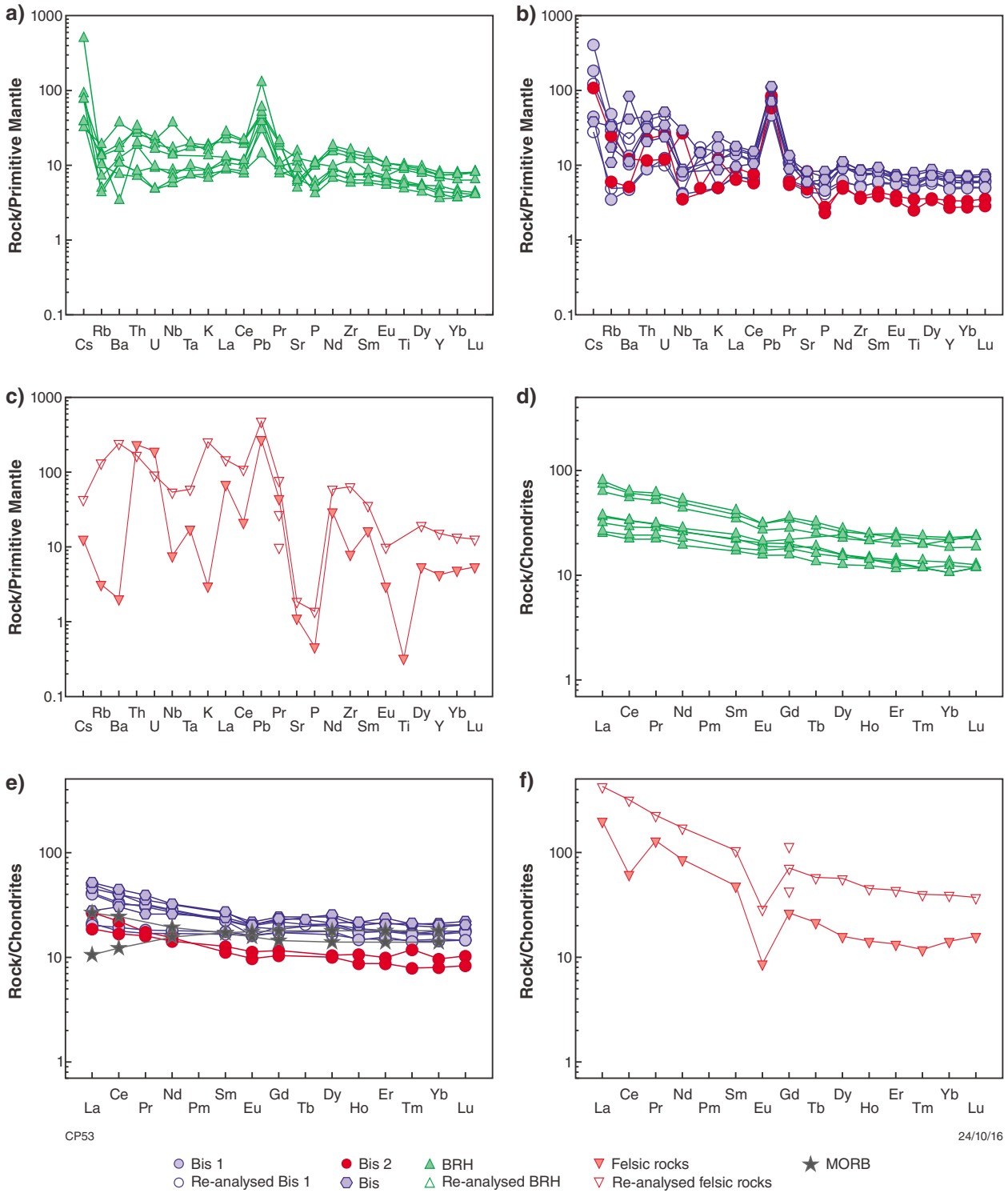

Figure 17. **Trace element and REE trends in Brim Rockhole and Biscay Formation mafic metavolcanic rocks. Normalizing values are from Sun and McDonough (1989): a) PM-normalized trace-element plots for Brim Rockhole metabasalts; b) PM-normalized trace element plots for Biscay Formation metabasalt rocks compared with MORB – Bis 1 and Bis 2 refer to the geochemical groups identified by Sheppard et al. (1999b); c) PM-normalized trace element plots for felsic metavolcanic rocks from the Brim Rockhole and Biscay Formations; d) C1-normalized REE plots for Brim Rockhole Formation metabasalt rocks; e) C1-normalized REE plots for Biscay Formation; f) C1-normalized REE plots for felsic metavolcanic rocks from the Brim Rockhole and Biscay Formations**

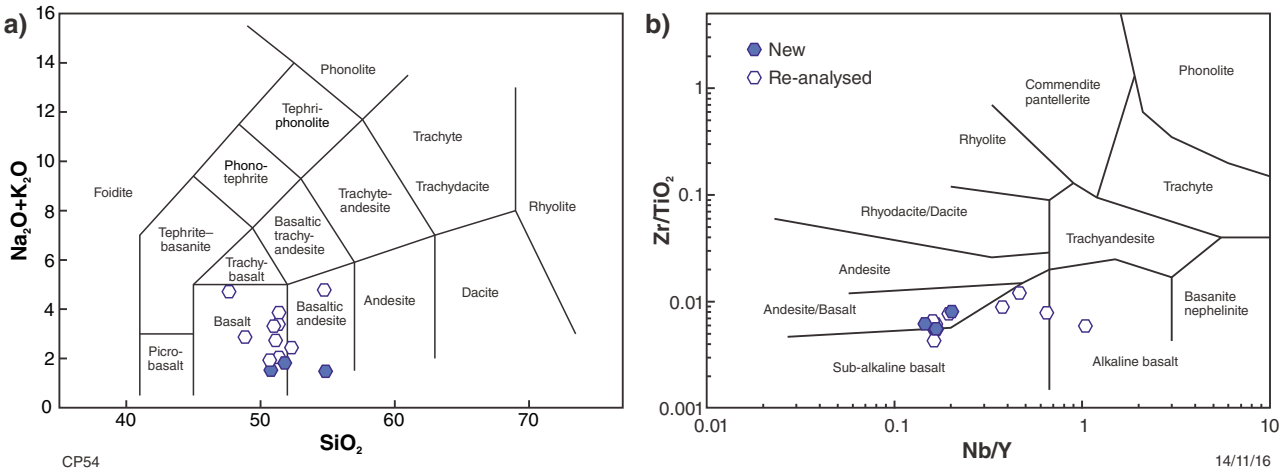

Figure 18. Volcanic rock classification of Woodward Dolerite samples: a) major element classification after Le Bas et al. (1986). All samples plot as basalt or basaltic andesite, one sample plots near the trachybasalt field; b) immobile element diagram showing most samples are subalkaline basalt to basalt/andesite. GSWA 108718 plots in the alkali basalt field (Winchester and Floyd, 1977). In other diagrams, GSWA 108718 is a transitional basalt (e.g. Zr vs Zr/Y). Re-analysed samples are from Sheppard et al. (1997a,b).

The highest V content is in samples with the highest TiO_2 and FeO^T. Yttrium and M–HREE show an overall negative trend with MgO. Most samples have low Zr/Y ratios (<5).

All PM-normalized spider diagrams show a strong positive Pb anomaly and elevated U and Th (Fig. 20). The majority of samples have depleted Nb with the exception of GSWA 108664 and GSWA 108718 (Nb 13–18 ppm). When normalized to chondrite (Sun and McDonough, 1989), low Zr/Y ratio Woodward Dolerite samples are 50 times more enriched in some of the LREE and 10 times more enriched in the HREE (Fig. 20d). The low Zr/Y ratio Woodward Dolerite samples are slightly elevated in LREE compared to normal ocean floor basalts (N-MORB).

Two low MgO samples (GSWA 108629 and GSWA 118101) are off trend in many of the bivariant major element oxide plots. They display high Al_2O_3 content (18–20 wt%), high K_2O (> 1 wt %) and P_2O_5 (>0.4wt%). Both contain more LILE, U, Th and LREE than other Woodward Dolerite samples, as well high Zr/Y ratios. Anomalous major oxide, trace elements and REE patterns of GSWA 118101 (leucogabbro) and GSWA 108629 (tonalite), suggest that they are highly evolved or contaminated portions of the Woodward Dolerite, or that their classification as Woodward Dolerite is uncertain.

Sm–Nd whole-rock isotope data

Five samples of the Ding Dong Downs Volcanics and one Sophie Downs Granite were analysed for whole-rock Sm–Nd isotope data (Appendix 1 — Table 9). All samples yield εNd_i ratios between –4.72 and +0.21, assuming an age of 1910 Ma. The Sophie Downs Granite (GSWA 108550) has an evolved signature (–3.82) most similar to the felsic volcanic sample from the Brim Anticline (GSWA 113434; εNd_i = –4.72). All other mafic and felsic samples are from the Saunders Creek Dome and are closer to Chondritic Uniform Reservoir (CHUR), with εNd_i values ranging between –0.78 and +0.21. T_{DM}^2 model ages for the Sophie Downs Granite and the Brim Creek rhyolite indicate a source at c. 2600 Ma. Mafic rocks with εNd_i values similar to CHUR have T_{DM}^2 model ages at c. 2300 Ma (Fig. 21).

Two samples of mafic rocks from Brim Rockhole Formation were analysed for Sm–Nd isotopes and produced an εNd_i value of +3.31 and +2.53 with T_{DM}^2 model ages at 1984 and 2045 Ma from GSWA 108608 and GSWA 108626, respectively (Fig. 21; Appendix 1 — Table 9). Three Biscay Formation samples are presumed to have an age of 1865 Ma (see the geochronology section below). The εNd_i value for these mafic samples is close to CHUR, between –0.78 and +0.72 with T_{DM}^2 model ages for the samples between c. 2290–2174 Ma (Fig. 21; Appendix 1 — Table 9).

Four samples from the Woodward Dolerite have εNd_i values between –0.86 and +3.05 at 1835 Ma (Fig. 21; Appendix 1 — Table 9). Although these rocks have not been directly dated, an age of c. 1835 Ma is considered a reasonable estimate based on the field relationships. The formation is overprinted by D_2/M_2 events during the Halls Creek Orogeny placing a minimum age of 1808 Ma on the dolerite.

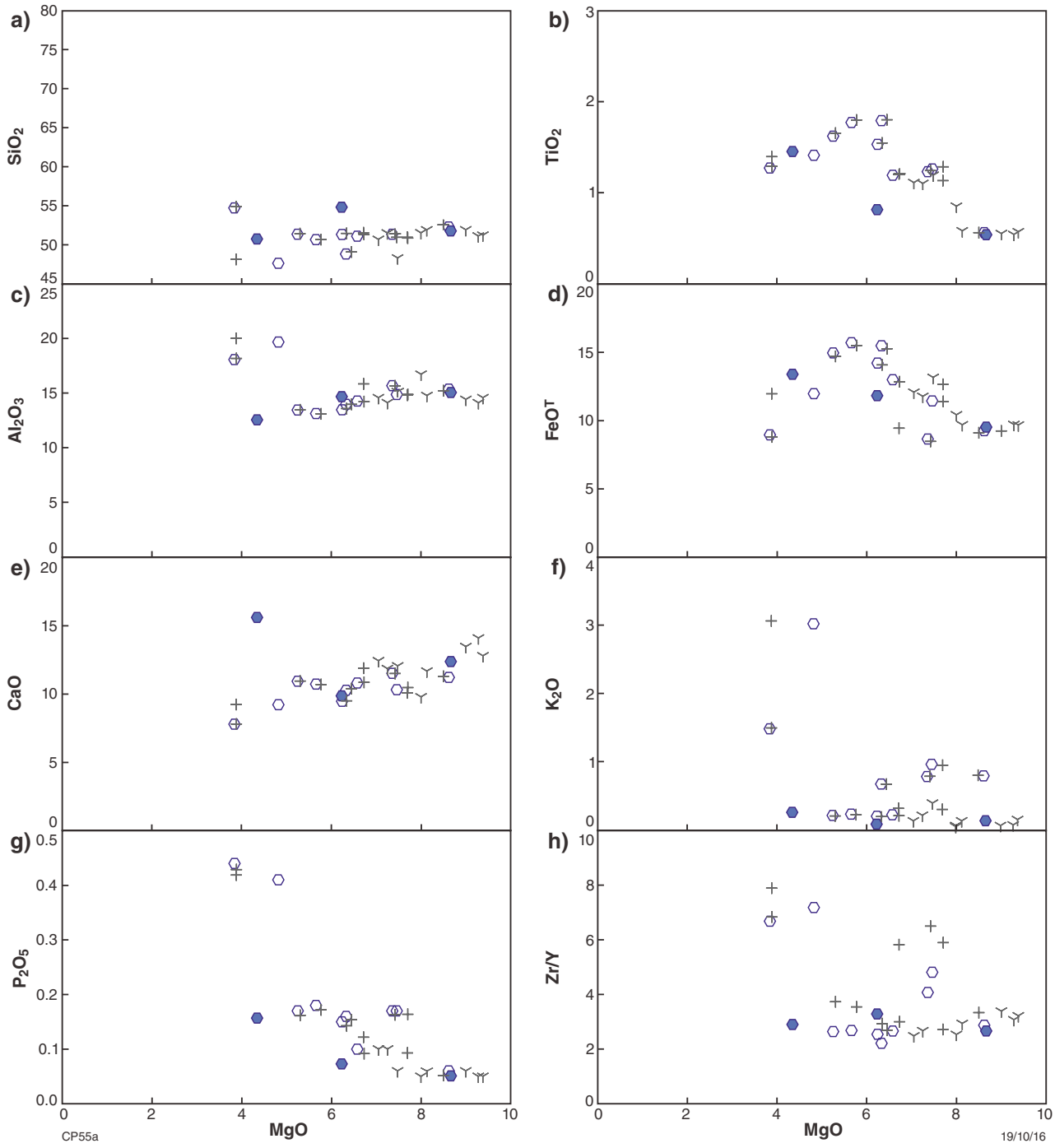

Figure 19. Major and selected trace-element plots against MgO for samples of Woodward Dolerite. Major oxides in wt% and trace elements in ppm. Other samples are from Sheppard et al. (1997a) and OZCHEM database maintained by Geoscience Australia (GA).

Figure 20. (bottom right) Spider diagrams for samples of Woodward Dolerite. Normalizing values are from Sun and McDonough (1989): a) primitive–mantle-normalized spider diagrams for mafic samples; d) C1-normalized REE plot. Most samples have a relatively flat pattern, with slight enrichment in light rare earth elements (LREE). Samples GSWA 108629 and 118101 have steeper slopes and more abundant LREE.

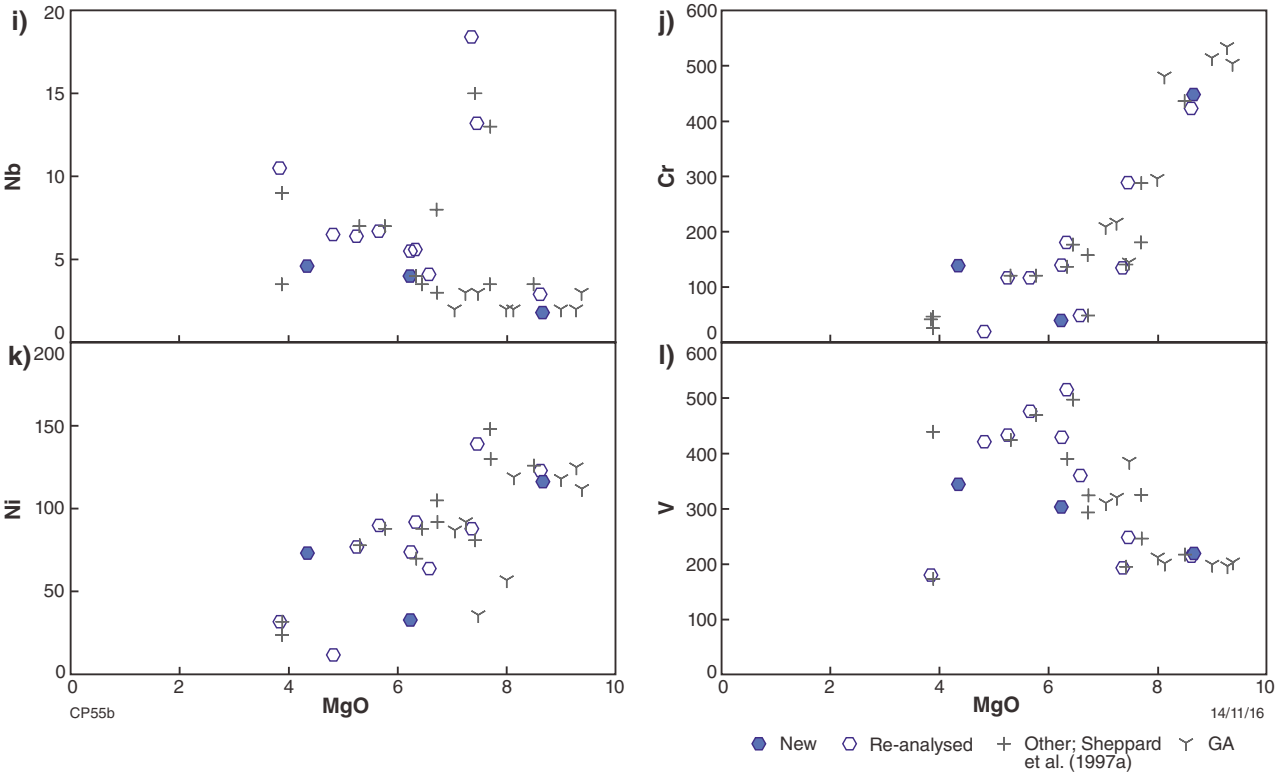

Figure 19. continued

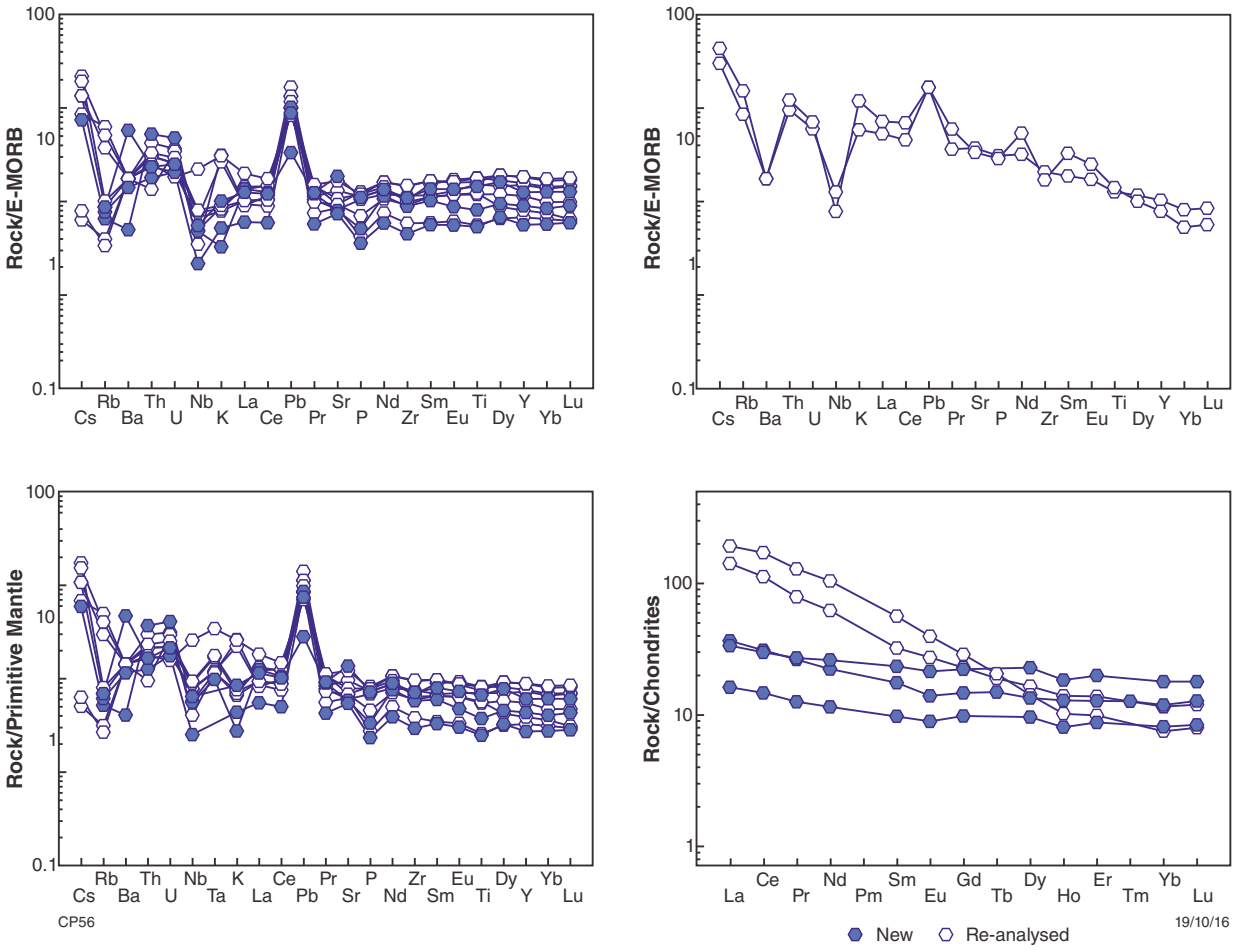

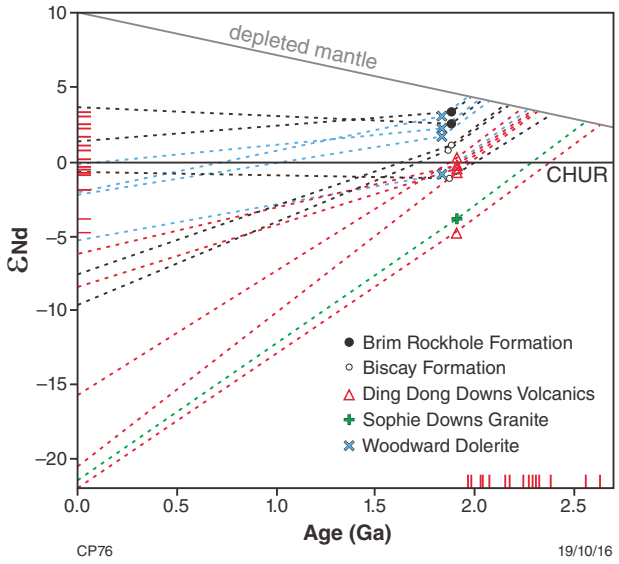

Figure 21. εNd values vs time for samples from the Eastern Zone

Zircon U–Pb geochronology and Lu–Hf isotopes

This section describes U–Pb zircon geochronology and hafnium isotope analyses on new and re-analysed samples from basement and basin rocks in the Eastern Zone. This section includes results from Geoscience Australia's OZCHRON database and Geochron Delivery web page, available at <www.ga.gov.au/geochron-sapub-web/>. Analytical methods and data tables are presented in Appendix 2. In this section, Pb* indicates radiogenic Pb, weighted mean $^{207}Pb^*/^{206}Pb^*$ dates are reported with 95% (tσ√MSWD) confidence intervals, and the statistical coherence of each mean is quantified by the mean square of weighted deviates (MSWD) parameter.

Sophie Downs Suite

GA 93526009: felsic volcanic rock — Ding Dong Downs Volcanics

Sample GA 93526009 is a foliated fragmental felsic volcanic rock of the Ding Dong Downs Volcanics. The sample contains euhedral plagioclase and opaque minerals, wispy aggregates (possibly fiamme) of biotite and muscovite in a very fine-grained quartzofeldspathic groundmass containing biotite, muscovite and sparse opaque minerals (Blake et al., 1999b). The sample was collected from the core of the Brim Anticline, 10 km northeast of Sophie Downs Homestead (Fig. 1).

U–Pb geochronology is reported in summary form in Blake et al. (1999b). Thirty-five analyses were obtained from 35 zircons. Excluding one analysis of a c. 2505 Ma inherited zircon, the remaining 32 analyses <5% discordant yield a weighted mean $^{207}Pb^*/^{206}Pb^*$ date of 1912 ± 3 Ma, interpreted as the age of volcanism (Fig. 22a, Table 1, Appendix 2 — Table 1; MSWD = 0.88).

GA 87598029: leucocratic granite — Sophie Downs Granite

Sample GA 87598029 is a foliated porphyritic granophyre of the Sophie Downs Granite. The sampled rock contains strained and partly recrystallized megacrysts of anhedral quartz along with microcline and plagioclase, scattered wispy aggregates of biotite, muscovite and opaque oxide minerals in a fine-grained recrystallized groundmass of quartz and microcline with a remnant micrographic texture (Blake et al., 1999b). The sample was collected 9 km north-northeast of Sophie Downs Homestead (Fig. 1).

U–Pb geochronology is reported in summary form in Blake et al. (1999b). Thirty-four analyses were obtained from 34 zircons. Thirty-two analyses <5% discordant yield a weighted mean $^{207}Pb^*/^{206}Pb^*$ date of 1912 ± 4 Ma, interpreted as the age of magmatic crystallization (Fig. 22b, Table 1, Appendix 2 — Table 2; MSWD = 0.43).

GSWA 108547: granite — Junda Microgranite

The Junda Microgranite crops out in the cores of a series of structural domes in the southeast on Dockrell (labelled as Sophie Downs Suite on Figure 1). It is overlain by the Saunders Creek Formation, except in the areas 6 km northeast of Junda Bore and 8 km southwest of Junda Bore, where it is overlain by the Brim Rockhole Formation. The Junda Microgranite comprises foliated and recrystallized, fine-grained leucocratic monzogranite. Biotite forms small clots that, together with fine-grained mafic inclusions, are flattened in the foliation. The microgranite is composed of fine-grained, granular quartz, plagioclase (albite–oligoclase) and microcline with a few percent biotite in small clots and very minor muscovite, commonly intergrown with biotite. Epidote, zircon, apatite and allanite typically occur with, or are included within, biotite (Tyler et al., 1998). The sample was collected 33 km south of Old Lamboo Homestead (Fig. 1).

A SHRIMP U–Pb age of 1913 ± 8 Ma is reported in Tyler et al. (1998). The sample was re-examined in this study. Sixteen analyses were obtained from 16 zircons. Fourteen analyses <5% discordant yield a weighted mean $^{207}Pb^*/^{206}Pb^*$ date of 1911 ± 5 Ma, interpreted as the age of magmatic crystallization (Fig. 22c, Table 1, Appendix 2 — Table 3; MSWD = 1.18).

Hafnium isotope data were collected from six zircons, five of which were <5% discordant. These five range in age from c. 1924 to 1903 Ma and show tightly grouped, radiogenic Hf isotope compositions (εHf = +2.7 to +1.5; Fig. 22f, Appendix 2 — Table 3).

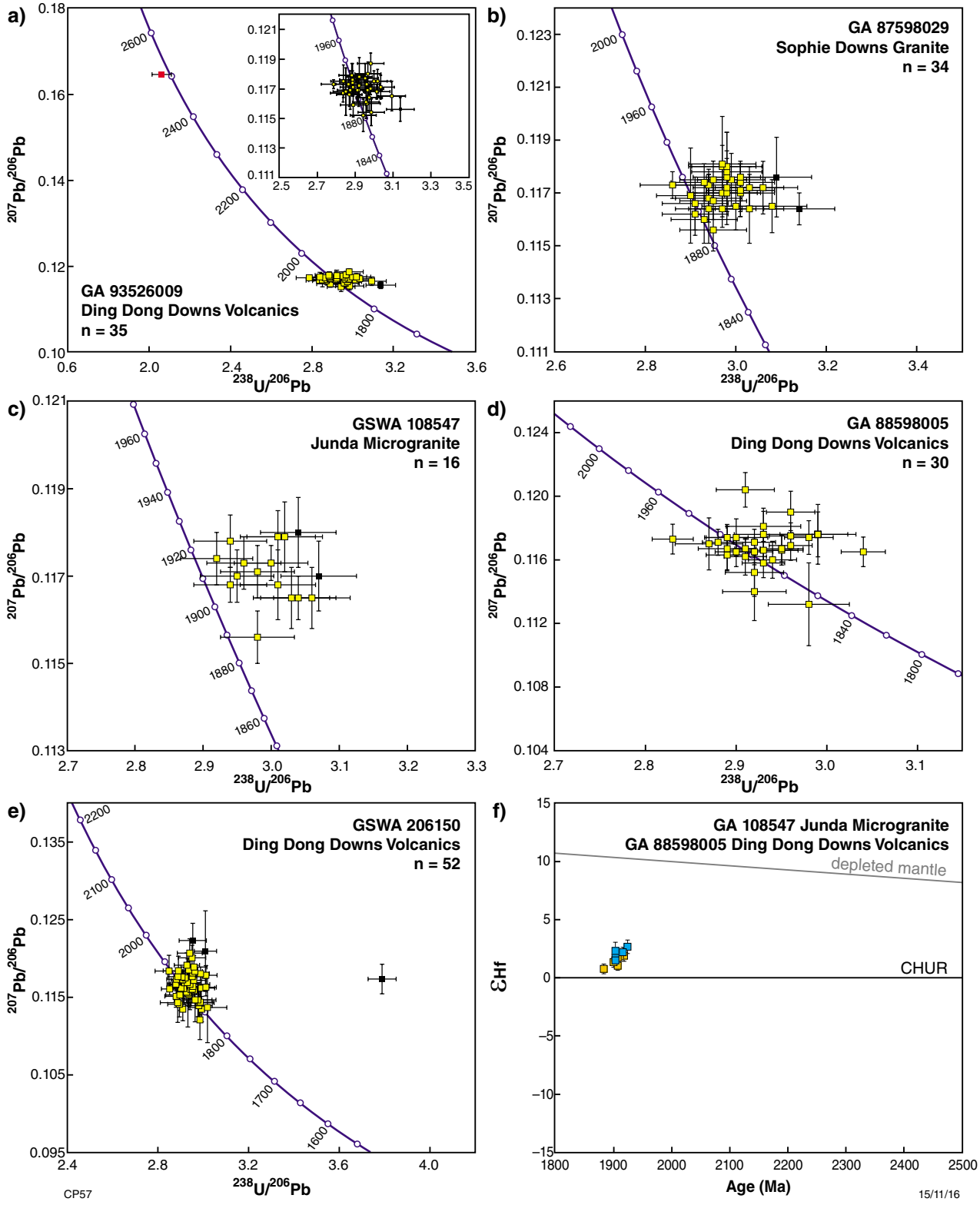

Figure 22. U–Pb and Lu–Hf analytical data for zircons from the Sophie Downs Suite: a) felsic volcanic rock (GA 93526009), Ding Dong Downs Volcanics with inset showing the main magmatic component; b) leucocratic granite (GA 87598029), Sophie Downs Granite; c) granite (GSWA 108547), Junda Microgranite; d) fragmental felsic volcanic rock (GA 88598005), Ding Dong Downs Volcanics; e) mylonitic felsic volcanic rock (GSWA 206150), Ding Dong Downs Volcanics; f) εHf vs age for zircons from the Junda Microgranite (GSWA 108547) shown in blue and the Ding Dong Downs Volcanics (GA 88598005) shown in orange. The grey line is the depleted mantle (DM) model, and the black line is the chondrite-normalized uniform earth (CHUR) model. Yellow squares indicate magmatic zircons, red square indicates inherited zircons, and black squares indicate data that are >5% discordant. Error bars are ± 1σ. Full details of U–Pb geochronology for these samples are available in published GSWA Geochronology Records.

Table 1. Summary of age data for samples analysed from the Eastern Zone, listed in top down stratigraphic order. Detrital samples are red and magmatic samples are black. Coherent group refers to the youngest analyses that are within 2.5σ of a common weighted mean age.

Sample	*Lithological unit*	*Youngest individual analysis (Group Y)*	*Youngest coherent detrital group (denoted by * in tables)*	*Detrital age components*	*Crystallization age*
GSWA 206184	Upper Olympio Formation	1797 ± 49	1834 ± 8	2205, 1928, 1871	
GA 92524896	Upper Olympio Formation	1821 ± 10	1848 ± 5	1848	
GA 92524993C	Butchers Gully Member	1832 ± 10			1846 ± 4
GA 87598023	Butchers Gully Member	2637 ± 4			none obtained
GA 87598022	Butchers Gully Member	1856 ± 10		1906, 1872, 1862	1868 ± 3
GA 87598001	Butchers Gully Member	1823 ± 25			1868 ± 5
GA 85598001	Maude Hedley Member				1856 ± 6
GA 93525128B	Lower Olympio Formation	1864 ± 5	1874 ± 3		
GSWA 206126	Lower Olympio Formation	1830 ± 9	1851 ± 6	2518, 2496, 1879, 1864	
GSWA 206187	Biscay Formation	1842 ± 27	1861 ± 3	2470, 2227, 1859	
GSWA 206183	Biscay Formation	1825 ± 28	1872 ± 5	2485, 1873	
GSWA 206185	Biscay Formation	1832 ± 18	1872 ± 6	2493, 1872	
GA 93526012	Brim Rockhole Formation				1881 ± 4
GSWA 206121	Brim Rockhole Formation	1894 ± 12	1909 ± 10	3613, 3528, 3456, 3309, 2523, 2491, 1909	
GSWA 206119	Brim Rockhole Formation	2487 ± 11	2512 ± 10	3388, 3420, 2521, 3309, 3282, 2496	
08TKHCO03	Saunders Creek Formation	2501 ± 5	2508 ± 8		
GA 87598028	Saunders Creek Formation	2437 ± 36	2512 ± 8	3576, 3318, 2512	
GSWA 206150	Ding Dong Downs Volcanics				1904 ± 5
GA 8859-8005	Ding Dong Downs Volcanics				1910 ± 5
GSWA 108547	Junda Microgranite				1911 ± 5
GA 87598029	Sophie Downs Granite				1912 ± 4
GA 93526009	Ding Dong Downs Volcanics				1912 ± 3

GA 88598005: fragmental felsic volcanic rock — Ding Dong Downs Volcanics

Sample GA 88598005 is a foliated fragmental felsic volcanic rock of the Ding Dong Downs Volcanics. The sample contains euhedral crystals of microcline and plagioclase and clasts of volcanic rocks, including basalt, andesite and rhyolite in a fine-grained recrystallized matrix, containing muscovite and chlorite (Blake et al., 1999b). The sample was collected from the northern part of the Saunders Creek Dome, 20 km northeast of Sophie Downs Homestead (Fig. 1).

U–Pb geochronology was reported in summary form in Blake et al. (1999b). Zircon separates from the same sample were remounted and analysed at Geoscience Australia in 2008 and these new data are presented here. Thirty analyses were obtained from 30 zircons. All 30 analyses (<5% discordant) yield a weighted mean $^{207}Pb^*/^{206}Pb^*$ date of 1910 ± 5 Ma interpreted as the age of crystallization (Fig. 22d; Table 1, Appendix 2 — Table 4; MSWD = 0.88).

Eight zircons that yielded dates of 1918–1883 Ma show tightly grouped, radiogenic Hf isotope compositions (εHf = +2.0 to +0.8; Fig. 22f, Appendix 2 — Table 4).

GSWA 206150: mylonitized quartzofeldspathic rock — Ding Dong Downs Volcanics

Sample GSWA 206150 is a mylonitized quartzofeldspathic rock of the Ding Dong Downs Volcanics. The sampled unit is a c. 70 m wide, moderately west-dipping unit of mylonitic quartzofeldspathic muscovite-bearing gneiss, interpreted as a felsic metavolcanic rock. The mylonitic S_2 fabric is cut by a shallower, west-dipping S_3 S–C fabric with a top to the east (west side up) movement sense. The sample was collected from a rocky slope on the west bank of a creek in the Saunders Creek Dome, 15 km northeast of Sophie Downs Homestead (Fig. 1).

U–Pb geochronology is reported in Kirkland et al. (2015b). Fifty-two analyses were obtained from 52

zircons. Forty-nine analyses (<5% discordant) yield a weighted mean $^{207}Pb^*/^{206}Pb^*$ date of 1904 ± 5 Ma (Fig. 22e; Table 1, Appendix 2 — Table 5; MSWD = 1.3), interpreted as the age of the volcanic protolith.

Halls Creek Group

GA 87598028: quartz sandstone — Saunders Creek Formation

Sample GA 87598028 is a medium- to coarse-grained, poorly sorted, cross-laminated, recrystallized quartz metasandstone of the Saunders Creek Formation. The sample contains clasts of strained quartz and fine-grained quartzite, as well as muscovite and opaque minerals that define heavy mineral layers within the cross-laminations (Blake et al., 1999b). The sample was collected from the northern part of the Saunders Creek Dome, 20 km northeast of Sophie Downs Homestead (Fig. 1).

U–Pb geochronology was reported in summary form in Blake et al. (1999b). Seventy-eight analyses were obtained from 47 zircons. Twenty-nine analyses <5% discordant yield $^{207}Pb^*/^{206}Pb^*$ dates of 3605–2437 Ma (Fig. 23a; Table 1, Appendix 2 — Table 6), and form a dominant age component at c. 2512 Ma (15 analyses, 52%), significant components at c. 3318 and 3576 Ma, and several minor components in the range 3605–2653 Ma interpreted as the ages of detrital sources. A maximum age of deposition is provided by the weighted mean $^{207}Pb^*/^{206}Pb^*$ date of 2512 ± 8 Ma (MSWD = 1.5) for the 15 youngest analyses. However, all detrital ages are much older than the underlying 1912–1904 Ma Ding Dong Downs basement, which provides a maximum age constraint on sediment deposition.

Hafnium isotope data were collected from 23 zircons, eight of which were <5% discordant. These eight range in age from c. 3581 to 2500 Ma (Fig. 23b; Appendix 2 — Table 6). The three youngest analysed zircons at c. 2672, 2527 and 2500 Ma yield unradiogenic εHf values of –9.1, –10.8 and –10.4 respectively, which suggest these zircons were derived by magmatic reworking of much older crust.

08TKHCO03: quartzite — Saunders Creek Formation

Sample 08TKHCO03 is a quartzite of the Saunders Creek Formation. The sample was collected from the northern part of the Saunders Creek Dome, 20 km northeast of Sophie Downs Homestead (Fig. 1).

Thirty-seven analyses were obtained from 36 zircons. All 37 analyses were <5% discordant and yielded $^{207}Pb^*/^{206}Pb^*$ dates of 3634–2501 Ma (Fig. 23c; Table 1, Appendix 2 — Table 7). These include a dominant age component at c. 2522 Ma (16 analyses, 43%) and several minor components in the range 3634–2501 Ma interpreted as the ages of detrital sources. A maximum age of deposition is provided by the weighted mean $^{207}Pb^*/^{206}Pb^*$ date of 2508 ± 8 Ma (MSWD = 1.6) for the six youngest analyses. However, all detrital ages are much older than the age of the underlying 1912–1904 Ma Ding Dong Downs basement, which provides a maximum age constraint on sediment deposition.

Hafnium isotope data were collected from 36 zircons ranging in age from c. 3634 to 2501 Ma (Fig. 23d; Appendix 2 — Table 7). The dominant age component 2501–2552 Ma yields Hf compositions that lie along a vertical array spanning εHf = –13.3 to –7.5, consistent with mixing between a Paleoarchean to Eoarchean source and a younger, relatively radiogenic Archean source.

GSWA 206119: metasandstone — Brim Rockhole Formation

Sample GSWA 206119 is a metasandstone of the Brim Rockhole Formation. The sample was collected within a metre of the basal contact of the Brim Rockhole Formation with underlying quartzite of the Saunders Creek Formation. It is a fine-grained metasandstone with very coarse-grained metasandstone lenses and poorly defined ripples. From the basal contact, the unit fines upward over tens of centimetres into a fine-grained massive metasiltstone. The sample was collected from a cliff on Sophie Downs Station, about 22 km northeast of Sophie Downs Homestead on the northern end of the Saunders Creek Dome (Fig. 1).

Seventy-five analyses were obtained from 75 zircons (Kirkland et al., 2015a). Sixty-two analyses <5% discordant yield $^{207}Pb^*/^{206}Pb^*$ dates of 3590–2487 Ma (Fig. 23e,f; Table 1, Appendix 2 — Table 8). These include significant age components at c. 3388 (14%), 3420 (10%), 2521 (10%), 3309 (8%), 3282 (7%) and 2496 Ma (6%) and several minor components in the range 3590–2487 Ma. These are interpreted as the ages of detrital sources. A maximum age of deposition is provided by the weighted mean $^{207}Pb^*/^{206}Pb^*$ date of 2511 ± 10 Ma (MSWD = 2.3) for the six youngest analyses. However, all detrital ages are much older than the age of the underlying 1912–1904 Ma Ding Dong Downs basement, which provides a maximum age constraint on sediment deposition.

GSWA 206121: metasandstone — Brim Rockhole Formation

Sample GSWA 206121 is a fine-grained psammitic metasandstone of the Brim Rockhole Formation. In this location, the Brim Rockhole Formation unconformably overlies the c. 1912 Ma Sophie Downs Granite. The sample was collected from a succession of upper greenschist facies laminated pelitic and psammitic metasandstones that fine upward into locally graphitic metapelitic rocks (Fig. 1). It is a laminated garnet- and hornblende-bearing psammitic rock that may have been formed either by airfall (i.e. tuff) or, more likely, by sedimentary reworking of at least some component of volcanic rocks.

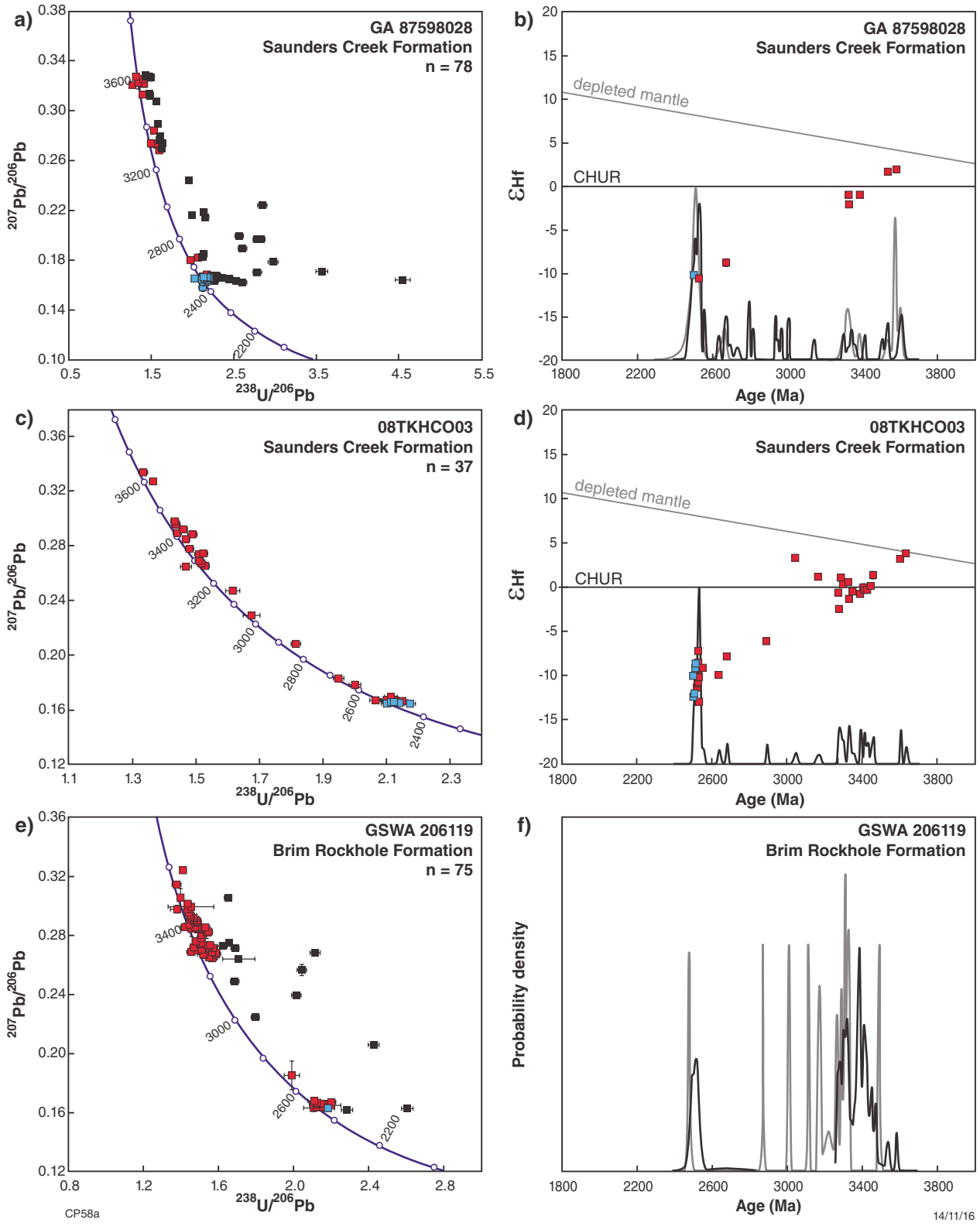

Figure 23. see opposite page for caption

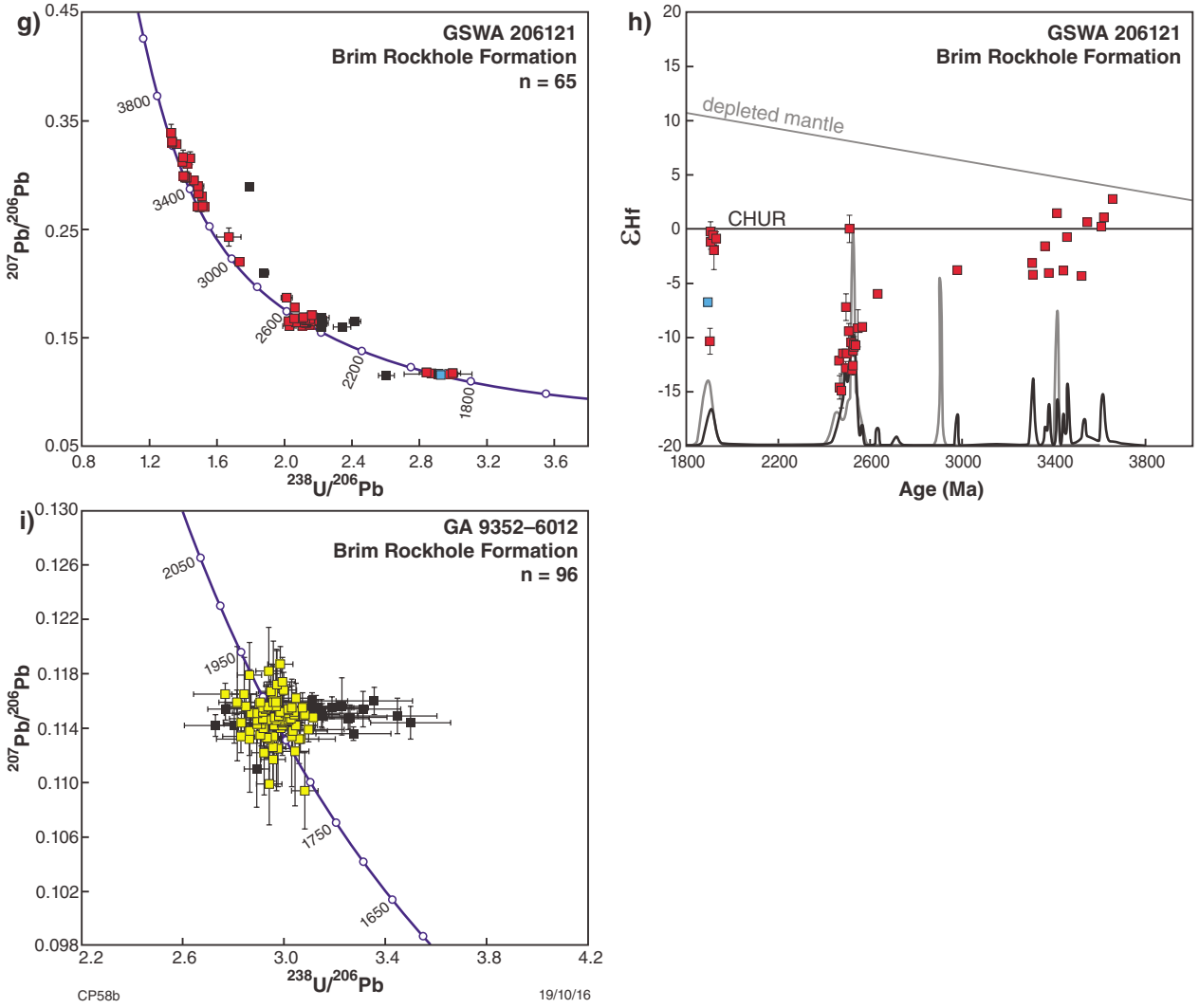

Figure 23. U–Pb and Lu–Hf analytical data for the Saunders Creek Formation and Brim Rockhole Formation: a) U–Pb data for quartz sandstone, Saunders Creek Formation (GA 87598028); b) Lu–Hf data and U–Pb probability density diagram for quartz sandstone, Saunders Creek Formation (GA 87598028); c) U–Pb data for quartzite, Saunders Creek Formation (08TKHCO03); d) Lu–Hf data and U–Pb probability density diagram for quartzite, Saunders Creek Formation (08TKHCO03); e) U–Pb data for metasandstone, Brim Rockhole Formation (GSWA 206119); f) U–Pb probability density diagram for metasandstone, Brim Rockhole Formation (GSWA 206119); g) U–Pb data for metasandstone, Brim Rockhole Formation (GSWA 206121); h) Lu–Hf data and U–Pb probability density diagram for metasandstone, Brim Rockhole Formation (GSWA 206121); i) U–Pb data for fragmental volcanic rock, Brim Rockhole Formation (GA 93526012). Probability density diagrams of all U–Pb detrital zircon results show <5% discordant data in black and >5% discordant data in grey; n is the number of analyses. Blue squares indicate the youngest detrital zircon(s), red squares indicate older detrital zircons, yellow squares indicate magmatic zircons, black squares indicate data that are >5% discordant. Error bars are ± 1σ. Full details of U–Pb geochronology for these samples are available in published GSWA Geochronology Records.

Sixty-five analyses were obtained from 65 zircons (Wingate et al., 2015a). Forty-nine analyses <5% discordant yield $^{207}Pb^*/^{206}Pb^*$ dates of 3656–1894 Ma (Fig. 23g; Table 1, Appendix 2 — Table 9), including main age components at c. 2523 (41%, 19 analyses) and 2491 Ma (39%, 18 analyses) and significant components at c. 3613, 3528, 3456, 3309, 2510 and 1909 Ma. A maximum age of deposition is provided by the weighted mean $^{207}Pb^*/^{206}Pb^*$ date of 1909 ± 10 Ma (MSWD = 0.54) for the seven youngest analyses. This is consistent with the age of the underlying c. 1912 Ma Sophie Downs Granite and Ding Dong Downs Volcanics, which may be sources of the detrital zircons.

Hafnium isotope data were collected from 40 zircons ranging in age from c. 3656 to 1894 Ma (Fig. 23h; Appendix 2 — Table 9). The latest Neoarchean to earliest Paleoproterozoic (2523–2493 Ma) zircons yield a vertical array spanning εHf = –13.0 to 0.0, consistent with mixing between a strongly evolved, Paleoarchean to Eoarchean mantle-derived magmatic source and a younger radiogenic Archean source.

GA 93526012: fragmental volcanic rock — Brim Rockhole Formation

Sample GA 93526012 is a foliated felsic fragmental volcanic rock of the Brim Rockhole Formation (Blake et al., 1999b) collected from a felsic volcanic layer on the western side of the Sophie Downs Dome, south of Little Mount Isa and about 14 km north-northeast of Sophie Downs Homestead (Figs 1 and 8). In this location, the Brim Rockhole Formation unconformably overlies the c. 1912 Ma Sophie Downs Granite. The sampled rock contains euhedral to fragmented crystals of microcline and quartz in a very fine- to fine-grained matrix of quartz, K-feldspar, muscovite and biotite with accessory iron oxide minerals and secondary calcite (Blake et al., 1999b).

U–Pb geochronology was reported in summary form in Blake et al. (1999b). Ninety-six analyses were obtained from 58 zircons. Seventy-seven analyses <5% discordant yield $^{207}Pb^*/^{206}Pb^*$ dates of 1937–1789 Ma (Fig. 23i; Table 1, Appendix 2 — Table 10), and a weighted mean $^{207}Pb^*/^{206}Pb^*$ date of 1881 ± 4 Ma (MSWD = 0.84), interpreted as the age of volcanism.

GSWA 206183: metasandstone — Biscay Formation

Sample GSWA 206183 is from a medium-grained feldspathic metasandstone of the Biscay Formation. The sample was collected 3 km southwest of Old Halls Creek (Fig. 1). At this location, immature metasandstone beds are intercalated with metabasalt.

Fifty-two analyses were obtained from 51 zircons (Lu et al., in prep.). Fifty-two analyses <5% discordant yield $^{207}Pb^*/^{206}Pb^*$ dates of 2491–1838 Ma (Fig. 24a, b; Table 1, Appendix 2 — Table 11). These included significant age components at c. 2485 (5%, three analyses) and 1873 Ma (75%, 39 analyses) interpreted as the age of detrital sources. A maximum depositional age is provided by the weighted mean $^{207}Pb^*/^{206}Pb^*$ date of 1872 ± 5 Ma (MSWD = 1.3) for the 43 youngest analyses.

GSWA 206185: metasandstone — Biscay Formation

Sample GSWA 206185 is from a medium-grained feldspathic metasandstone of the Biscay Formation collected from an outcrop off the Duncan Road 3.5 km southeast of Old Halls Creek (Fig. 1).

Fifty-two analyses were obtained from 52 zircons (Lu et al., in prep.). Fifty analyses <5% discordant yield $^{207}Pb^*/^{206}Pb^*$ dates of 2682–1832 Ma (Fig. 24c, d; Table 1, Appendix 2 — Table 12). These included significant age components at c. 2493 (6%, three analyses) and 1872 Ma (62%, 39 analyses) interpreted as the age of detrital sources. A maximum depositional age is provided by the weighted mean $^{207}Pb^*/^{206}Pb^*$ date of 1872 ± 6 Ma (MSWD = 1.7) for the 39 youngest analyses.

GSWA 206187: pelitic schist — Biscay Formation

Sample GSWA 206187 is from an andalusite–garnet–biotite–muscovite schist that is interleaved on a kilometre scale with metabasaltic, metavolcaniclastic and metacarbonate rocks, and which has been mapped as part of the Biscay Formation (Blake et al., 1999b). In this location, lower amphibolite facies pelitic to psammitic schists are isoclinally folded with metabasaltic rocks. Andalusite forms large, randomly orientated porphyroblasts that overgrow a regional fabric defined by biotite and muscovite. Garnet porphyroblasts overgrow biotite and locally forms trails of small porphyroblasts. The sample was collected 8.5 km west-northwest of Ruby Plains Homestead (Fig. 1).

Fifty analyses were obtained from 50 zircons (Kirkland et al., 2015c). Forty-seven analyses <5% discordant yield $^{207}Pb^*/^{206}Pb^*$ dates of 2471–1842 Ma (Fig. 24e; Table 1, Appendix 2 — Table 13), including a major age component at c. 1858 Ma (68%) and significant components at c. 2470 (6%) and 2226 Ma (9%). A maximum age of deposition is provided by the weighted mean $^{207}Pb^*/^{206}Pb^*$ date of 1861 ± 3 Ma (MSWD = 1.3) for the 36 youngest analyses.

Hafnium isotope data were collected from 24 zircons ranging in age from c. 2471 to 1842 Ma (Fig. 24f; Appendix 2 — Table 13). The dominant age component at c. 1861 Ma shows a range of εHf compositions from –10.3 to +3.0, consistent with their derivation from mixed early Paleoproterozoic and older Archean sources. A few older Paleoproterozoic and Neoarchean detrital grains have mainly unradiogenic Hf compositions.

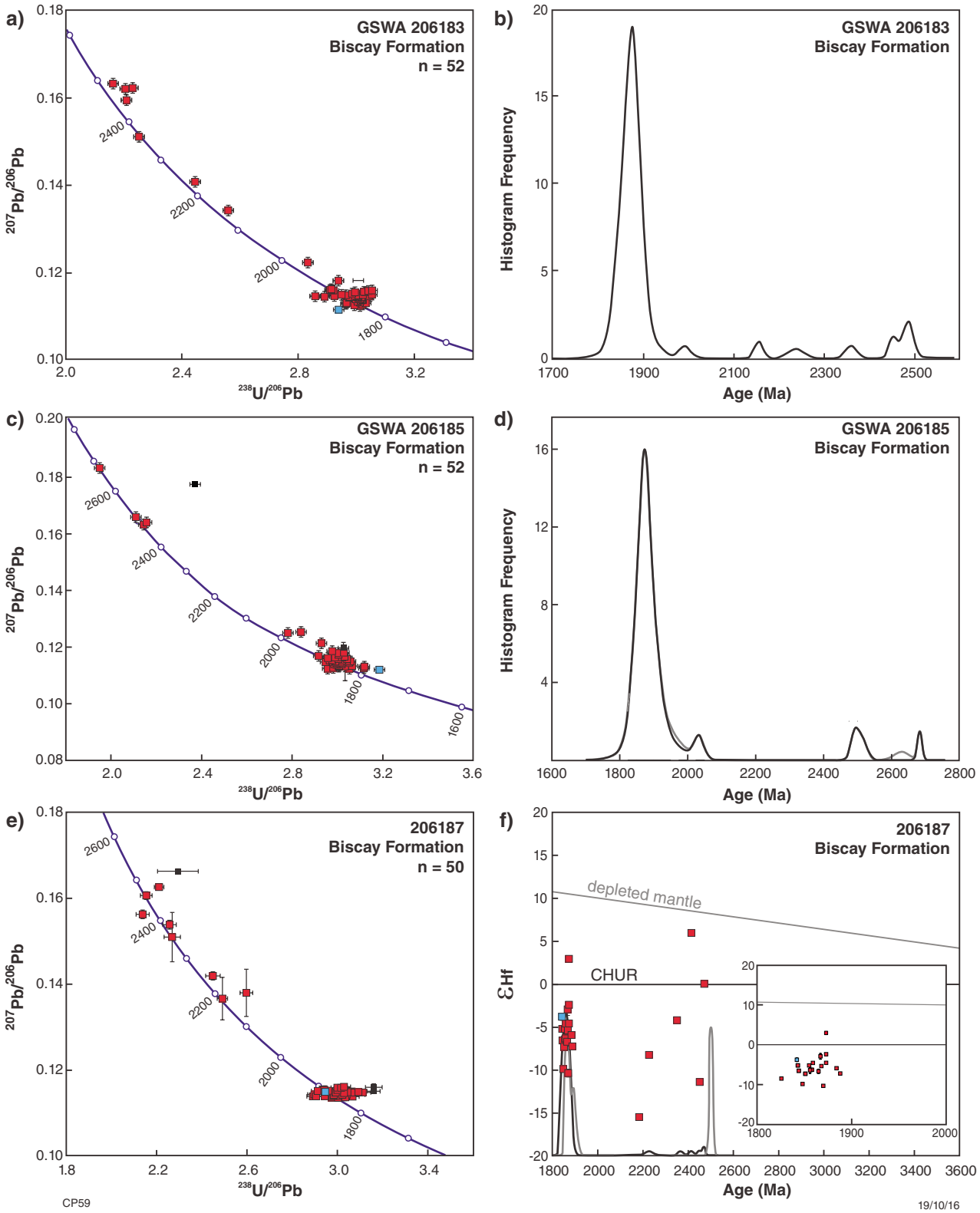

Figure 24. U–Pb and Lu–Hf analytical data for the Biscay Formation: a) U–Pb data for metasandstone, Biscay Formation (GSWA 206183); b) U–Pb probability density diagram for metasandstone, Biscay Formation (GSWA 206183); c) U–Pb data for metasandstone, Biscay Formation (GSWA 206185); d) U–Pb probability density diagram for metasandstone, Biscay Formation (GSWA 206185); e) U–Pb data for a pelitic schist, Biscay Formation (GSWA 206187); f) Lu–Hf data and U–Pb probability density diagram for sample GSWA 206187. For explanation, see the caption to Figure 23.

GSWA 206126: metasandstone — lower Olympio Formation

Sample GSWA 206126 is a fine-grained, massive recrystallized metasandstone collected from the Olympio Formation, stratigraphically below the Maude Headley Member and therefore deposited prior to c. 1856 Ma (GA 85598001; Blake et al., 1999b; this study). It was collected from a low-lying boulder outcrop on Sophie Downs Station, about 34 km northeast of Sophie Downs Homestead and 4 km west of the Saunders Creek Dome (Fig. 1).

Sixty-four analyses were obtained from 64 zircons (Wingate et al., 2015b). Fifty-seven analyses <5% discordant yield $^{207}Pb^*/^{206}Pb^*$ dates of 2847–1830 Ma (Fig. 25a,b; Table 1, Appendix 2 — Table 14), including major age components at c. 1864 (44%) and 1879 Ma (47%), significant components at c. 2496 (7%) and 2518 (14%) and several minor components in the range 2847–1830 Ma. A maximum age of deposition is provided by the weighted mean $^{207}Pb^*/^{206}Pb^*$ date of 1857 ± 3 Ma (MSWD = 1.0) for the 36 youngest analyses.

GA 93525128B: metagreywacke — lower Olympio Formation

Sample GA 93525128B is a coarse-grained, subarkosic turbiditic metagreywacke of the lower Olympio Formation, collected from immediately below the Maude Headley Member. It contains angular quartz and K-feldspar, biotite and metasiltstone clasts. The sample was collected 1 km southeast of the Maude Headley gold deposit and abandoned mine site (Fig. 1).

Nineteen analyses were obtained from 19 zircons. All 19 analyses are <5% discordant and yield $^{207}Pb^*/^{206}Pb^*$ dates of 1864–1918 Ma (Fig. 25c; Table 1, Appendix 2 — Table 15). A maximum age of deposition is provided by the weighted mean $^{207}Pb^*/^{206}Pb^*$ date of 1874 ± 3 Ma (MSWD = 1.5) for the 18 youngest analyses.

Hafnium isotope data were collected from 19 zircons. The dominant age component at c. 1874 Ma shows a range of εHf compositions from –6.6 to –1.3 (Fig. 25d; Appendix 2 — Table 15).

GA 85598001: felsic volcanic rock — Maude Headley Member, Olympio Formation

Sample GA 85598001 is a porphyritic felsic volcanic rock of the Maude Headley Member of the Olympio Formation. Blake et al. (1999b) interpreted this rock as a pyroclastic flow deposit, rather than a sill as previously reported by Page and Hancock (1988). The sample was collected from a volcanic unit concordant with adjacent bedded volcaniclastic rocks in a volcanic succession near the base of the Olympio Formation that, in this location, conformably overlies the Brim Rockhole Formation. It was collected about 24 km northeast of Sophie Downs Homestead (Fig. 1).

Thermal ionization mass spectrometric (TIMS) U–Pb geochronology was described in Page and Hancock (1988), who reported a minimum age of 1856 ± 5 Ma (MSWD = 3.3, n = 10) for zircon crystallization related to volcanism. The same sample was revisited using SHRIMP U–Pb geochronology by Blake et al. (1999b), and these data are reproduced and re-interpreted here. Twenty-one analyses were obtained from 21 zircons. Sixteen analyses <5% discordant yield $^{207}Pb^*/^{206}Pb^*$ dates of 1865–1823 Ma (Fig. 25e; Table 1, Appendix 2 — Table 16) and all 16 analyses yield a weighted mean $^{207}Pb^*/^{206}Pb^*$ date of 1856 ± 6 Ma (MSWD = 0.65), interpreted as the age of volcanism.

Hafnium isotope measurements of 11 zircons ranging in age from c. 1865 to 1833 Ma yielded well-grouped εHf compositions between –2.5 and –0.5 (Fig. 25f; Appendix 2 — Table 16).

GA 87598001: siliciclastic rock — Butchers Gully Member, Olympio Formation

Sample GA 87598001 is a fine-grained siliciclastic rock, previously described as a schistose volcaniclastic rock, viz the 'niobium-tuff' of Chalmers (1990), but which may be a mylonitic metasedimentary or metavolcaniclastic rock. The sampled rock is a fine-grained, strongly foliated rock with angular fragments of quartz, microcline, and vesicular volcanic rock containing fluorite. It was collected about 16 km southeast of Halls Creek (Fig. 1).

U–Pb geochronology was reported in Taylor et al. (1995b) and those data are re-interpreted here. Fifty-five analyses were obtained from 44 zircons. Forty-four analyses <5% discordant yield $^{207}Pb^*/^{206}Pb^*$ dates of 2654–1823 Ma (Fig. 26a; Table 1, Appendix 2 — Table 17). The oldest nine analyses yield $^{207}Pb^*/^{206}Pb^*$ dates of 2654–1921 Ma and are interpreted as having derived from inherited xenocrystic or detrital sources. The youngest 35 analyses are interpreted as representing a single magmatic source and yield a weighted mean $^{207}Pb^*/^{206}Pb^*$ date of 1868 ± 5 Ma (MSWD = 1.4). This was interpreted as an eruption age by Taylor et al. (1995b). In this study, this age is re-interpreted as the age of a xenocrystic or detrital source, given that it is older than the c. 1856 Ma age of the underlying Maude Headley Member.

GA 87598022: siliciclastic rock — Butchers Gully Member, Olympio Formation

Sample GA 87598022 is a very fine-grained siliciclastic rock, previously described as a schistose volcaniclastic rock, the 'niobium-tuff' of Chalmers (1990), but which may be a mylonitic metasedimentary or metavolcaniclastic rock. The sampled rock is a very fine-grained, mylonitic, fluorite-bearing rock, which is possibly a deformed and metamorphosed tuff or volcaniclastic rock collected from the base of the Butchers Gully Member about 15 km southeast of Halls Creek (Fig. 1).

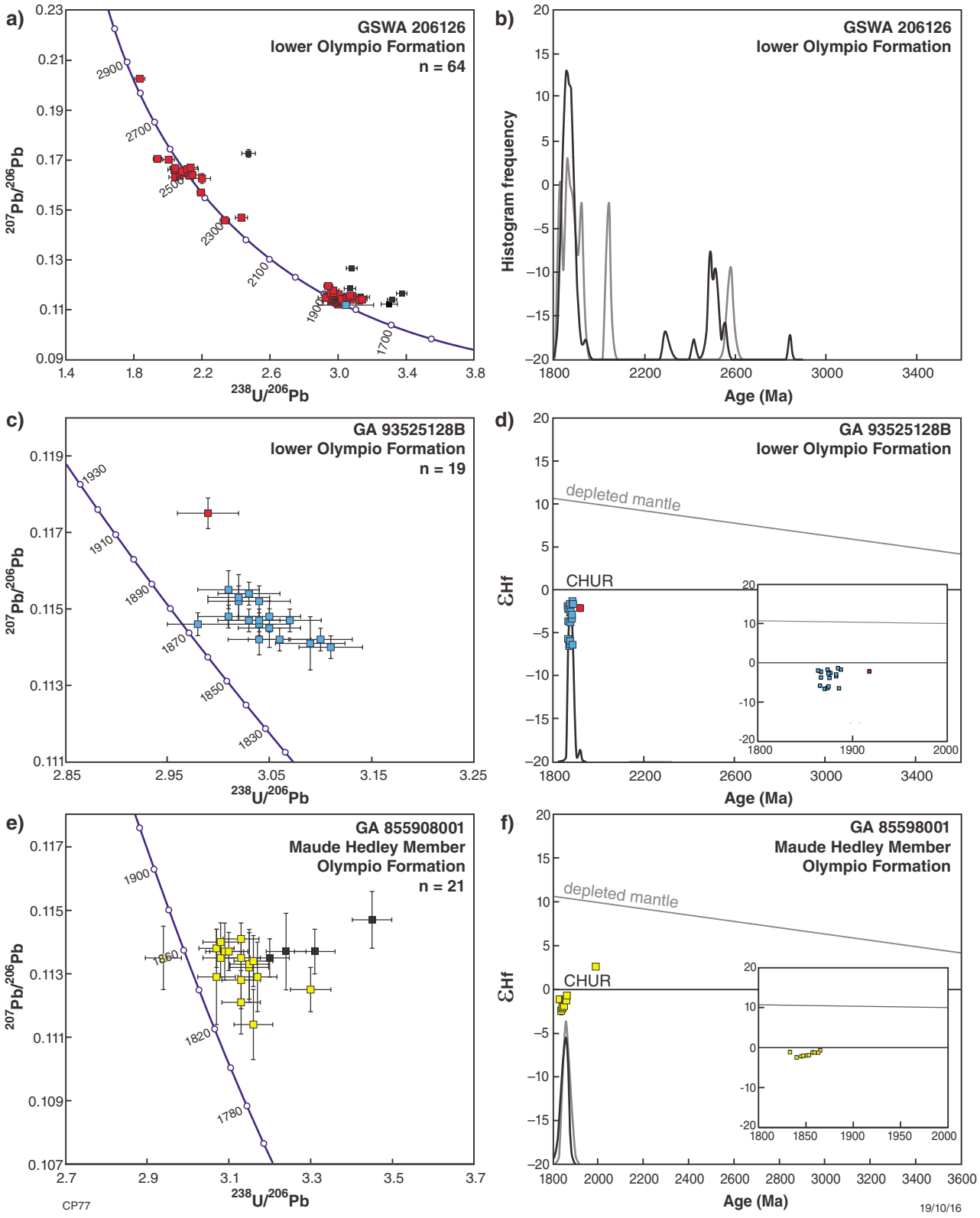

Figure 25. U–Pb and Lu–Hf analytical data for the lower Olympio Formation including the Maude Headley Member: a) U–Pb data for metasandstone, lower Olympio Formation (GSWA 206126); b) U–Pb probability density diagram for sample GSWA 206126; c) U–Pb data for metagreywacke, Olympio Formation (GA 93525128B); d) Lu–Hf data and U–Pb probability density diagram for sample GA 93525128B; e) U–Pb data for a felsic volcanic rock, Maude Headley Member, Olympio Formation (GA 85598001; f) Lu–Hf data and U–Pb probability density diagram for sample GA 85598001. For explanation, see the caption to Figure 23.

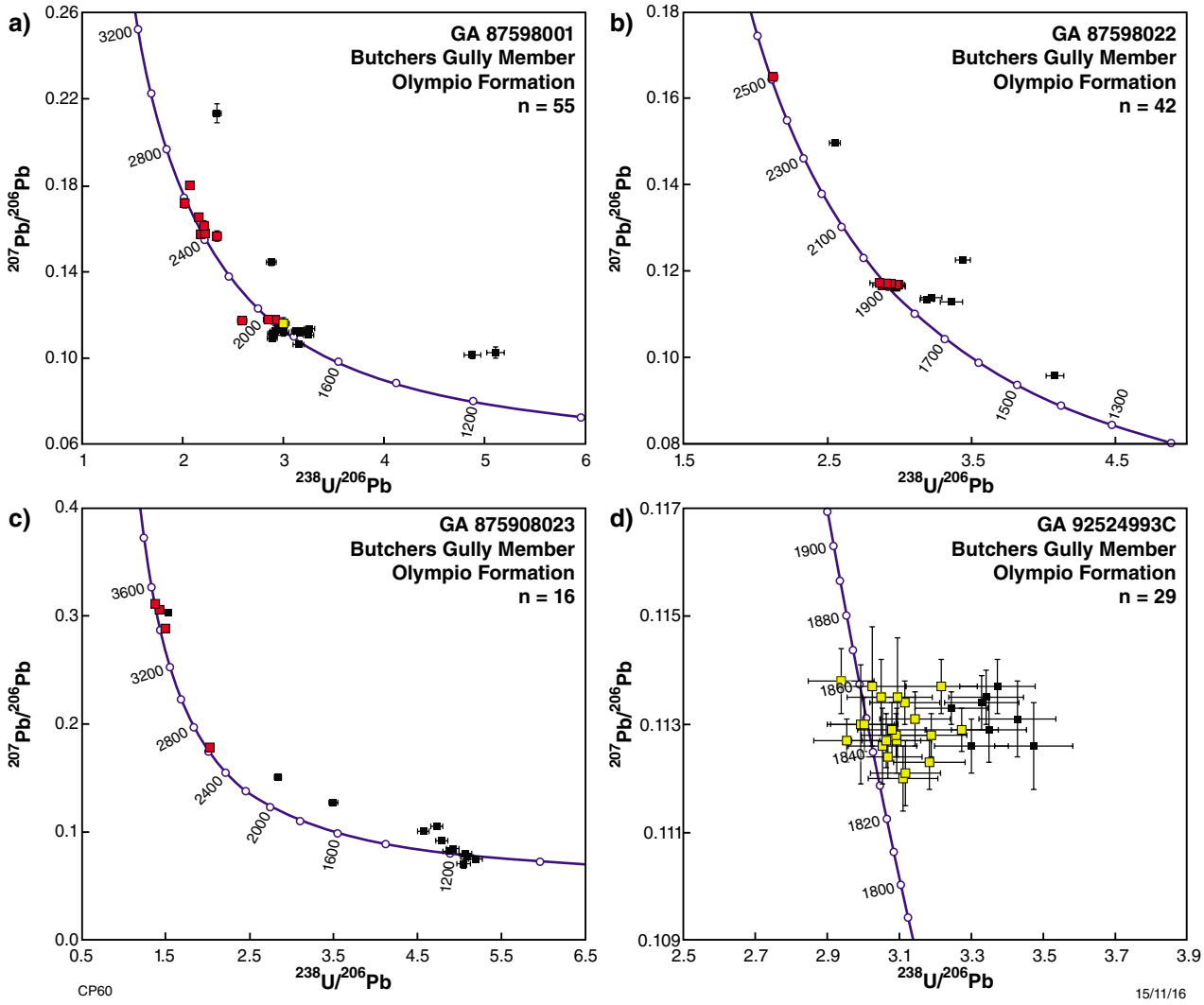

Figure 26. U–Pb analytical data for the Butchers Gully Member, Olympio Formation: a) U–Pb data for a siliciclastic rock (GA 87598001); b) U–Pb data for a siliciclastic rock (GA 87598022); c) U–Pb data for an amygdaloidal trachytic lava (GA 87598023); d) U–Pb data for a trachytic lava (GA 92524993C). Red squares indicate xenocrystic zircons, yellow squares indicate magmatic zircons, black squares indicate data that are >5% discordant. Error bars are ± 1σ. n is the number of analyses. Full details of U–Pb geochronology for these samples are available in published GSWA Geochronology Records.

Forty-two analyses were obtained from 41 zircons. Thirty-six analyses <5% discordant yield $^{207}Pb^*/^{206}Pb^*$ dates of 2506–1856 Ma (Fig. 26b; Table 1, Appendix 2 — Table 18), including significant age components at c. 1906, 1872 and 1862 Ma. These are interpreted as the ages of detrital sources. A maximum age of deposition is provided by the weighted mean $^{207}Pb^*/^{206}Pb^*$ date of 1868 ± 3 Ma (MSWD = 1.15) for the 19 youngest analyses. This is interpreted as a detrital or xenocrystic zircon component, rather than an eruption age as interpreted by Taylor et al. (1995b), because it is older than the c. 1856 Ma age of the stratigraphically underlying Maude Headley Member. The c. 1906 Ma detrital age component is consistent, within uncertainty, with derivation from the underlying c. 1912 Ma Sophie Downs Granite and Ding Dong Downs Volcanics or similar-aged magmatic rock.

GA 87598023: trachytic lava — Butchers Gully Member, Olympio Formation

Sample GA 87598023 is an amygdaloidal trachytic lava of the Butchers Gully Member collected from the same location as sample GA 87598022, about 15 km southeast of Halls Creek (Fig. 1).

Sixteen analyses were obtained from 15 zircons. Four analyses <5% discordant yield $^{207}Pb^*/^{206}Pb^*$ dates of c. 3526, 3499, 3408 and 2637 Ma (Fig. 26c; Table 1, Appendix 2 — Table 19) interpreted as xenocrystic zircons. The remainder of the analyses are >5% discordant or show evidence of Pb loss.

GA 92524993C: trachytic lava — Butchers Gully Member, Olympio Formation

Sample GA 92524993C is an amygdaloidal trachytic pillow lava of the Butchers Gully Member collected 17 km southeast of Halls Creek (Fig. 1).

Twenty-nine analyses were obtained from 26 zircons. Nineteen analyses <5% discordant yield a weighted mean $^{207}Pb^*/^{206}Pb^*$ date of 1846 ± 4 Ma (Fig. 26d; Table 1, Appendix 2 — Table 20; MSWD = 0.76), interpreted as the age of volcanism.

GA 92524896: metasandstone — upper Olympio Formation

Sample GA 92524896 is a coarse-grained subarkosic metasandstone, collected from turbiditic metasedimentary rocks of the upper Olympio Formation, stratigraphically above the Maude Headley Member.

Twenty-three analyses were obtained from 22 zircons. Twenty-one analyses <5% discordant yield $^{207}Pb^*/^{206}Pb^*$ dates of 2528–1809 Ma (Fig. 27a; Table 1, Appendix 2 — Table 21). The youngest analysis, at 1809 ± 11 Ma (1σ), shows evidence of Pb loss. Excluding the single older

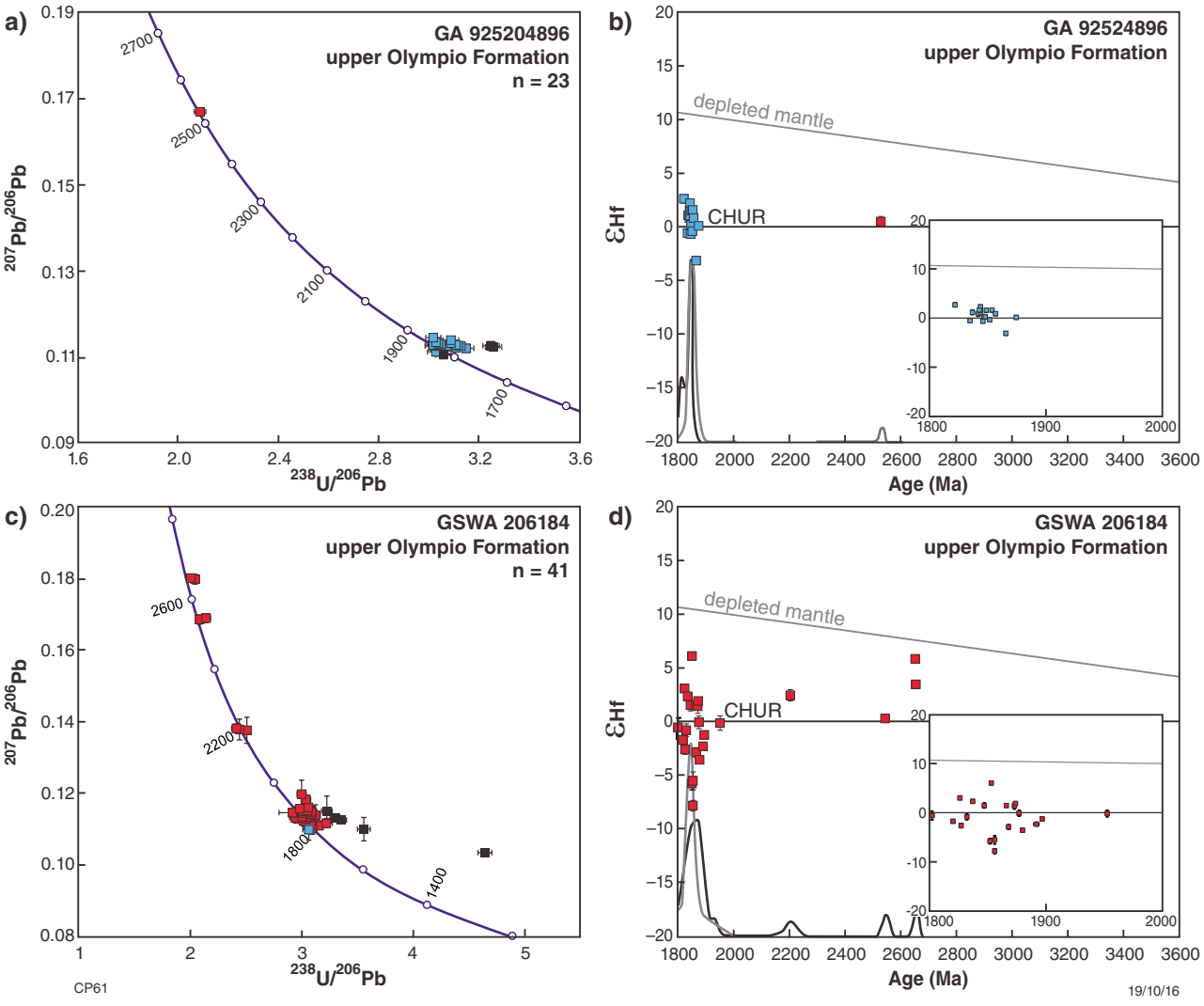

Figure 27. Lu–Hf data and U–Pb probability density diagram for the upper Olympio Formation: a) U–Pb data for metasandstone, upper Olympio Formation (GA 92524896); b) Lu–Hf data and U–Pb probability density diagram for sample GA 92524896; c) U–Pb data for metasandstone, upper Olympio Formation (GSWA 206184); d) Lu–Hf data and U–Pb probability density diagram for sample GSWA 206184. For explanation, see the caption to Figure 23.

individual at c. 2528 Ma, a maximum age of deposition is provided by the weighted mean $^{207}Pb^*/^{206}Pb^*$ date of 1848 ± 5 Ma (MSWD = 1.7) for the remaining 19 analyses. This is within uncertainty of the eruption age of the c. 1846 Ma Butchers Gully Member.

Hafnium isotope data for these 19 zircons range in age from c. 2528 to 1821 Ma (Fig. 27b; Appendix 2 — Table 21). The c. 1848 Ma population yielded a spread in Hf composition with εHf = –3.3 to +2.5.

GSWA 206184: metasandstone — upper Olympio Formation

Sample GSWA 206184 is a fine-grained, normal-graded, medium- to very thick-bedded turbidite metasandstone and represents the stratigraphic top of the exposed succession of the Olympio Formation collected from a low scarp about 2 km east-northeast of Sawpit Gorge (Fig. 1).

Forty-one analyses were obtained from 41 zircons (Wingate et al., 2015c). Thirty-six analyses <5% discordant yield $^{207}Pb^*/^{206}Pb^*$ dates of 2656–1797 Ma (Fig. 27c; Table 1, Appendix 2 — Table 22), including significant age components at c. 2205, 1928 and 1871 Ma. A maximum age of deposition is provided by the weighted mean $^{207}Pb^*/^{206}Pb^*$ date of 1834 ± 8 Ma (MSWD = 1.1) for the 14 youngest analyses. This is significantly younger than the eruption age of the underlying 1846 ± 4 Ma Butchers Gully Member and is within uncertainty of the magmatic age of the 1832 ± 5 Ma Mabel Downs Tonalite of the Sally Downs Supersuite (Bodorkos et al., 2000), which was emplaced during the Halls Creek Orogeny.

Hafnium isotope data from 25 zircons ranging in age from c. 2656 to 1797 Ma (Fig. 27d; Appendix 2 — Table 22) yielded a range of εHf compositions between –7.8 and +6.1.

Discussion

The Eastern Zone of the Lamboo Province represents more than 124 Ma of geological history on the western margin of the North Australian Craton. In this discussion sedimentology, volcanology, geochemistry and geochronology combine to elucidate the development of the Eastern Zone and the evolution of the margin of the North Australian Craton as well as the implications for regional geology. This Report also proposes a new formation, the Brim Rockhole Formation, to describe siliciclastic and carbonate metasedimentary rocks and intercalated bimodal metavolcanic rocks formerly at the base of the Biscay Formation. The separation into a new formation is based on different sedimentology and U–Pb zircon ages.

Evolution of the Eastern Zone

Basement development: 1912–1904 Ma Sophie Downs Suite

The age of the Sophie Downs Suite is tightly constrained to between c. 1912 and 1904 Ma, based on the five samples dated here (Fig. 22a–f; Table 1, Appendix 2 — Tables 1–5). This age is relatively uncommon within the North Australian Craton and Proterozoic Australia in general. This study focused on extrusive bimodal metavolcanic rocks of the Ding Dong Downs Volcanics intercalated with mafic-derived and pelitic metasedimentary rocks. Peperitic margins to the metabasalt units indicate contemporaneous volcanism and sedimentation. The depositional environment is uncertain, but may have been partially subaerial (Blake et al., 2000). Low Ni contents indicate that the mafic rocks underwent olivine crystal fractionation prior to eruption while depletions in Sr and significant negative Eu anomalies suggest plagioclase crystallization. Depletions in Nb and Ta and initial εNd values close to crust or CHUR suggest some crustal contamination (Fig. 21).

Metafelsic rocks of the Sophie Downs Suite have A-type granite geochemical signatures and are metaluminous to peraluminous (Fig. 13d,e). Some zircons from the felsic rocks have radiogenic εHf zircon values (+0.8 to +2.7; Fig. 22f) suggesting a mantle contribution. Ogasawara (1988) suggested that the Sophie Downs Suite could have formed in a rift environment. Similar geochemical characteristics of A-type magmatism and moderate Nd-isotopic values with more juvenile zircon Hf-isotopic values are apparent in granites of the Delamarian and Lachlan Fold Belt of eastern Australia (Kemp et al., 2005, 2009). Analogous metaluminous A-type granites in the Lachlan Fold Belt reflect a large degree of crustal assimilation, and the juvenile isotope signature of these magmas indicate significant extensional collapse (Kemp et al., 2009). These authors suggested that these granites formed in back-arc environments, related to slab rollback concomitant with crustal accretion. Although the geochemical characteristics of the Sophie Downs Suite are not unique as they share continental and back-arc affinities, it is probable that the basement rocks of the Eastern Zone represent passive margin volcanism, magmatism and crustal assimilation on the North Australian Craton.

Comparing Sm–Nd whole-rock data of felsic and mafic rocks in the Sophie Downs Suite, mafic rocks have lower radiogenic εNd_i values (–0.78 to +0.21) with T_{DM}^2 model ages of c. 2300 Ma while felsic rocks have εNd_i values of –4.72 to –3.82 with model ages at c. 2600 Ma (Fig. 21; Appendix 1 — Table 9). These Sm–Nd data and T_{DM}^2 model ages indicate mixing of juvenile mafic magma with sediment or older crust to produce near CHUR εNd values.

Basin initiation: 1904–1881 Ma Saunders Creek and Brim Rockhole Formations

The Halls Creek Group marks a new phase of deposition in the Eastern Zone beginning with deposition of the Saunders Creek Formation. These rocks are texturally and mineralogically immature with poor sorting, angular grains and coarse grain size, indicative of proximal-to-source settings. Abundant trough cross-bedding, overturned cross-bedding and heavy mineral cross-laminations containing magnetite, ilmenite, monazite, rutile and zircon suggest a high current energy setting with stacked channels typical of braided river systems

(Fig. 6a,b). The Saunders Creek Formation locally fines upward to planar-laminated metasiltstone punctuated by erosive metasandstone beds interpreted as overbank or floodplain deposits or possibly high current energy events in a lacustrine setting (Figs 6c and 28a).

The Saunders Creek Formation was deposited after c. 1904 Ma, the age of the youngest rocks in the underlying basement, but before c. 1881 Ma, the age of felsic metavolcanic rocks in the overlying Brim Rockhole Formation. Gradational contacts between the Saunders Creek and Brim Rockhole Formations suggest fluvial deposition began closer to c. 1881 Ma. The two formations have similar detrital zircon age spectra, both dominated by Neoarchean to Paleoarchean grains (c. 3585, 3530, 3350, 2680 and 2508 Ma; Fig. 23a–h, Table 1). The nearest, currently exposed, magmatic Archean rocks are found in the c. 2550 Ma Billabong Complex of the Granites–Tanami Orogen to the southeast (Page et al., 1995; Blake et al., 2000; Cross and Crispe, 2007; Crispe et al., 2007). The 2550–2510 Ma magmatic zircons from the Billabong Complex show a greater spread of unradiogenic and radiogenic data (εHf = –5.8 to +4.1) (Whelan et al., 2014), compared to similar aged detrital zircons in the Saunders Creek and Brim Rockhole Formations, which have dominantly unradiogenic isotopic compositions (εHf = –13.3 to +0.0; Figs 23b,d,h). Limited data and minor overlap in Hf isotope compositions are inconsistent and insufficient to identify confidently the magmatic sources of detrital zircons in the Saunders Creek and Brim Rockhole Formations, possibly suggesting recycled sedimentary terranes as the direct source.

The absence of c. 1910 Ma detrital zircons in the Saunders Creek Formation is consistent with a partially or entirely buried local basement during development of the fluvial system. The c. 1910 Ma detrital zircon components in the Brim Rockhole Formation display Hf isotope data indicating an unradiogenic source (εHf = –10.4 to –0.2; GSWA 206121; Fig. 23h, Appendix 2, Table 13). Hafnium isotope data from magmatic zircons in the c. 1910 Ma Sophie Downs Suite are relatively juvenile (εHf = +0.8 to +2.7; Fig. 22f) but are within uncertainty of data from the Brim Rockhole Formation possibly indicating that the Sophie Downs Suite may have been exposed for a brief time during deposition of the Brim Rockhole Formation.

Brim Rockhole Formation lithofacies have a broadly shallow-marine origin with laminated quartzites becoming finer grained, carbonaceous, micaceous and heavy mineral-bearing up section (Fig. 7a–c). Planar-laminated and fine-grained carbonaceous metasedimentary lithofacies indicate a current-restricted depositional setting, possibly in topographically controlled depocentres around basement highs. Graphitic schists contain 4.24 wt% C, 7.04 wt% Fe_2O_3 and elevated Mo relative to average continental crust (Taylor and McLennan, 1995). This chemistry has been used to indicate anoxic or dysoxic and reducing conditions in ancient settings (Reinhard et al., 2013). The source of the carbon could be organic although no microbial textures are preserved. However, the intensity of deformation would probably have erased this evidence if it were present. Exposed carbonate metasedimentary rocks consist of 150 m of interbedded greenschist facies limestone, sandy limestone, calcareous siltstone, carbonate schists and lesser marble (Fig. 7d–f). There is no evidence for subaerial exposure to suggest carbonate deposition in an emergent setting. Likewise, there are no evaporitic textures or minerals and no correlation between Ca/Na, Ca/Mg and Ca/Sr ratios which have been used to infer ancient evaporitic environments (Sass and Katz, 1982). Deposition of Brim Rockhole Formation metasedimentary carbonates took place above fair-weather wave base in a shallow-marine or possibly lacustrine setting. The $CaO:SiO_2$ ratio in calcareous metasedimentary samples is commonly around 1:1, indicating carbonate deposition on or near a continental margin with constant input of terrigenous material. Sample GSWA 206047 has a $CaO:SiO_2$ ratio of 5:1, possibly indicating periods of clastic dilution and decreased continental runoff. Fragmentary metafelsic material intercalated with calcareous metasedimentary rocks northwest of the Sophie Downs Dome indicates active volcanism in the basin and proximity to a volcanic centre. Volcanism was coeval with carbonate sedimentation at c. 1881 Ma (GA 93526012; Fig. 23i). The unconformity at the top of the calcareous unit (Fig. 8) suggests a depositional hiatus, probably due to basin subsidence and flooding followed by deposition of the shallow-marine Biscay Formation.

Continuing extension, magmatism and subsidence: c. 1881–1861 Ma Biscay Formation

The Biscay Formation is redefined in this Report to describe immature lithic metasandstone beds commonly massive or wavy to planar-laminated, interbedded with massive or cleaved metasiltstone deposited on the Brim Rockhole Formation. Metasedimentary packages have either a planar geometry or gently pinch and swell along strike with uncommon erosive contacts. These features suggest deposition in an unrestricted shallow-marine setting, probably tidally influenced. Higher current energy episodes produced erosive contacts and rare coarse-grained beds, possibly tempestite facies. Immature and lithic metasandstone with clasts of metasiltstone and metasandstone indicate sourcing from a proximal continental province with grains of pyroxene, actinolite, biotite, chlorite and magnetite (some now hematite) probably indicative of partial derivation from the concomitant mafic volcanism.

There is a considerable difference in detrital zircon modal ages between the Brim Rockhole Formation and the Biscay Formation. The Brim Rockhole Formation is dated at 1881 ± 4 Ma (GA 93526012; Fig. 23i; Table 1) with detrital zircons yielding dominant age components at 3656–2496 Ma (Fig. 23e–h) similar to those from the Saunders Creek Formation. Biscay Formation metasedimentary rocks, however, contain detrital zircons that have dominant components at 2493–2226 Ma and 1873–1858 Ma (Fig. 24a–f) with maximum depositional ages of 1872 ± 5, 1872 ± 6 and 1861 ± 3 Ma (GSWA 206183, 206185 and 206187, respectively; Table 1).

Hafnium data from the Biscay Formation indicate a mix of radiogenic and unradiogenic sources (εHf = –10.3 to +3.0; Fig. 24f) supporting sedimentology which indicates a mix of autochthonous and allochthonous sources. These maximum depositional ages are closer in age to the c. 1856 Ma age of volcanism of the Maude Headley Member in the overlying Olympio Formation. Indeed, Biscay Formation metasedimentary samples have a similar detrital zircon age spectrum to GSWA 206126 and GA 93525128B of the lower Olympio Formation, with which it shares a similar spread in unradiogenic zircon Hf compositions for the youngest age component (Fig. 25) as well as similar REE trends in metasandstone samples (Fig. 14). These data indicate the Biscay Formation and Olympio Formation share similar sources with similar chemistry.

Sheppard et al. (1999b) described two geochemical groups of mafic rocks in the Biscay Formation. Although some new samples have affinities with these groups, many do not. These new data indicate fractionation trends involving olivine, pyroxene and feldspar. Interestingly, group 1 samples of Sheppard et al. (1999b) are all from the Brim Rockhole Formation, and two of the three samples Sheppard et al. (1999b) defined as group 2 are from the Biscay Formation. Brim Rockhole Formation and Biscay Formation metamafic samples are petrographically and geochemically similar and fall on a trend consistent with fractionation of pyroxene (CaO, Cr), olivine (Ni) and feldspar (Al_2O_3, Sr, Eu; Winter et al., 1992). Incompatible elements such as Zr, Y and REE are concentrated in less MgO-rich rocks. PM-normalized spider diagram patterns are consistent with lower crust contamination (Naldrett, 2004) although Nb anomalies are less prominent in the older succession. Strontium depletion and negative Eu anomalies indicate feldspar fractionation, which is most prominent in more evolved samples. No samples of primary mantle-like magmas are present. The most primitive samples have flat trace element pattern in chondrite-normalized spider diagrams but high Pb and LILE contents indicate crustal contamination. The least fractionated, isotopically most primitive, metabasalts from what Sheppard et al. (1999b) called group 1 Biscay Formation are now redefined as Brim Rockhole Formation samples (εNd_i = +2.53 and +3.31; Fig. 21). They may represent volcanism accompanying crustal attenuation and the development of a basin within older continental crust. These authors considered these metabasalts to be most similar to the enriched metabasalt of the 1865–1850 Ma Tickalara Metamorphics, interpreted as having formed in an island arc, continental back-arc or ensialic basin margin setting (Sheppard et al., 1999b; Griffin et al., 2000a). However, similar basalts are also present as the least-enriched end members of continental flood basalts (Hooper and Hawkesworth, 1993; Hooper, 1997).

Nearly all basaltic rocks around Ruby Plains Homestead belong to the least fractionated samples (highest MgO contents) of the Biscay Formation. Sheppard et al. (1999b) considered the geochemical patterns of these rocks to be similar to continental flood basalts derived by melting of the subcontinental lithosphere. The geographical clustering of these metabasalts suggests that they may all belong to a local volcanic centre.

The most evolved metabasaltic rocks may represent continental flood basalts with elevated LILE and LREE and elevated M–HREE (Fig. 17a,b). This interpretation is supported by Sm–Nd whole-rock isotope data that indicate that the most isotopically evolved samples (εNd_i = –0.78) of the Biscay Formation are from and the most fractionated basalts (Fig. 21). These data are consistent with a prolonged magmatic event, which commenced during basin initiation, marked by intercalated metabasalt in the Brim Rockhole Formation at c. 1881 Ma, to the end of the Biscay Formation at c. 1861 Ma. This study proposes that the magmas became more isotopically evolved through time, consistent with increasing proportions of crustal contamination, and may be related to extension on the passive margin of the North Australian Craton.

Basin drowning: c. 1856–1808 Ma Olympio Formation

The Olympio Formation consists of >4 km of siliciclastic metasedimentary rocks deposited in a turbidite fan system over a period of at least 22 Ma from c. 1856 to <1834 Ma. A disconformable surface is present at the base of the Olympio Formation, where it transgresses the Biscay Formation. The contact is marked by basalt (Fig. 10a) or chert. Blake et al. (1999b) interpreted these cherts as a flooding surface. Warren (1997) suggested that the disconformable surface may represent a low-angle D_1 structure. The abrupt change in lithofacies and the erosive nature of the contact in various places on Halls Creek and McIntosh suggest that the contact is probably a transgressive erosion surface, marking major basin subsidence and flooding. Basin drowning was probably the result of significant subsidence caused by extension elsewhere in the Lamboo Province at this time (i.e. emplacement of the Paperbark Supersuite at 1864–1852 Ma in the Western Zone or the beginning of layered mafic–ultramafic intrusions in the Central Zone at c. 1855 Ma).

Volumetrically abundant metasedimentary lithofacies include immature metasandstone turbidites interbedded with quartz-rich metasiltstone hemipelagite. Metasandstone-rich turbidites contain sedimentary structures characteristic of Bouma divisions T_{ABD} whereas silty metasandstone beds and metasiltstone-dominated units probably represent Bouma divisions T_{DEF} (Bouma, 1962). These lithofacies are present at all stratigraphic levels. Sheet-like geometry and dominance of massive beds suggests an intrachannel setting in middle to outer turbidite fan lobes on a continental shelf or slope (Fig. 28c; Pickering et al., 1989; Phillips et al., 2011). Conglomeratic lags and coarse-grained meta-arkose are rare and probably indicate proximity to intralobe channels or deposition from high-volume, high-current energy turbidity currents delivering coarser material to the depocentre.

Submarine alkaline lavas and associated volcaniclastic units punctuate deep-marine sedimentation, producing two distinct members — the 1856 ± 5 Ma Maude Headley Member and the 1846 ± 4 Ma Butchers Gully Member.

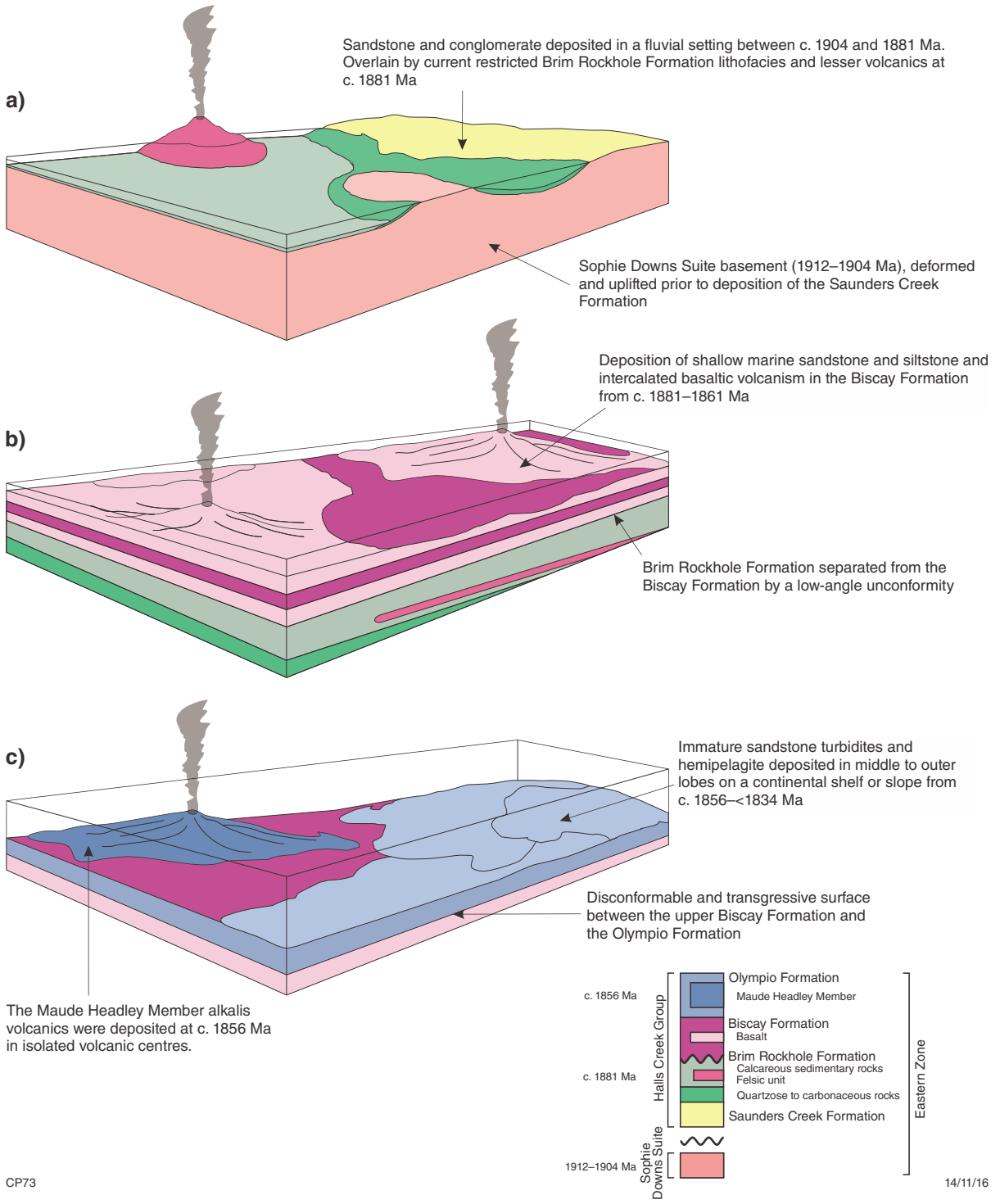

Figure 28. Depositional models of the Halls Creek Group: a) Saunders Creek Formation fluvial system and probable shallow marine restricted lithofacies of the Brim Rockhole Formation sourced from Archean rocks; b) Biscay Formation depositional environment, probably a shallow marine shelf setting with mafic volcanic centres; c) deposition of turbidites in the Olympio Formation on a deeper shelf or slope with intercalated alkalis volcanic centre. The c. 1846 Ma Butchers Gully Member was probably deposited in a similar setting.

Both members represent discrete volcanic centres made of lavas, volcaniclastic rocks and debrites intercalated with turbidite sedimentation (Fig. 28c). Carbonate breccia beds may represent collapse of local fringing carbonate lithofacies deposited on volcano flanks. Pillow lavas from the Butchers Gully Member in the Gardner Creek Anticline on Ruby Plains and Dockrell (Fig. 2) indicate subaqueous deposition and some breccia beds may be the product of fire fountaining (Tyler et al., 1998). Fire fountaining and explosive volcanism are reported from seamounts (Smith and Batiza, 1989) and deep-marine successions (Allen et al., 1997; Simpson and McPhie, 2001). Recent observations of explosive submarine mafic eruptions suggest that they can occur at depths greater than 1000 m below sea level (Chadwick Jr et al., 2008).

Despite the similarity in lithofacies throughout the formation, Hf isotopic composition and detrital zircon age profiles are distinct between lower and upper turbidite units (i.e. metasandstone turbidite units stratigraphically below the Maude Headley Member and above the Butchers Gully Member, respectively). Lower Olympio Formation turbidite metasandstone beds contain detrital zircon grains with dominant age modes at 1875–1860 Ma. These grains have a range of Hf isotopic compositions that are slightly more evolved than CHUR (Hf = –6.6 to –1.3; Fig. 25d). Upper Olympio Formation turbidites also contain an age mode at 1875–1860 Ma and a younger detrital source with dominant ages modes at 1848–1834 Ma, and have a range of Hf isotopic compositions that are mostly more radiogenic than CHUR (εHf typically –3.5 to +6.1; Fig. 27b,d). Notably, the youngest detrital zircon in the Olympio Formation has been dated at 1834 ± 8 Ma (Fig. 27c) which overlaps with the beginning of the Halls Creek Orogeny defined by D_1 deformation of the 1832 ± 3 Ma Mabel Downs Tonalite (Page et al., 2001). This suggests that sedimentation in the upper part of the Olympio Formation may represent deposition into a foreland basin off the North Australian Craton.

Intrusion of the Woodward Dolerite: c. 1835 Ma

Primitive mafic magma represented by sills of the Woodward Dolerite was emplaced into the Sophie Downs Suite and throughout the Halls Creek Group prior to deformation and metamorphism during the Halls Creek Orogeny. The dolerite is younger than the Butchers Gully Member dated at c. 1846 Ma and the upper Olympio Formation, which has a maximum deposition age of 1834 ± 8 Ma (Fig. 28c; GSWA 206184). The Woodward Dolerite was deformed by the Halls Creek Orogeny and therefore must have a minimum age >1832–1808 Ma (Tyler and Page, 1996; Tyler et al., 1998; Blake et al., 2000; Page et al., 2001). An age of c. 1835 Ma is assumed to be an acceptable estimate for the intrusion of the Woodward Dolerite. The Woodward Dolerite displays geochemical characteristics similar to those of mafic rocks of the Ding Dong Downs Volcanics, and more primitive mafic rocks of the Brim Rockhole and Biscay Formations (Fig. 21). The εNd_i values (–0.86 to +3.05; Appendix 1, Table 9) indicate derivation from a primitive source (Sun et al., 1991; Sun and Hoatson, 2000) and the depleted Nb and Ta contents coupled with elevated LILE concentrations are consistent with some crustal contamination (Fig. 20). The Woodward Dolerite possibly represents the final opening of conduits and heating associated with tapping the lithospheric mantle beneath this portion of the crust just prior to the onset of the Halls Creek Orogeny.

Correlations with the Granites–Tanami Orogen

Regional correlations with the Halls Creek Orogen have focused on the Paleoproterozoic Granites–Tanami Orogen (Crispe et al., 2007; Cross and Crispe, 2007; Bagas et al., 2008, 2010; Joly et al., 2010). This study interprets a portion of shared provenance between these coeval orogens and reinterprets some Granites–Tanami Orogen stratigraphy based on evidence from new detrital zircon age data (Fig. 3). Metasedimentary units of the 1880–1830 Ma Tanami Group include the Stubbins Formation, Dead Bullock Formation and Killi Killi Formation, interpreted to be broadly a deep-marine succession with constituent lithofacies commonly, or exclusively, turbiditic (Crispe et al., 2007; Lambeck et al., 2008, 2012; Bagas et al., 2014). Bagas et al. (2014) included the Mount Charles Formation and Stubbins Formation in the Dead Bullock Formation based whole-rock and trace-element geochemistry, geochronology and lithostratigraphy at the Coyote gold mine. In this Report, the Mount Charlies and Subbins Formations are kept separate based on the lack of outcropping structural relationships between the Stubbins Formation and Dead Bullock Formation but are considered correlatives within the Tanami Group (Fig. 3; Crispe et al., 2007; Lambeck et al., 2008). The enigmatic Mount Charles Formation consists of volcano-sedimentary units, probably deposited from turbidity currents (Tunks and Cooke, 2007; Huston et al., 2007). The age and stratigraphic position of the Mount Charles Formation is poorly constrained. The 1825–1815 Ma Ware Group overlies the Tanami Group with apparent unconformity and consists of submarine to subaerial volcanic and siliciclastic sedimentary rocks (Huston et al., 2007).

Mount Charles Formation

The Mount Charles Formation is a package of fine- to coarse-grained siliciclastic sedimentary rocks and intercalated massive and pillowed basalt with some basalt breccia (Tunks and Cooke, 2007). Fine-grained lithofacies are commonly ferruginous and carbonaceous and host significant gold mineralization (Tunks, 1996; Crispe et al., 2007; Tunks and Cooke, 2007). Detrital zircons from arkosic sandstone beds in the Mount Charles Formation are dominated by Archean grains with dominant age modes at 3500–3320 Ma and c. 2504 Ma with subordinate Paleoproterozoic grains dated at 1913 ± 18 Ma and 1905 ± 12 Ma (Cross and Crispe, 2007). The detrital zircon age spectra are very similar to samples from the Saunders Creek and Brim Rockhole

Formations, especially GSWA 206121 of the Brim Rockhole Formation that has age modes at 3613–2510 Ma and c. 1909 Ma. Zircons dated at c. 1910 Ma are rare on the North Australian Craton, and are only observed as detrital grains from the Brim Rockhole Formation and Mount Charles Formation and as magmatic zircons from the 1912–1909 Ma Sophie Downs Suite. A maximum depositional age of 1916 ± 8 Ma for the Mount Charles Formation was provided by the youngest 14 detrital zircon analyses (Page, 1998). Cross and Crispe (2007) considered the formation to have been deposited at c. 1800 Ma and placed it stratigraphically above the Tanami and Ware Groups (fig. 3 in Cross and Crispe, 2007). However, c. 1870 Ma detrital zircons are ubiquitous in the Tanami and Ware Group rocks but are absent in the Mount Charles Formation, which exclusively contains much older grains (Cross and Crispe, 2007). In their model, Cross and Crispe (2007) suggested that c. 1910 Ma detrital zircons in the Mount Charles Formation were sourced from the Ding Dong Downs Volcanics; however, at c. 1800 Ma the Lamboo Province was most likely buried beneath the Speewah and Kimberley Basins. Paleocurrents from the Speewah and Kimberley Groups indicate detrital sources from the northeast and northwest with no change in paleocurrent direction adjacent to the Lamboo Province (Gellatly et al., 1970). This would suggest that the Lamboo Province, particularly the Sophie Downs Suite, was buried during deposition of the Speewah and Kimberley Groups (Hollis et al., 2014). Based on the available evidence, it is possible that the Mount Charles Formation was deposited closer in time to its youngest constituent detrital zircon grains (i.e. c. 1916 Ma) and is roughly coeval with the Saunders Creek Formation and Brim Rockhole Formation with which it shares very similar detrital zircon age spectra. This interpretation of an older Mount Charles Formation is in agreement with Bagas et al. (2014). With the absence of other exposed c. 1910 Ma sources on the North Australian Craton, it is possible that the Sophie Downs Suite was the source of material for the Mount Charles Formation during a brief interval prior to deposition of the Tanami Group. Alternatively, the Brim Rockhole Formation, which also contains a number of c. 1910 Ma zircon grains, may have been reworked and deposited in the Granites–Tanami Orogen. At present, there are no Hf isotopic data from the Mount Charles Formation to test these hypotheses.

Stubbins Formation

The Stubbins Formation consists of sandstone and siltstone turbiditic rocks overlain by ferruginous and carbonaceous fine-grained lithofacies with intercalated basalt and dolerite (Bagas et al., 2008). The timing of deposition has been constrained at 1864 ± 3 Ma from a rhyolitic porphyry within the formation (Fig. 3; Cross and Crispe, 2007; Bagas et al., 2008). Two sedimentary samples from the Stubbins Formation provide maximum depositional ages of c. 1875 Ma and c. 1869 Ma (Maidment et al., written comm., 2016). These dates indicate that deposition of the Stubbins Formation (i.e. between c. 1869 and 1864 Ma) was broadly coeval with: 1) extension and the start of emplacement of the 1864–1852 Ma Paperbark Supersuite in the Western Zone; 2) deposition of the sedimentary protoliths to the Tickalara Metamorphics in the Central Zone and; 3) deposition of the Biscay Formation and lower Olympio Formation in the Eastern Zone. Detrital zircons from the Biscay Formation and lower Olympio Formation are dominated by age components at 1879–1858 Ma sharing similar detrital age spectra with the Stubbins Formation that are dominated by 1875–1864 Ma zircons (Maidment et al., written comm., 2016). Based on these data, it is possible that the Stubbins Formation was deposited at the same time as the Biscay and lower Olympio Formations, possibly from the same sources (Fig. 3).

Killi Killi Formation

The Olympio Formation in the Eastern Zone and the Killi Killi Formation in the Granites–Tanami Orogen have similar lithofacies, REE trends and detrital zircon ages. The Killi Killi Formation consists of up to 4 km of monotonous, variably micaceous and lithic, turbiditic metasandstone that are interbedded with metasiltstone (Cross and Crispe, 2007) interpreted as part of a basin-floor fan system (Lambeck et al., 2012). The formation was deposited after c. 1864 Ma (the age of a rhyolitic porphyry in the underlying Stubbins Formation) but before the 1840–1825 Ma Tanami Orogeny (Vandenberg et al., 2001). Detrital zircons from the Killi Killi Formation have dominant age components at 1870–1860 Ma and at c. 2500 Ma (Cross and Crispe, 2007). These age spectra are very similar to those of the lower Olympio Formation, which have dominant zircon age components at c. 2500 Ma and 1875–1860 Ma (GSWA 206106 and GA 9352–5128B). REE contents, when normalized to PAAS for both the Olympio Formation and the Killi Killi Formation turbiditic metasandstones, show a similar flat pattern (Fig. 14) which probably reflects derivation from chemically similar sources. These data suggest that there is a common source between these turbidite-dominated units. There are no zircon Hf isotopic data currently available from the Killi Killi Formation; however, c. 1875–1860 Ma detrital zircons from the lower Olympio Formation have relatively unradiogenic Hf compositions (εHf = –6.6 to –1.3; Fig. 25a–d). The age and isotopic composition of these grains are consistent with derivation from granitic rocks of the Paperbark Supersuite in the Western Zone of the Lamboo Province (εHf = –4.2 to –2.7) (Hollis et al., 2014). In the model proposed by Griffin et al. (2000a) and Sheppard et al. (1999b), the Paperbark Supersuite lay inboard of an intervening oceanic arc (Central Zone) at the time of turbidite deposition in the Eastern Zone. The detrital zircon ages and isotopic compositions are also consistent with derivation from granitic rocks of the 1871–1857 Ma Nimbuwah Complex of the Pine Creek Orogen (εHf = –5.5 to –2.5) (Hollis et al., 2010). The Olympio Formation and the Killi Killi Formation may have formed at an active margin, possibly contiguous with the Kimberley margin (Hollis et al., 2010; Hollis and Glass, 2012). Few paleocurrent data are available, but rare climbing ripples from the Olympio Formation suggest a paleocurrent from the northwest (Hancock and Rutland, 1984; Hancock, 1991). It is possible, therefore, that the Olympio Formation and the Killi Killi Formation detritus were sourced from either the Pine Creek Orogen by south-

directed transport along the margin of the North Australian Craton and/or from the Paperbark Supersuite to the west. These formations may have been part of a large turbidite system deposited in a foreland basin offshore of the North Australian Craton from c. 1856 Ma. Upper Olympio Formation turbidite metasandstones contain fewer 1875–1860 Ma detrital zircons and a younger detrital source with dominant age components at 1848–1834 Ma (Fig. 27). These younger detrital zircon age populations are not recorded in the Killi Killi Formation suggesting that either deep-marine sedimentation continued for longer in the Eastern Zone (until at least c. 1834 Ma), that younger portions of the Killi Killi Formation are not exposed or turbidite sedimentation is restricted to c. 1864–1840 Ma in the Granites–Tanami Orogen.

Conclusions

This Report has revised the tectonostratigraphy of the Eastern Zone of the Lamboo Province by splitting the Biscay Formation into a lower unit, now renamed the Brim Rockhole Formation, and an upper unit which retains the name Biscay Formation. This Report has also proposed times of shared provenance between turbiditic metasedimentary rocks in the Eastern Zone and broadly coeval Granites–Tanami Orogen.

The oldest exposed rocks in the Eastern Zone comprise greenschist facies bimodal volcanic and magmatic rocks of the Sophie Downs Suite emplaced contemporaneously with shallow-marine sedimentary rocks at c. 1912–1904 Ma. Radiogenic zircon εHf values from the Sophie Downs Suite suggest mantle contribution during passive margin magmatism along the western margin of the North Australian Craton. Initial deposition of the Halls Creek Group took place between c. 1904 and 1881 Ma in a terrestrial to shallow-marine basin. Fluvial Saunders Creek Formation and lacustrine or shallow-marine Brim Rockhole Formation metasandstone units contain detrital zircons dominated by Paleoarchean to Neoarchean ages with a felsic metavolcanic rock in the Brim Rockhole Formation dated at c. 1881 Ma, interpreted as the age of volcanism. Metabasalts of the Brim Rockhole Formation are characterized by radiogenic εNd values and elevated Pb and LILE, and may represent volcanism accompanying crustal attenuation. The unconformable surface mapped between the Brim Rockhole Formation and Biscay Formation may be indicative of basinwide subsidence and drowning after c. 1881 Ma. Interbedded lithic and quartzofeldspathic metasandstone and metasiltstone in the Biscay Formation are dominated by Paleoproterozoic detrital zircons with a dominant age component at 1870–1858 Ma and a maximum depositional age at c. 1861 Ma. The least fractionated metabasalts in the Biscay Formation have affinities similar to continental flood basalts derived from melting of subcontinental lithosphere. Data from metabasalts in the Brim Rockhole Formation and Biscay Formation are consistent with progressive fractionation and increasing crustal contamination of a continuous magmatic event on the margin of the North Australian Craton from c. 1881 to 1861 Ma.

The disconformable to unconformable surface between the Biscay Formation and the Olympio Formation is indicative of basinwide subsidence and marine transgression. The Olympio Formation consists of immature turbidite metasandstone and hemipelagic metasiltstone deposited on a continental shelf or slope on the margin of the North Australian Craton. Alkalic volcanic centres represented by the c. 1856 Ma Maude Headley Member and c. 1846 Ma Butchers Gully Member punctuate turbidite sedimentation. Turbidite metasandstone deposited before the Maude Headley Member contains detrital zircons with a dominant age mode at 1875–1860 Ma and unradiogenic Hf isotopic compositions. These data are similar to the c. 1864 to 1840 Ma Killi Killi Formation of the Tanami Group in the Granites–Tanami Orogen. Killi Killi Formation turbidite metasandstones are lithologically and geochemically similar to the lower Olympio Formation and also dominated by detrital zircons with age components at c. 1860 Ma. These data suggest shared provenance between deepwater lithofacies in the Eastern Zone and the Tanami region. Detrital zircon modal ages and Hf isotopic compositions from the lower Olympio and Killi Killi Formations indicate two possible detrital sources: 1) the 1864–1852 Ma Paperbark Supersuite in the Western Zone of the Lamboo Province; 2) the 1867–1862 Ma Nimbuwah Complex in the Pine Creek Orogen. The Olympio Formation and the Killi Killi Formation may have been part of a large turbidite system deposited off the North Australian Craton during the early stages of the Halls Creek Orogeny. Deep-marine sedimentation continued for longer in the Eastern Zone, until at least c. 1834 Ma, as evidenced by younger dominant age modes at 1848–1834 Ma in the upper Olympio Formation. The Woodward Dolerite intrudes the entire Halls Creek Group and the Sophie Downs Suite at c. 1835 Ma. The Woodward Dolerite probably represents mantle input during magmatism, evidenced by positive εNd values, related to onset of tectonism of the Halls Creek Orogeny.

References

Allen, RL, Weihed, P and Svenson, S 1997, Setting of Zn–Cu–Au–Ag massive sulfide deposits in the evolution and facies architecture of a 1.9 Ga marine volcanic arc, Skellefte district Sweden: Economic Geology, v. 91, p. 1022–1053.

Bagas, L, Bierlein, FP, Anderson, JAC and Maas, R 2010, Collision-related granitic magmatism in the Granites–Tanami Orogen: Precambrian Research, v. 177, p. 212–226.

Bagas, L, Bierlein, FP, English, L, Anderson, J, Maidment, D and Huston, DL 2008, An example of a Paleoproterozoic back-arc basin: petrology and geochemistry of the ca. 1864 Ma Stubbins Formation as an aid towards an improved understanding of the Tanami Orogen, Western Australia: Precambrian Research, v. 166, no. 1–4, p. 168–184.

Bagas, L, Broucher, R, Li, B, Miller, J, Hill, P, Depauw, G, Pascoe, J and Eggers, B 2014, Paleoproterozoic stratigraphy and gold mineralisation in the Granites-Tanami Orogen, North Australian Craton: Australian Journal of Earth Sciences, v. 61, p. 89–111.

Black, LP, Kamo, SL, Allen, CM, Aleinikoff, JN, Davis, DW, Korsch, RJ and Foudoulis, C 2003, TEMORA 1: a new zircon standard for Phanerozoic U–Pb geochronology: Chemical Geology, v. 200, p. 155–170.

Blake, DH, Griffin, TJ, Tyler, IM, Thorne, AM and Warren, RG 1999a, Halls Creek, WA Sheet 4461: Australian Geological Survey Organisation, 1:100 000 Geological Series.

Blake, DH, Tyler, IM, Griffin, TJ, Sheppard, S, Thorne, AM and Warren, RG 1999b, Geology of the Halls Creek 1:100 000 Sheet area (4461), Western Australia: Australian Geological Survey Organisation, Explanatory Notes, 36p.

Blake, DH, Tyler, IM and Sheppard, S 1997, Geology of the Ruby Plains 1:100 000 sheet area (4460), Western Australia: Australian Geological Survey Organisation, Canberra, 15p.

Blake, DH, Tyler, IM and Warren, RG 2000, Gordon Downs, Western Australia – 1:250,000 Geological Series (2nd edition): Australian Geological Survey Organisation, Explanatory Notes SE/52-10, 58p.

Blichert-Toft, J and Albarède, F 1997, The Lu–Hf isotope geochemistry of chondrites and the evolution of the mantle–crust system: Earth and Planetary Science Letters, v. 148, p. 243–258.

Bodorkos, S, Cawood, PA and Oliver, NHS 2000, Timing and duration of synmagmatic deformation in the Mabel Downs Tonalite, northern Australia: Journal of Structural Geology, v. 22, p. 1181–1198.

Bodorkos, S, Oliver, NHS and Cawood, PA 1999, Thermal evolution of the central Halls Creek Orogen, northern Australia: Australian Journal of Earth Sciences, v. 46, p. 453–465.

Bouma, AH 1962, Sedimentology of some Flysch deposits: a graphic approach to facies interpretation: Elsevier, Amsterdam, 168p.

Buckovic, WA 1984, Niobium-enriched alkaline volcanics, Brockman Project, Kimberley Region, Western Australia: Union Oil Development Corporation Report (unpublished).

Chadwick Jr, WW, Cashman, KV, Embley, RW, Matsumoto, H, Dziak, RP, de Ronde, CEJ, Lau, TK, Deardorff, ND and Merle, SG 2008, Direct video and hydrophone observations of submarine explosive eruptions at NW Rota-1 volcano, Mariana arc: Journal of Geophysical Research, v. 113, no. B8, doi:10.1029/2007JB005215.

Chalmers, DI 1990, Brockman multi-metal and rare-earth deposit, *in* Geology of the mineral deposits of Australia and Papua New Guinea, Volume 1 *edited by* FE Hughes: Australasian Institute of Mining and Metallurgy, Monograph 14, p. 707–709.

Collins, CDN, Drummond, BJ and Nicoll, MG 2003, Crustal thickness patterns in the Australian continent: Geological Society of America Special Papers, v. 372, p. 121–128.

Crispe, AJ, Vandenberg, LC and Scrimgeour, IR 2007, Geological framework of the Archean and Paleoproterozoic Tanami Region, Northern Territory: Mineralium Deposita, v. 42, p. 3–26.

Cross, AJ and Crispe, AJ 2007, SHRIMP U–Pb analyses of detrital zircon: a window to understanding the Paleoproterozoic development of the Tanami Region, northern Australia: Mineralia Deposita, v. 42, p. 27–50.

DeBievre, P and Taylor, PDP 1993, Table of the isotopic composition of the elements: International Journal of Mass Spectrometry and Ion Processes, v. 123, p. 149.

Dow, DB and Gemuts, I (compilers) 1967, Dixon Range, Western Australia: Geological Survey of Western Australia, 1:250 000 Geological Series Explanatory Notes, 14p.

Dow, DB and Gemuts, I 1969, Geology of the Kimberley region, Western Australia: the East Kimberley: Geological Survey of Western Australia, Bulletin 120, 135p.

Downes, PP, Griffin, BJ and Griffin, WL 2007, Mineral chemistry and zircon geochronology of xenocrysts and altered mantle and crustal xenoliths from the Aries micaceous kimberlite: Constraints on the composition and age of the central Kimberley Craton, Western Australia: Lithos, v. 93, p. 175–198.

Doyle, MG 2000, Clast shape and textural associations in peperite as a guide to hydromagmatic interactions: Upper Permain basaltic and basaltic andesite examples from Kiama, Australia: Australian Journal of Earth Sciences, v. 47, no. 1, p. 167–177.

Eggins, SM, Woodhead, JD, Kinsley, LPJ, Mortimer, GE, Sylvester, PJ, McCulloch, MT, Hergt, JM and Handler, MR 1997, A simple method for the precise determination of >40 trace elements in geological samples by ICPMS using enriched isotope internal standardisation: Chemical Geology, v. 134, p. 311–326.

Esslemont, G 1990, The geology and geochemistry of the Brockman alkaline volcanics and rare metal deposit: University of Western Australia, Perth, Western Australia, BSc thesis (unpublished), 166p.

Gellatly, DC, Derrick, GM and Plumb, KA 1970, Proterozoic palaeocurrent directions in the Kimberley region, northwestern Australia: Geological Magazine, v. 107, p. 249–257.

Gellatly, DC and Halligan, R (compilers) 1971, Charnley, Western Australia: Geological Survey of Western Australia, 1:250 000 Geological Series Explanatory Notes, 34p.

Gemuts, I and Smith, JW (compilers) 1968, Gordon Downs, Western Australia: Geological Survey of Western Australia, 1:250 000 Geological Series Explanatory Notes, 23p.

Goolaerts, A, Mattielli, N, de Jong, J, Weis, D and Scoates, JS 2004, Hf and Lu isotopic reference values for the zircon standard 91500 by MC-ICP-MS: Chemical Geology, v. 206, p. 1–9.

Grey, K and Griffin, TJ 1990, King Leopold and Halls Creek Orogens — local sedimentary successions related to the orogens, *in* Geology and mineral resources of Western Australia: Geological Survey of Western Australia, Memoir 3, p. 249–252.

Griffin, TJ and Grey, K 1990, King Leopold and Halls Creek Orogens, *in* Geology and mineral resources of Western Australia: Geological Survey of Western Australia, Memoir 3, p. 232–254.

Griffin, TJ, Page, RW, Sheppard, S and Tyler, IM 2000a, Tectonic implications of Palaeoproterozoic post-collisional, high-K felsic igneous rocks from the Kimberley region of northwestern Australia: Precambrian Research, v. 101, p. 1–23.

Griffin, TJ and Tyler, IM 1993, Geology of the southern Halls Creek Orogen — a summary of fieldwork in 1992: Geological Survey of Western Australia, Record 1992/17, 28p.

Griffin, TJ, Tyler, IM, Orth, K and Sheppard, S 1998, Geology of the Angelo 1:100 000 sheet: Geological Survey of Western Australia, 1:100 000 Geological Series Explanatory Notes, 27p.

Griffin, TJ, Tyler, IM and Playford, PE 1993, Explanatory notes on the Lennard River 1:250 000 geological sheet SE/51-8, Western Australia (3rd edition): Geological Survey of Western Australia, Record 1992/5, 85p.

Griffin, TJ, Tyler, IM and Playford, PE 1994, Lennard River, Western Australia (3rd edition): Geological Survey of Western Australia, 1:250 000 Geological Series Explanatory Notes, 56p.

Griffin, WL, Pearson, NJ, Belousova, EA, Jackson, SE, O'Reilly, SY, van Achterbergh, E and Shee, SR 2000b, The Hf isotope composition of cratonic mantle: LAM–MC–ICPMS analysis of zircon megacrysts in kimberlites: Geochimica et Cosmochimica Acta, v. 64, p. 133–147.

Griffin, WL, Wang, X, Jackson, SE, Pearson, NJ, O'Reilly, SY, Xu, X and Zhou, X 2002, Zircon chemistry and magma genesis, SE China: in-situ analysis of Hf isotopes, Pingtan and Tonglu igneous complexes: Lithos, v. 61, p. 237–269.

Gunn, PJ and Meixner, AJ 1998, The nature of the basement to the Kimberley Block, northwestern Australia: Exploration Geophysics, v. 29, p. 506–511.

Hancock, SL 1991, Tectonic development of the Lower Proterozoic basement in the Kimberley district of northwestern Western Australia: University of Adelaide, Adelaide, South Australia, PhD thesis (unpublished).

Hancock, SL and Rutland, RWR 1984, Tectonics of an early Proterozoic geosuture: the Halls Creek Orogenic Sub-province, northern Australia: Journal of Geodynamics, v. 1, p. 387–432.

Hoatson, DM and Blake, DH (editors) 2000, Geology and economic potential of the Palaeoproterozoic layered mafic–ultramafic intrusions in the East Kimberley, Western Australia: Australian Geological Survey Organisation, Canberra, ACT, Bulletin 246, 476p.

Hollis, JA and Glass, LM 2012, UNCLEAR – Howship and Oenpelli 5572, 5573: Northern Territory Geological Survey, 1:100 000 Geological Map Series Explanatory Notes.

Hollis, JA, Glass, LM, Carson, CJ, Kemp, AIS, Yaxley, G, Armstrong, R and Scherstén, A 2010, U–Pb–Hf–O character of Neoarchean basement to the Pine Creek Orogen, North Australian Craton, *in* Fifth International Archean Symposium Abstracts *edited by* IM Tyler and CM Knox-Robinson: Geological Survey of Western Australia, Record 2010/18; Fifth International Archean Symposium, Perth, 5 September 2010, p. 65–67.

Hollis, JA, Kemp, AIS, Tyler, IM, Kirkland, CL, Wingate, MTD, Phillips, C, Sheppard, S, Belousova, E and Greau, Y 2014, Basin formation by orogenic collapse: zircon U–Pb and Lu–Hf isotope evidence from the Kimberley and Speewah Groups, northern Australia: Geological Survey of Western Australia, Report 137, 46p.

Hooper, P 1997, The Columbia River Flood Basalt Province: Current status, *in* Large Igneous Provinces *edited by* JJ Mahoney and MF Coffin: Geophysical Monograph 10, p. 1–28.

Hooper, PR and Hawkesworth, CJ 1993, Isotopic and geochemical constraints on the origin and evolution of the Columbia River Basalt: Journal of Petrology, v. 34, p. 1203–1246.

Huston, DL, Vandenberg, L, Wygralak, AS, Mernagh, TP, Bagas, L, Crispe, A, Lambeck, A, Cross, A, Fraser, G, Williams, N, Worden, K, Meixner, T, Goleby, B, Jones, L, Lyons, P and Maidment, D 2007, Lode-gold mineralization in the Tanami region, northern Australia: Mineralium Deposita, v. 42, p. 175–204.

Joly, A, McCuaig, TC and Bagas, L 2010, The importance of early crustal architecture for subsequent basin-forming, magmatic and fluid flow events. The Granites–Tanami Orogen example: Precambrian Research, v. 182, no. 1–2, p. 15–29.

Kemp, AIS, Hawkesworth, CJ, Collins, WJ, Gray, CM, Blevin, PL and EIMF 2009, Isotopic evidence for rapid continental growth in an extensional accretionary orogen: the Tasmanides, eastern Australia: Precambrian Research, v. 284, no. 3–4, p. 455–466.

Kemp, AIS, Wormald, RJ, Whitehouse, MJ and Price, RC 2005, Hf isotopes in zircon reveal contrasting sources and crystallization histories for alkaline to peralkaline granites of Temora, southeastern Australia: Geology, v. 33, p. 797–800.

Kirkland, CL, Smithies, RH, Woodhouse, A, Howard, HM, Wingate, MTD, Belousova, EA, Cliff, JB, Murphy, RC and Spaggiari, CV 2012, A multi-isotopic approach to the crustal evolution of the west Musgrave province, Central Australia: Geological Survey of Western Australia, Report 115, 47p.

Kirkland, CL, Wingate, MTD, Hollis, JA and Phillips, C 2015a, 206119: metasandstone, Bullman Copper prospect; Geochronology Record 1239: Geological Survey of Western Australia, 6p.

Kirkland, CL, Wingate, MTD, Hollis, JA and Phillips, C 2015b, 206150: mylonitic quartzofeldspathic rock, Bullaman Rockhole; Geochronology Record 1242: Geological Survey of Western Australia, 5p.

Kirkland, CL, Wingate, MTD, Hollis, JA and Phillips, C 2015c, 206187: pelitic schist, Tanami Road; Geochronology Record 1244: Geological Survey of Western Australia, 6p.

Lambeck, A, Barovich, K, George, AD, Cross, A, Huston, D and Meixner, T 2012, Proterozoic turbiditic depositional system (Tanami Group) in the Tanami region, northern Australia, and implications for gold mineralization: Austrlain Journal of Earth Sciences, v. 59, p. 383–397.

Lambeck, A, Huston, D, Maidment, D and Southgate, PN 2008, Sedimentary geochemistry, geochronology and sequence stratigraphy as tools to typecast stratigraphic units and constrain basin evolution in the gold mineralised Palaeoproterozoic Tanami Region, Northern Australia: Precambrian Research, v. 166, p. 185–203.

Le Bas, MJ, Le Maitre, RW, Streckeisen, A, Zannettin, B and IUGS Subcommission on the Systematics of Igneous Rocks 1986, A chemical classification of volcanic rocks based on the total alkali–silica diagram: Journal of Petrology, v. 27, no. 3, p. 745–750.

McPhie, J, Doyle, M and Allen, R 1993, Volcanic textures: a guide to the interpretation of textures in volcanic rocks: CODES, University of Tasmania, Hobart, Tasmania, 198p.

Myers, JS, Shaw, RD and Tyler, IM 1996, Tectonic evolution of Proterozoic Australia: Tectonics, v. 15, p. 1431–1446.

Næraa, T, Scherstén, A, Rosing, MT, Kemp, AIS, Hoffman, JE, Kokfelt, TF and Whitehouse, MJ 2012, Hafnium isotope evidence for a transition in the dynamics of continental growth 3.2 Gyr ago: Nature, v. 485, p. 627–631.

Naldrett, AJ 2004, Magmatic sulfide deposits — geology, geochemistry and exploration: Springer-Verlag, Berlin, Germany, 728p.

O'Nions, RK, Carter, SR, Evensen, NM and Hamilton, PJ 1979, Geochemical and cosmochemical applications of Nd isotope analysis: Annual Review of Earth and Planetary Sciences, v. 7, p. 11–38.

Ogasawara, M 1988, Geochemistry of the Early Proterozoic granitoids in the Halls Creek orogenic subprovince, northern Australia: Precambrian Research, v. 40–41, p. 469–486.

Orth, K 1997, Notes on the geology of the Koongie Park Formation southwest of Halls Creek, Western Australia (1997 edition): Australian Geological Survey Organisation, Record 25, p. 1–18.

Page, RW 1998, Sample 94495025. Unpublished data in Geoscience Australia OZCHRON database: Geoscience Australia (unpublished).

Page, RW, Blake, DH, Sun, S-S, Tyler, IM, Griffin, TJ and Thorne, AM 1994, New geological and geochronological constraints on volcanogenic massive sulphide prospectivity near Halls Creek (WA): AGSO Research Newsletter, v. 20, p. 5–7.

Page, RW, Griffin, TJ, Tyler, IM and Sheppard, S 2001, Geochronological constraints on tectonic models for Australian Palaeoproterozoic high-K granites: Journal of the Geological Society, v. 158, p. 535–545.

Page, RW and Hancock, SL 1988, Geochronology of a rapid 1.85–1.86 Ga tectonic transition: Halls Creek orogen, northern Australia: Precambrian Research, v. 40, p. 447–467.

Page, RW and Hoatson, DM 2000, Geochronology of the mafic–ultramafic intrusions, *in* Geology and economic potential of the Palaeoproterozoic layered mafic–ultramafic intrusions in the East Kimberley, Western Australia *edited by* DM Hoatson and DH Blake: Australian Geological Survey Organisation, Bulletin 246, p. 163–172.

Page, RW and Sun, S-S 1994, Evolution of the Kimberley Region, W.A. and adjacent Proterozoic inliers — new geochronological constraints: Geological Society of Australia; Geoscience Australia — 1994 and Beyond, Abstracts v. 37, p. 332–333.

Page, RW, Sun, S-S and Blake, DH 1995, Geochronology of an exposed late Archean basement terrane in The Granites–Tanami Region: ASGO Research Newsletter 22, p. 19–20.

Pearce, JA 1983, The role of sub-continental lithosphere in magma genesis at destructive plate margins, *in* Continental basalts and mantle xenoliths *edited by* CJ Hawkesworth and MJ Norry: Shiva Publishing Ltd, Nantwich, UK, p. 230–249.

Phillips, C, McIlroy, D and Elliott, T 2011, Ichnological characterization of Eocene/oligocene turbidites from the Grès d'Annot Basin, French Alps, SE France: Palaeogeography, Palaeoclimatology, Palaeoecology, v. 300, no. 1–4, p. 67–83.

Pickering, K, Hiscott, RN and Hein, F 1989, Deep marine environments: clastic sedimentation and tectonics: Unwin Hyman, London, UK, 424p.

Pidgeon, RT, Furfaro, D, Kennedy, AK, Nemchin, AA and van Bronswik, W 1994, Calibration of zircon standards for the Curtin SHRIMP II, in Circular: United States Geological Survey; Eighth International Conference on Geochronology, Cosmochronology, and Isotope Geology, Berkeley, USA, Abstracts v. 1107, p. 251.

Plumb, KA, Allen, R and Hancock, SL 1985, Proterozoic evolution of the Halls Creek Province, Western Australia: Bureau of Mineral Resources, Geology and Geophysics, Record 1985/25, 87p.

Pyke, J 2000, Minerals laboratory staff develops ICP-MS preparation method: Australian Geological Survey Organisation Newsletter, v. 33, p. 12–14.

Reinhard, CT, Planavsky, NJ, Robbins, LJ, Partin, CA, Gill, BC, Lalonde, SV, Bekker, A, Konhauser, KO and Lyons, TW 2013, Proterozoic ocean redox and biogeochemical stasis: Proceedings of the National Academy of Sciences of the United States of America, v. 110, no. 14, p. 5357–5362.

Roberts, HG, Halligan, R and Playford, PE (compilers) 1968, Mount Ramsay, Western Australia: Geological Survey of Western Australia, 1:250 000 Geological Series Explanatory Notes, 24p.

Sass, E and Katz, A 1982, The origin of platform dolomites: new evidence: American Journal of Science, v. 282, p. 1184–1213.

Saygin, E and Kennett, BLN 2010, Ambient noise tomography for the Australian Continent: Tectonophysics, v. 481, p. 116–125, doi:10.106/j.tecto.2008.11.013.

Scherer, E, Münker, C and Mezger, K 2001, Calibration of the lutetium–hafnium clock: Science, v. 293, p. 683–687.

Schminke, HU 1967, Fused tuffs and pepperite in south-central Washington: Geological Society of America Bulletin, v. 78, p. 319–330.

Segal, I, Halicz, L and Platzner, IT 2003, Accurate isotope ratio measurements of ytterbium by multiple collection inductively coupled plasma mass spectrometry applying erbium and hafnium in an improved double external normalization procedure: Journal of Analytical Atomic Spectrometry, v. 18, p. 1217–1223.

Shaw, RD, Tyler, IM, Griffin, TJ and Webb, A 1992, New K–Ar constraints on the onset of subsidence in the Canning Basin, Western Australia: BMR Journal of Australian Geology and Geophysics, v. 13, p. 31–35.

Sheppard, S 1997, Mafic-felsic magma mingling in the Bow River batholith of the Halls Creek Orogen, *in* Geological Survey of Western Australia Annual Review 1995–96: Geological Survey of Western Australia, Perth, Western Australia, p. 56–60.

Sheppard, S, Griffin, TJ and Tyler, IM 1997a, Compilation of whole-rock geochemical data for the King Leopold and Halls Creek Orogens: Geological Survey of Western Australia, Record 1997/4, 138p.

Sheppard, S, Griffin, TJ and Tyler, IM 1997b, The tectonic setting of granites in the Halls Creek and King Leopold Orogens, northwest Australia: Australian Geological Survey Organisation, Record 1997/44.

Sheppard, S, Page, RW, Griffin, TJ, Rasmussen, B, Fletcher, IR, Tyler, IM, Kirkland, CL, Wingate, MTD, Hollis, J and Thorne, AM 2012, Geochronological and isotopic constraints on the tectonic setting of the c. 1800 Ma Hart Dolerite and the Kimberley and Speewah Basins, northern Western Australia: Geological Survey of Western Australia, Record 2012/7, 28p.

Sheppard, S, Thorne, AM and Tyler, IM 1999a, Geology of the Bow 1:100 000 sheet: Geological Survey of Western Australia, 1:100 000 Geological Series Explanatory Notes, 36p.

Sheppard, S, Tyler, IM, Griffin, TJ and Taylor, RW 1999b, Palaeoproterozoic subduction-related and passive margin basalts in the Halls Creek Orogen, northwest Australia: Australian Journal of Earth Sciences, v. 46, p. 679–690.

Sheppard, S, Tyler, IM and Hoatson, DM 1997c, Geology of the Mount Remarkable 1:100 000 sheet: Geological Survey of Western Australia, 1:100 000 Geological Series Explanatory Notes, 27p.

Simpson, K and McPhie, J 2001, Fluidal-clast breccia generated by submarine fire fountaining, Trooper Creek Formation, Queensland, Australia: Journal of Volcanology and Geothermal Research, v. 109, p. 339–355.

Smith, TL and Batiza, R 1989, Field and laboratory evidence for the origin of hyaloclatite on seamount summits: Bulletin of Volcanology, v. 51, p. 96–114.

Stacey, JS and Kramers, JD 1975, Approximation of terrestrial lead isotope evolution by a two-stage model: Earth and Planetary Science Letters, v. 26, p. 207–221.

Stern, RA 2001, A new isotopic and trace-element standard for the ion microprobe: preliminary thermal ionization mass spectrometry (TIMS) U–Pb and electron microprobe data: Geological Survey of Canada, Report 2001-F1, 11p.

Stern, RA, Bodorkos, S, Kamo, SL, Hickman, AH and Corfu, F 2009, Measurement of SIMS instrumental mass fractionation of Pb isotopes during zircon dating: Geostandards and Geoanalytical Research, v. 33, p. 145–168.

Sun, S-S and Hoatson, DM 2000, Trace-element geochemical and Nd isotopic study of the mafic-ultramafic intrusions: implications for their petrogenesis and tectonic environment, *in* Geology and economic potential of the Palaeoproterozoic layered mafic-ultramafic intrusions in the East Kimberley, Western Australia *edited by* DM Hoatson and DH Blake: Australian Geological Survey Organisation, Canberra, ACT, Bulletin 246, p. 163–172.

Sun, S-S and McDonough, WF 1989, Chemical and isotopic systematics of oceanic basalts: implications for mantle composition and processes, *in* Magmatism in the Ocean Basins *edited by* AD Saunders and MJ Norry: Geological Society, London, Special Publication 42, p. 313–345.

Sun, S-S, Wallace, DA, Hoatson, DM, Glikson, AY and Keays, RR 1991, Use of geochemistry as a guide to platinum group element potential of mafic–ultramafic rocks: examples from the west Pilbara Block and Halls Creek Mobile Zone, Western Australia: Precambrian Research, v. 50, p. 1–35.

Taylor, SR and McLennan, SM 1985, The continental crust: its composition and evolution: Blackwell Scientific Publications, Oxford, U.K., 312p.

Taylor, SR and McLennan, SM 1995, The geochemical evolution of the continental crust: Reviews of Geophysics, v. 33, no. 2, p. 241–265, doi:10.1029/95RG00262.

Taylor, WR, Esslemont, G and Sun, S-S 1995a, Geology of the volcanic-hosted Brockman rare-metals deposit, Halls Creek Mobile Zone, northwest Australia. II. Geochemistry and petrogenesis of the Brockman volcanics: Mineralogy and Petrology, v. 52, no. 3–4, p. 231–255.

Taylor, WR, Page, RW, Esslemont, G, Rock, NMS and Chalmers, DI 1995b, Geology of the volcanic-hosted Brockman rare-metals deposit, Halls Creek Mobile Zone, northwest Australia. I. Volcanic environment, geochronology, and petrography of the Brockman volcanics: Mineralogy and Petrology, v. 52, p. 209–230.

Thom, JH 1975, Kimberley region, *in* The geology of Western Australia: Geological Survey of Western Australia, Memoir 2, p. 160–193.

Thorne, AM, Sheppard, S and Tyler, IM 1999, Lissadell, Western Australia (2nd edition): Geological Survey of Western Australia, 1:250 000 Geological Series Explanatory Notes, 68p.

Tunks, AJ and Cooke, D 2007, Geological and structural controls on gold mineralization in the Tanami District, Northern Territory: Mineralium Deposita, v. 42, no. 1, p. 107–126, 10.1007/s00126-006-0097-z.

Tyler, IM 2004, Geology of the Dixon 1:100 000 sheet: Geological Survey of Western Australia, 1:100 000 Geological Series Explanatory Notes, 30p.

Tyler, IM and Griffin, TJ 1990, Structural development of the King Leopold Orogen, Kimberley region, Western Australia: Journal of Structural Geology, v. 12, p. 703–714.

Tyler, IM, Griffin, TJ, Page, RW and Shaw, RD 1995, Are there terranes within the Lamboo Complex of the Halls Creek Orogen?, *in* Geological Survey of Western Australia Annual Review 1993–94: Geological Survey of Western Australia, Perth, Western Australia, p. 37–46.

Tyler, IM, Griffin, TJ and Sheppard, S 1998, Geology of the Dockrell 1:100 000 sheet: Geological Survey of Western Australia, 1:100 000 Geological Series Explanatory Notes, 24p.

Tyler, IM, Hocking, RM and Haines, PW 2012, Geological evolution of the Kimberley region of Western Australia: Episodes, v. 35, p. 298–306.

Tyler, IM and Page, RW 1996, Palaeoproterozoic deformation, metamorphism and igneous intrusion in the central zone of the Lamboo Complex, Hall Creek Orogen: Geological Society of Australia; Australian Geological Convention, Canberra, February 1996; Abstract 41, 450p.

Tyler, IM, Page, RW and Griffin, TJ 1999, Depositional age and provenance of the Marboo Formation from SHRIMP U–Pb zircon geochronology: Implications for the early Palaeoproterozoic tectonic evolution of the Kimberley region, Western Australia: Precambrian Research, v. 95, no. 3, p. 225–243.

Vandenberg, LC, Hendrick, MA and Crispe, AJ 2001, Structural geology of the Tanami region: Northern Territory Geological Survey, Record 2001-004, 28p.

Vervoort, JD, Patchett, JP, Söderlund, U and Baker, M 2004, Isotopic composition of Yb and the determination of Lu concentrations and Lu/Hf ratios by isotope dilution using MC-ICPMS: Geochemistry Geophysics Geosystems, v. 5, no. 11, DOI: 10.1029/2004GC000721.

Warren, RG 1997, Reconnaissance geological mapping in Dixon, SE McIntosh and northermost Halls Creek 1:100 000 Sheet areas, East Kimberley, WA 1992–3: Australian Geological Survey Organisation, Record 1997/026.

Whelan, JA, Woodhead, JD and Cliff, J 2014, Zircon LA-ICPMS Hf and SIMS O isotopic data for granitic gneiss of the Billabong Complex, Tanami Region: Northern Territory Geological Survey, Record 2014-002, 8p.

Wiedenbeck, M, Alle, P, Corfu, F, Griffin, WL, Meier, M, Oberli, F, Vonquadt, A, Roddick, JC and Speigel, W 1995, Three natural zircon standards for U–Th–Pb, Lu–Hf, trace-element and REE analyses: Geostandards Newsletter, v. 19, p. 1–23.

Wilson, M 1989, Igneous Petrogenesis: Chapman and Hall, London, England, 466p.

Winchester, JA and Floyd, PA 1977, Geochemical discrimination of different magma series and their differentiation products using immobile elements: Chemical Geology, v. 20, p. 325–343.

Wingate, MTD, Kirkland, CL, Griffin, TJ and Sheppard, S 2011, 95406: porphyritic microgranite, Wotjulum Mission; Geochronology Record 973: Geological Survey of Western Australia, 4p.

Wingate, MTD, Kirkland, CL, Hollis, JA and Phillips, C 2015a, 206121: metasandstone, Sophie Downs homestead; Geochronology Record 1240: Geological Survey of Western Australia, 6p.

Wingate, MTD, Kirkland, CL, Hollis, JA and Phillips, C 2015b, 206126: metasandstone, Dry Creek mine; Geochronology Record 1241: Geological Survey of Western Australia, 6p.

Wingate, MTD, Kirkland, CL, Hollis, JA and Phillips, C 2015c, 206184: metasandstone, Palm Springs; Geochronology Record 1243: Geological Survey of Western Australia, 6p.

Wingate, MTD and Kirkland, CL 2013, Introduction to geochronology information released in 2013: Geological Survey of Western Australia, 5p.

Woodhead, JD and Hergt, JM 2005, A preliminary appraisal of seven natural zircon reference materials for in situ Hf isotope determination: Geostandards and Geoanalytical Research, v. 29, p. 183–195.

Woodhead, JD, Hergt, JM, Shelley, M, Eggins, S and Kemp, R 2004, Zircon Hf-isotope analysis with an excimer laser, depth profiling, ablation of complex geometries, and concomitant age estimation: Chemical Geology, v. 209, no. 1–2, p. 121–135.

Appendix 1

Analytical data and methodology for geochemistry

Analytical techniques and data preparation

Samples collected in the field were as unweathered as possible and representative of their units. Rocks were cut, crushed and milled to a powder using a tungsten carbide mill at the GSWA Laboratory. Powdered samples were dispatched to Australian Laboratory Services (ALS) or GENALYSIS for geochemical analysis. Pulps of samples from earlier work by Sheppard et al. (1997a) were re-analysed in 2010 at Geoscience Australia (GA) laboratories. Newly collected samples were analysed in 2012 (three batches), 2013 (one batch) and 2014 (one batch). All samples underwent major element analysis using XRF for SiO_2, TiO_2, Fe_2O_3, MgO, MnO, CaO, K_2O, Na_2O and P_2O_5. Some powders were made into pellets whereas others were fused into lithium borate glasses. Loss on ignition (LOI) was also completed by weighing samples then drying and reweighing (gravimetric/thermogravimetric techniques). FeO titration was employed as a check in the 2010 GA batch. REE were analysed on all samples submitted. These analyses were on digested lithium borate glasses. For more refractory elements, samples underwent a four-acid digest using HF, HNO_3, $HClO_4$ and HCl prior to analysis. ICP–MS and in some cases ICP–OES were used for analyses. For some elements, both XRF and ICP–MS techniques were used to crosscheck analytical accuracy. Precious metal analyses, including Ag, Au, Pd, Pb, and in some cases Ir, Os, Rh and Ru, were undertaken on some samples using fire assay and ICP–MS on small amounts of sample. The raw analyses are presented in this Appendix, Tables 1–8. Techniques used by these laboratories are listed below.

GSWA laboratories: powder preparation (all batches)

The procedures used at different laboratories for preparing the samples for analysis are summarized in the following sections.

C1M1S0 — plate jaw crusher — tungsten carbide ring mill — not screened | CGMGSG — crush at gannet — mill at gannet — screen at gannet | CUMUSU — crush unknown — mill unknown — screen unknown

GA (batch gsd13122010_26691)

TITR — FeO determined by titration | XRF major and some trace elements using XRF | GRAV — gravimetric LOI | ICP–MS — trace elements and some REE, ICP–MS determination of dissolved XRF fused glass disc (Eggins et al., 1997; Pyke, 2000)

ALS (batches gs12092012, gs10102012 and gs56210122013)

Powdered samples were made into lithium borate fusion disks (FB). These disks underwent either XRF, ICP–MS, or for ore-forming metals, ICP–OES analyses. For more refractory trace elements (Ag, As, Be, Bi, Cd, Co, Ge, In, Li, Mo, Pb, Re, Sb, Se, Te and Tl), the samples underwent a four-acid digest (4A) prior to analysis with either ICP–MS or ICP–OES.

ME–XRF26 — major elements, lithium borate fusion, XRF | ME–XRF05 — major elements by pressed pellet XRF | MEGRA05 — thermogravimetric analysis, LOI at 37.1, 425, 550, 650 and 1000°C | ME–MS81 — trace and REE element, lithium borate fusion then 4A digest prior to ICP–MS | ME–4ACD81 — trace and REE element, lithium borate fusion then 4A digest prior to ICP–MS | PGM–MS23 — Pt, Pd and Au by fire assay and ICP–MS finish

GENALYSIS (batches gs08112012, gs2609012 and gs07042014)

Powdered samples were made into lithium borate fusion disks (FB). These disks underwent either XRF, ICP–MS or, for ore-forming metals, ICP–OES analyses. For more refractory trace elements (Ag, As, Be, Bi, Cd, Co, Ge, In, Li, Mo, Pb, Re, Sb, Se, Te and Tl), the samples underwent a four-acid digest (4A, HF–HNO_3–$HClO_4$–HCl) prior to analysis with either ICP–MS or ICP–OES. Carbon and sulfur were analysed using a CS analyser. Abbreviations for the techniques are listed below.

CSA — total carbon and sulfur analyses by CS analyser | FA25/MS is a lead collection fire assay and ICP–MS analysis on a 25 g powder aliquot | FB1/XRF — major elements, lithium borate fusion, XRF analyses | FB6/MS — some traces and REE, lithium borate fusion, ICP–MS | FB6/OE — traces and REE, lithium borate fusion, ICP–OES | NS25/MS – PGM (Ag, Ir, Os, Pd, Pt, Rh, Ru) fire assay and ICP–MS analysis on a 25 g powder aliquot | NS25/MS is a nickel sulfide fire assay and ICP–MS analysis on a 25 g powder aliquot | TGA — thermogravimetric LOI | 4A/MS — some trace elements (Ag, As, Be, Bi, Cd, Co, Ge, In, Li, Mo, Pb, Re, Sb, Se, Te, Tl), a four-acid (HF–HNO_3–$HClO_4$–HCl) digest, ICP–MS | 4A/OE — Cu, Zn, Ni, a four-acid digest, ICP–OES

Geochemical data

Standards and acceptable analyses

All data were scrutinized and each batch contained internal standards and duplicates. The comparison for reference materials and recommended value or parent and duplicate is given by the following equation:

$$\text{HRD} = 100^* \frac{(\textit{analysis}\ 1 - \textit{analysis}\ 2)}{(\textit{analysis}\ 1 + \textit{analysis}\ 2)}$$

A half relative difference (HRD) of <5 is considered acceptable. Although this is the optimum HRD, what is acceptable may vary, as the HRD value is a function of: 1) the analysis in question [e.g. high field strength elements (HFSE), such as Nb, Ta and Zr, are usually found in minerals that are difficult to digest — a disadvantage of more aggressive digests is an elevated lower level of detection]; 2) the homogeneity of the sample; 3) the concentration level (HRD will increase when the concentration approaches the lowest level of detection (Paul Morris, personal comm., 2015).

Comparison of analyses

Sheppard et al. (1997a) examined all the first-generation geochemical data from the Halls Creek Group, Sophie Downs Suite and Woodward Dolerite. All the analyses tabulated in that report were considered to be reasonable on the basis of well-constrained geological and location information. Samples that did not fit these criteria were rejected. Many of the possibly comparative, older geochemical analyses (Hancock in Plumb et al., 1985) or contemporary data gathered by AGSO, now GA and other workers in the area were rejected because of poor lithological constraints or lack of full location information. However, in this Report, where samples from GA (in OZCHEM) are well documented, these samples have been retained (e.g. GA sample of Biscay Formation basalts along the Tanami Road north of Ruby Plains Homestead). The analyses reported in Sheppard et al. (1997a) have been scrutinized and compared with the re-analysed batch from 2010. Some REE analyses from the old dataset showed greater variability than new analyses, and thus often display apparent anomalies, which were not repeated in the new dataset. REE abundances can be low in the old data compared with the new data. For these reasons, the old REE data of Sheppard et al. (1997a) have not been incorporated into calculations, diagrams, or discussions in this Report. Other anomalous data, not caused by analytical problems, are discussed in the appropriate sections of the main body of the Report.

Volatiles

LOI was variable, with the highest values around 12 wt%. Samples with high LOI were re-examined and in some cases considered too inaccurate to be included in the major element plots or calculations. Volatiles have been removed and all major elements recalculated on a volatile-free basis to 100 wt% prior to any other forms of major element manipulation. Although the data in this Appendix are reported in their original form, all plots and calculations in the body of the Report were done on a volatile-free basis.

Fe oxide

All Fe was recalculated to total Fe as Fe^{2+} (FeO^{T}). This is considered a reasonable assumption as much of the Fe^{3+} is probably altered to Fe^{2+} in these ancient rocks. Furthermore, Mg-number (Mg#) is used in many of the plots. The Mg#, which reports molecular proportion, rather than weight percentage oxide, is considered to be more robust and comparable between analyses generated in different laboratories with different equipment and at different times.

Trace elements

Where ICP–MS and XRF analyses are available, plots of results were made and examined. In general, some techniques are better than others for providing accurate elemental data. For example, arsenic analyses by ICP–MS always yield lower concentrations than arsenic analysed by XRF in the same sample.

Metamorphism

Many of the analysed samples have undergone greenschist to amphibolite facies metamorphism. The geochemistry of the rocks will reflect the protolith, provided metamorphism did not involve large fluid fluxes. Samples were chosen to avoid veins but some elements such as Na, Ca, K, Ba, Rb and Sr may be mobile and reflected in high Na_2O/K_2O ratios as in the Butchers Gully Member (Taylor et al., 1995a; Taylor et al., 1995b). Anomalous CaO or SiO_2 values may indicate addition or removal of CaO or SiO_2. Classification schemes which use immobile elements Ti, Nb, Y and immobile element ratios, such as Winchester and Floyd (1977), are used as a check against major element classifications throughout the Report (Le Bas et al., 1986). Samples with high LOI and problematic analyses were not used for classification, plots and comparisons.

Sm–Nd whole-rock isotope methods

Samarium–Nd isotope measurements were determined on crushed whole-rock samples by isotope dilution at several different laboratories over several years. Samples were spiked with ^{150}Nd–^{149}Sm mixed solutions and dissolved in HF–HNO_3. REE were separated using solution column chemistry. Samarium and Nd were separated and collected by passing the solution through an additional set of ion exchange columns. Samarium and Nd were loaded with acid onto filaments and analysed using mass spectrometry. In each analytical session, the unknowns were analysed together with isotope standards. All analyses of the unknowns are adjusted to a nominal $^{143}Nd/^{144}Nd$ value of 0.511850 for the La Jolla Standard. Mass fractionation was monitored and corrected using the value for $^{146}Nd/^{144}Nd$ of 0.7219 (O'Nions et al., 1979). Procedural blanks analysed during these analyses were always less than <200 pg, and are considered to be negligible compared to the total quantity of Nd in the samples.

Data tables

This section presents the analytical data from whole-rock, trace element and Sm–Md whole-rock isotope geochemistry used in this Report. Appendix 1 Geochem_ Tables are available as a downloadable zip file on eBookshop.

Appendix 2

Zircon U–Pb geochronology and Lu–Hf isotopes

Analytical methods

U–Pb geochronology

Analytical methods for U–Pb zircon geochronology by secondary ion mass spectrometry (SIMS) using the sensitive high-resolution ion microprobe (SHRIMP) are described in detail in Wingate and Kirkland (2013) so only a brief summary is provided here. Handpicked zircons were mounted with zircon standards in epoxy disks and polished to about half-grain thickness to expose crystal interiors. Transmitted-light, reflected-light, and cathodoluminescence (CL) images were used to target analytical locations. Zircon standard BR266 (Stern, 2001) and Temora-2 (Black et al., 2003) were used for U/Pb calibration and BR266 or CZ3 (Pidgeon et al., 1994) used for ^{238}U concentration. Fractionation of $^{207}Pb^*/^{206}Pb^*$ ratios (Pb* refers to radiogenic Pb) was monitored by comparison with the 3465 Ma OGC1 zircon standard (Stern et al., 2009). Calibration uncertainties are included in the errors of $^{238}U/^{206}Pb^*$ ratios and dates are listed in Tables 1–22. Common-Pb corrections were applied to all analyses using contemporaneous isotopic compositions determined according to the model of Stacey and Kramers (1975).

Lu–Hf isotopes

GEMOC

Hafnium isotope analyses were conducted on previously dated zircons in samples GSWA 206184, 206121 and 206187 of the Biscay and Olympio Formations at the ARC National Key Centre for Geochemical Evolution and Metallogeny of Continents (GEMOC), in the ARC Centre for Excellence for Core to Crust Fluid Systems, Macquarie University. Analyses were conducted using a New Wave/Merchantek LUV213 laser ablation microprobe attached to a Nu Plasma multicollector inductively coupled plasma mass spectrometer (LA–MC–ICPMS). The analyses employed a beam diameter of approximately 55 µm and a 5 Hz repetition rate, and energies of 0.6 – 1.3 mJ per pulse, which resulted in ablation pits typically 40–60 µm deep during a 30–120 s ablation. The ablated sample material was transported from the laser cell to the ICPMS torch by helium carrier gas. Interference of ^{176}Lu on ^{176}Hf was corrected by measuring interference-free ^{175}Lu, and using the invariant $^{176}Lu/^{175}Lu$ correction factor of 0.02669 (DeBievre and Taylor, 1993). Measurement of accurate $^{176}Hf/^{177}Hf$ ratios in zircon requires correction for isobaric interference of ^{176}Lu and ^{176}Yb on ^{176}Hf. The interference of ^{176}Yb on ^{176}Hf was corrected by measuring the interference-free ^{172}Yb isotope and using $^{176}Yb/^{172}Yb$ to calculate the intensity of ^{176}Yb. The appropriate value of $^{176}Yb/^{172}Yb$ (0.5865) was determined by successively doping a JMC475 Hf standard (100 ppb solution) with various amounts of Yb, and determining the value of $^{176}Yb/^{172}Yb$ required to yield the value of $^{176}Hf/^{177}Hf$ in the undoped solution.

Zircons from the Mud Tank Carbonatite locality were analysed, together with the samples, as a measure of the accuracy of the results. Excluding one outlier, the remaining data and the mean (0.282501 ± 0.000024; 2σ, n = 54) are within 2σ uncertainty of the recommended value 0.282507 ± 0.000006 (2s, n = 5; Woodhead and Hergt, 2005). The average $^{176}Hf/^{177}Hf$ ratio for the Temora-2 zircon standard (Wiedenbeck et al., 1995; Goolaerts et al., 2004), analysed concurrently with unknown zircons, was 0.282686 ± 7 (2σ), which is well within analytical uncertainty of the accepted value, 0.282680 ± 0.000024 (2σ), by LA–MC–ICPMS (Woodhead et al., 2004).

Advanced Analytical Centre, James Cook University

For the remaining five samples presented here, hafnium isotope analyses were measured using a ThermoScientific Neptune MC–ICPMS and GeoLas Pro 193nm ArF laser system in the Advanced Analytical Centre, James Cook University, Townsville (analyst T Kemp). Instrumental operating parameters and analytical protocols followed those described by Kemp et al. (2009) and Næraa et al. (2012). Data were acquired using a 42 µm or 58 µm beam diameter and 4 Hz laser pulse repetition rate over a 60 s ablation period. The power density at the sample was maintained at 5–6 J/cm^2. Ablation was carried out in He, which was combined with Ar and a small (~0.005 l/min) N_2 flow before transport into the ICPMS. Ablation was conducted as close as practical to the pits, resulting from the previous U–Pb isotope analyses. The isobaric interference of Lu and Yb on ^{176}Hf was corrected by monitoring the interference-free ^{171}Yb and ^{175}Lu intensities during the analysis and then deriving ^{176}Yb and ^{176}Lu using $^{176}Yb/^{171}Yb = 0.897145$ (Segal et al., 2003) and $^{176}Lu/^{175}Lu = 0.02655$ (Vervoort et al., 2004). Yb isotope ratios were normalized to $^{173}Yb/^{171}Yb = 1.130172$ (Segal et al., 2003) and Hf isotope ratios to $^{179}Hf/^{177}Hf = 0.7325$ using an exponential law. The mass bias of Lu was assumed to follow that of Yb. Data were processed offline using a customized Microsoft Excel spreadsheet; within-run outlier rejection was set at three standard errors of the mean (3).

Reference zircons of moderate (Yb+Lu)/Hf analysed concurrently with the unknowns yielded mean $^{176}Hf/^{177}Hf$ values (± 2σ) of 0.282181 ± 20 (n = 66) for FC1 and 0.282689 ± 22 (n = 10) for Temora-2, identical to the solution $^{176}Hf/^{177}Hf$ values reported by (Woodhead and Hergt, 2005), and 0.282129 ± 16 (n = 12) for the synthetic zircons of Fisher et al. (2011). All Hf isotope data are

normalized to the accepted solution $^{176}Hf/^{177}Hf$ value of Mud Tank zircon (Woodhead and Hergt, 2005) using laser ablation data generated from this zircon during the same analytical session (combined Mud Tank zircon measurements from all sessions yielded 0.282491 ± 19, n = 78). Quoted εHf uncertainties for sample zircons combine in quadrature within-run analytical errors plus the session reproducibility of Mud Tank zircon measurements.

Calculation of model ages

Calculation of initial $^{176}Hf/^{177}Hf$ values is based on the ^{176}Lu decay constant (1.865×10^{-11} y^{-1}) of Scherer et al. (2001) and εHf values are based on the present-day chondritic measurement (0.282772) of Blichert-Toft and Albarède (1997). Calculation of Hf model ages (T_{DM}^2) is based on a depleted mantle source with $(^{176}Hf/^{177}Hf)_i$ = 0.279718 at 4.56 Ga and $^{176}Lu/^{177}Hf$ = 0.0384 (Griffin et al., 2000b). For each analysis, a two-stage model age is calculated, which assumes that the parent magma was produced from a volume of average continental crust with a $^{176}Lu/^{177}Hf$ ratio of 0.015 (Griffin et al., 2002). This ratio has been demonstrated to be appropriate for collision settings by evaluation of global whole-rock compilations (Kirkland et al., 2012).

Data tables

This section presents analytical data from SHRIMP U–Pb dating and Lu–Hf isotope data from the 22 geochronology samples described in this Report. Appendix 2 Geochronology_Tables are available on the downloadable zip file.

Appendix 3

Definition of the Brim Rockhole Formation (new formation)

Derivation of name

Brim Rockhole (MGA Zone 52, 382771E 7993817N), 10 km northeast of Sophie Downs Homestead

Parent unit

Halls Creek Group

Distribution

The Brim Rockhole Formation crops out around structural domes and basement inliers of the Sophie Downs Suite including the Sophie Downs Dome, Saunders Creek Dome, Brim Anticline, Castle Creek Anticline on Sophie Downs Station (HALLS CREEK and ANTRIM) and around basement inliers near Taylor Lookout (DOCKRELL).

Stratigraphic thickness

The maximum stratigraphic thickness is 200 m north of the Sophie Downs Dome, but this may be locally variable due to the inferred topographic control on deposition and distribution.

Type area

The proposed type area is exposed north and east of the Sophie Downs Dome on HALLS CREEK, 10 km northeast of Sophie Downs Homestead.

Lithology

The lithology is composed of greenschist facies quartzite, ferruginous sandstone and siltstone, graphitic schist, calcareous metasandstone and metasiltstone, calc-silicate schist, carbonate schist, and marble intercalated with metabasalt and lesser metarhyolite, felsic volcaniclastic schist.

Relationships

The Brim Rockhole Formation is locally unconformable on basement rocks of the Sophie Downs Granite on the eastern flank of the Sophie Downs Dome. The formation is conformable or locally gradational on the Saunders Creek Formation. The Brim Rockhole Formation is unconformably or disconformably overlain by the Biscay Formation. The formation is intruded by the Woodward Dolerite.

Age

The Brim Rockhole Formation is dated at 1881 ± 4 Ma from a foliated fragmental felsic metavolcanic rock (Figs 1 and 24i; GA 93526012; Blake et al., 1999b; this study), interpreted as the age of volcanism.

This Report presents the results of new mapping and sampling as well as new and previously unpublished geochemistry and geochronology revising the tectonostratigraphy of the Eastern Zone of the Lamboo Province, Halls Creek Orogen. The Eastern Zone records magmatism, volcanism and sedimentation associated with extension of the western margin of the North Australian Craton from c. 1912 to 1788 Ma. Basement rocks consist of c. 1912 to 1904 Ma rift-related units in the Sophie Downs Suite. The Sophie Downs Suite is unconformably overlain by greenschist to amphibolite facies volcano-sedimentary rocks of the c. 1904 and 1834 Ma Halls Creek Group. New mapping and geochronology divides the Biscay Formation of the Halls Creek Group into an older Brim Rockhole Formation (new formation) and a younger Biscay Formation (redefined). Detrital zircon modal ages and Hf-isotope compositions suggest correlation of the Olympio Formation (Halls Creek Group) with Killi Killi Formation in the Granites–Tanami Orogen indicating an extensive turbidite system off the western margin of the North Australian Craton from c. 1856 to 1834 Ma. These turbidites were probably derived from within the Western Zone of the Lamboo Province or the Pine Creek Orogen in the Northern Territory.

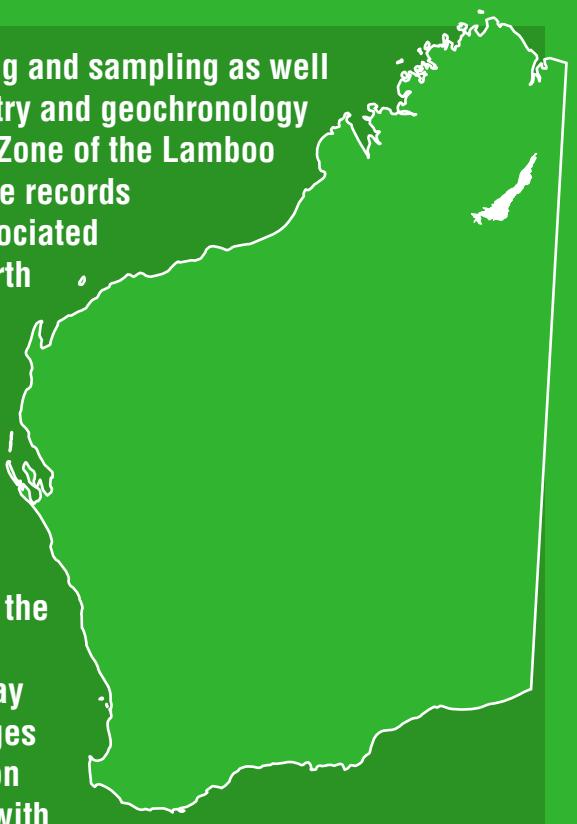

Further details of geological products and maps produced by the Geological Survey of Western Australia are available from:

Information Centre
Department of Mines and Petroleum
100 Plain Street
EAST PERTH WA 6004
Phone: (08) 9222 3459 Fax: (08) 9222 3444

www.dmp.wa.gov.au/GSWApublications

PHILLIPS et al.

GEOLOGY OF THE EASTERN ZONE OF THE LAMBOO PROVINCE, HALLS CREEK OROGEN, WESTERN AUSTRALIA

REPORT 164